Evaluating the influence of DNA damage substrates and DNA context on recognition and repair by the NEIL Family of DNA Repair Enzymes

By

ELIZABETH ROSE LOTSOF
DISSERTATION

Submitted in partial satisfaction of the requirements for the degree of

DOCTOR OF PHILOSOPHY

in

Chemistry

in the

OFFICE OF GRADUATE STUDIES

of the

UNIVERSITY OF CALIFORNIA

DAVIS

Approved:

Sheila S. David, Chair

Peter A. Beal

Andrew J. Fisher

Committee in Charge

2022

To my family,

Henry, Sue, and David

Abstract

The DNA nucleobases are highly susceptible to modification from a wide variety of oxidizing and alkylating agents. Alterations to the nucleobase can threaten genomic integrity by disrupting normal cellular processes including replication and transcription or by introducing mutations. Damage to the DNA base is identified and removed by DNA glycosylases that initiate the base excision repair pathway (BER). The diversity of DNA damage, the location of damage, and how that DNA damage is identified has given valuable insights into disease related to DNA repair. The NEIL family of DNA glycosylases can excise lesions arising from all four nucleobases in a variety of DNA contexts, including duplex, single stranded, and G-quadruplex (G4). The loss or dysfunction of NEIL enzymes is associated with a diverse set of disease phenotypes, such as immune deficiencies, anxiety, impaired memory retention, and cancer. Yet, it remains unclear how NEIL dysfunction is related to these phenotypes. In this work, I evaluate the molecular and structural features involved in recognition and excision of a diverse set of lesions across multiple DNA contexts by the NEIL family of glycosylases.

First, I examine the features of the damaged nucleobase that influence differences in excision between the two isoforms of NEIL1. RNA editing of the NEIL1 pre-mRNA by the Adenosine Deaminase Acting on RNA (ADAR1) creates two isoforms of NEIL1 via a recoding event that converts a lysine to arginine in the lesion recognition loop of NEIL1. Notably, previous studies have demonstrated that the two isoforms display different enzymatic properties on the pyrimidine lesion, thymine glycol (Tg), where the unedited (UE, K242) isoform showed a significantly faster rate of excision compared to edited NEIL1 (Ed, R242). To further the understanding of NEIL1 activity, I continued this analysis on lesion processing by the two NEIL1 isoforms on a large number of substrates to evaluate the impact of the ADAR1-mediated recoding

event. Notably, UE NEIL1 demonstrates better excision of U/T pyrimidines, such as Tg, uracil glycol (Ug), 5-hydroxyuracil (5-OHU), and 5-hydroxymethyluracil (5-hmU), than the edited isoform. However, the relative difference in the rate of excision between Ed and UE NEIL1 is not consistent between lesions and decreases markedly in the series with Tg > Ug > 5-OHU > 5-hmU. Calculations performed in the gas phase examine tautomer stability (2-OH vs 4-OH) and N3 proton affinity of each lesion, and the relative rates of base excision track with the N3 proton affinity of the most stable tautomer. These data suggest that enzyme-promoted tautomerization affects cleavage of the glycosidic bond and enhances excision observed with the unedited enzyme. As a result, the differences in activity between the two isoforms of NEIL1 imply a unique regulatory mechanism for DNA repair by RNA editing.

Additionally, the ability of NEIL enzymes to excise DNA damage from G4 structures was evaluated. The G-rich nature of G4 sequences makes them highly susceptible to oxidative damage, and DNA damage in promoter containing G4 sequences and interaction of BER enzymes have been implicated in gene regulation. An oxidation product of guanine, guanidinohydantoin (Gh), was positioned at varying locations in G4 sequences from *VEGF*, *KRAS*, and *RAD17* promoters, and excision by NEIL1 and mouse NEIL3 (mNeil3), was monitored using *in vitro* glycosylase assays. The production curves are biphasic providing two rates, indicating that a fraction of Gh within the G4 is excised rapidly, while another fraction is processed more slowly. Also, the percent base removed does not reach 100% despite excess enzyme. The G4 sequence was the largest contributing factor to the differences in rates, associated amplitudes, and overall Gh excision by the NEIL enzymes. These observations suggest that the G4 structure and stability impact accessibility and ability of NEIL1 and mNeil3 to position Gh for cleavage. Thus, reduced repair by NEIL may increase the persistence of mutations or alter gene regulation.

In the last chapter, I evaluated the repair of Tg, Gh, and 2,6-diamino-4-hydroxy-5-formamidopyrimidine (FapyG) in human cell lines, as repair can vary between them, using a green fluorescent protein (GFP) reporter that had been previously used to evaluate the repair of Gh and Tg initiated by Neil1 in MEFs. Here, I evaluated the repair of Tg, Gh, and FapyG in HEK293FT cells and the cancer cell lines, HeLa and U87. The extent of repair was the greatest in HEK 293FT cells, while reduced repair of all lesions was observed in HeLa and U87 cells. In comparing the lesions, FapyG was repaired to the greatest extent followed by Gh and Tg across all cell lines. These lesions have never been explored in a cell-based assay, and lesion containing plasmid based cellular assays are useful tool to examine DNA damage and DNA repair capacity as they reflect the influence of factors such as protein expression and stability, which can be altered in disease states.

My dissertation evaluates the molecular basis of NEIL initiated repair to provide insights between NEIL activity and its diverse disease phenotypes. These results demonstrate that the type of damage and the location of damage can influence excision by the NEIL DNA glycosylases and altered NEIL activity can impact cellular function and progression of disease. NEIL1 specificity can be modified by RNA editing, and aberrant RNA editing and high levels Ed NEIL1 is associated with cancer. Also, NEIL enzymes interact with G4 structures and reduced excision may lead to increase mutation or participate in regulatory mechanisms. Each chapter examines unique repair properties of the NEIL enzymes and its DNA damage substrates and provides further opportunities to explore repair of these diverse lesions.

Table of Contents

List of Abbreviations

2’-F-Gh	2'-fluoro-guanidinohydantoin
2’-F-Tg	2'-fluorothymidine glycol
2-OH lactim	2-hydroxy lactim
4-OH lactim	4-hydroxy lactim
5-caC	5-carboxycytosine
5-fC	5-formylcytosine
5-hmC	5-hydroxymethylcytosine
5-hmU	5-hydroxymethyluracil
5-mC	5-methylcytosine
5-OHC	5-hydroxycytosine
5-OHU	5-hydroxyuracil
A	adenine
aa	amino acids
AFB_1-FapyG	methyl-FapyG, 8,9-dihydro-8-(2,6-diamino-4-oxo-3,4-dihydropyrimid-5-yl-formamido)-9-hydroxyaflatoxin B_1
AP	apurinic/apyrimidinic
APE	AP endonuclease
BER	base excision repair
Cg	cytosine glycol
CPD	cyclobutane pyrimidine dimers
CYP	cytochrome P450
DHT	dihydrothymine

DHU	dihydrouracil
E	glutamic acid
Ed	edited
EMSA	electrophoretic mobility shift assays
FapyA	4,6-diamino-5-formamidopyrimidine
FapyG	2,6-diamino-4-hydroxy-5-formamidopyrimidine
FEN1	flap endonuclease 1
Fpg	formamidopyrimidine-DNA-glycosylase
G	guanine
G4	G-quadruplex
GFP	green-fluorescent protein
Gh	guanidinohydantoin
H2TH	helix-two-turn-helix
hnRNP-U	heterogeneous nuclear ribonucleoprotein-U
HR	homologous recombination
I	inosine
IFN-α	interferon alpha
K	lysine
K_d	dissociation constant
k_g	rate constant of glycosidic bond cleavage
Lig1	DNA ligase 1
Lig3α	DNA ligase 3α
MBD4	methyl-CpG binding domain protein 4

MEF	mouse embryonic fibroblasts
MPG	methylpurine DNA glycosylase
Nei	endonuclease VII
NEIL	Nei-like glycosylase
NER	nucleotide excision repair
NHEJ	nonhomologous end joining
nt	nucleotide
nth/NTH1	endonuclease III
OA	8-oxo-7,8-dihydroadenine
OG	8-oxo-7,8-dihydroguanine
OGG1	8-oxoG DNA glycosylase
OI	8-oxoinosine
PAHs	polycyclic aromatic hydrocarbons
PCNA	proliferating cell nuclear antigen
Pol β	polymerase beta
Pol δ	polymerase delta
PQS	potential quadruplex forming sequence
pT	pTurbo
R	arginine
RFP	red-fluorescent protein
RNA pol II	RNA polymerase II
RONS	reactive oxygen and nitrogen
RPA	replication protein A

SAM	S-adenosyl methionine
SMUG	single-stranded monofunctional uracil DNA glycosylase
SNP	single nucleotide polymorphisms
Sp	spiroiminodihydantoin
SS DNA	single stranded DNA
T	thymine
TDG	thymine DNA glycosylase
TET	Ten-Eleven-Translocation enzyme
Tg	thymine glycol
THF	tetrahydrofuran
TPM	transcripts per million
U	uracil
UE	unedited
Ug	uracil glycol
UNG	uracil DNA glycosylase
WRN	Werner syndrome helicase
XRCC1	X-ray repair cross-complementing protein 1

List of Tables

List of Schemes

List of Figures

Acknowledgements

My PhD journey was supported by many people who helped me to become the scientist that I am today. First, I have to thank Dr. Sheila David for your years of mentorship and guidance. You have created an incredible laboratory that fosters community and innovation paired with scientific rigor. Your CARE philosophy, being curious, active, responsible, and engaged with our research, helped me to develop critical thinking, creativity, and communication skills that were essential to my success. This philosophy also extended outside of the laboratory, and you supported my growth in leadership, service, and mentorship. I will forever cherish our conversations, the research, developing the CURE class, and our work on the Miller Symposium. Thank you, Sheila!

The Department of Chemistry is truly an exceptional place to learn and grow as a scientist. The faculty and my peers had a profound impact on my graduate journey, and I can't thank them enough. I first have to thank my thesis committee Dr. Peter Beal and Dr. Andrew Fisher for all their guidance on my dissertation and broadening my education on nucleic acids. Dr. Dean Tantillo, thank you for your continued encouragement and support. Dr. Jared Shaw, I appreciate your thoughtfulness and dedication to addressing graduate student concerns and improving the department. Dr. Kyle Crabtree, it was incredible working with you on the outreach committee and continuing to promote scientific education while navigating the challenges of the pandemic. Additionally, the Designated Emphasis in Biotechnology greatly supported my professional development and helped me find a career path that I am so excited about. Thank you Dr. Judy Kjelstrom and Dr. Denneal Jamison-McClung for creating such fantastic program and providing opportunities for career exploration and professional development. I am also extremely grateful for the collaborative projects and the wonderful scientific stories produced with Dr. Jeehiun Lee

at Rutgers University, Dr. Eric Kool at Stanford University, and Dr. Cynthia Burrows and Dr. Aaron Fleming at the University of Utah.

My family and friends were truly my rock throughout my graduate school experience sending love from near and far. Thank you mom for teaching me to be fearless and bold, and dad, you taught me the value of hard work, dedication, and to push boundaries. These combined lessons helped me to take the leap into graduate school and explore opportunities that I never thought were possible. David, thank you for all the laughs and conversations about cars that provided fun and necessary breaks. My dear friends, Kay, Becky, Jess, Louis, Kelsey, and Danielle, you all reminded me to believe in myself and were my constant champions. Anna and Nina, we went through our graduate school journey together, and thank you for being my sounding board and continual sources of support and laughter.

I am incredibly grateful to all the members of the David laboratory, who made the lab such a wonderful place to work and provided endless support through the ups and downs of the PhD journey. Nicole, Doug, Brittany, Carlos, Alan, Kori, Cindy, Merve, Robert, Savannah, Jonathan, Steven, Nhu, Josh, Nicole, Melody, Mo, and Summer, I am so thankful for every single one of you. Nicole, Doug, Brittany, thank you for getting me started in my graduate career and setting me up for success. Carlos and Alan, you both were a constant source of knowledge and helping hand when I needed it the most. Team NEIL, Josh and Savannah, I am so proud of what we have accomplished and foundation that we have laid to for NEIL projects to come. Josh, I will forever appreciate your creativity, intellect, and enthusiasm, and Savannah, your diligence and passion helped to drive our many projects. Steven, thank you for all of your kindness in addition to the coffee, dance parties, and jokes that brought so much joy to the laboratory. I especially want to thank Chandrima and Cindy. Chandrima, you were a huge help during my academic journey and

constant mentor but, more importantly, an amazing, creative, and thoughtful friend. Plus, we had the best crochet and cooking nights. Cindy, I learned so much from you, and I could have not succeeded in graduate school without you. It is truly special when you get to work with a dear friend, whose constant support encourages you to be the best version of yourself. My team of amazing undergraduate researchers, Kelsey, Alyssa, Sara, and Olivia, it was a privilege to work with each of you, and thank you for all your contributions to our projects. I know all of you are going to reach great heights, and I can't wait to see what you do!

Lastly, I am grateful the financial support I received during my Ph.D. Thank you to the Department of Chemistry, the Bradford Borge fellowship, and the Wakeham fellowship: mentorship in critical transitions, and additionally, the NIH for GM143557, written by team NEIL, and CA090689 grants. Without their support, this work would not have been possible.

Chapter 1 Introduction

This chapter is adapted with permission from an invited chapter entitled "Chemical Approaches to Genomic Integrity," by Elizabeth R. Lotsof, Savannah G. Conlon, and Sheila S. David, in the book entitled "Advanced Chemical Biology: Chemical Dissection and Reprogramming of Biological Systems," Edited by Howard C. Hang, Matthew R. Pratt, and Jennifer A. Prescher, Wiley-VCH, © 2023. in Advanced Chemical Biology.

DNA is a dynamic molecule that undergoes structural changes for normal cellular function, such as replication and transcription, and its highly dynamic nature makes DNA susceptible to modification. Some modifications are required to regulate mechanisms like gene expression, while others are deleterious and threaten the integrity of the human genome.[1] Our cells have several mechanisms to repair such modification in DNA and to maintain genomic integrity.[2] The study of DNA damage and repair mechanisms illustrated the important role of chemistry in identifying critical features of this complex biological processes such that Tomas Lindahl, Aziz Sancar, and Paul Modrich were awarded the 2015 Chemistry Nobel Prize for their discovery of the mechanisms of DNA repair.[3]

Types of DNA damage and base modifications

All four DNA bases can undergo structural modification from oxidizing agents, alkylating agents, and radiation (Figure 1.1).[4] Such modifications can alter structural features of the nucleobase, including changing hydrogen bonding properties and mediating mutations during DNA replication, or hindering DNA replication and transcription.[4] Additionally, modifications to nucleobases may weaken the *N*-glycosidic linkage between the base and sugar, which may result in base loss (depurination or depyrimidination) producing a base-less, apurinic/apyrimidinic (AP) site. AP sites are inherently unstable and may also be enzymatically processed to generate DNA strand breaks.[5] All modifications have some consequence to the cell requiring recognition and repair. The next sections discuss some of the common types of DNA base damage and how they arise.

Oxidation: Reactive oxygen and nitrogen species (RONS) are potent oxidants that mediate structural modifications to all biomolecules including the nucleobase, deoxyribose sugar, and phosphate backbone of DNA.[6,7] The hydroxyl radical ($HO^{\bullet}$) and carbonate radical ($CO_3^{\bullet-}$) are

reactive one-electron oxidants that can form as a by-product of cellular respiration, Fenton chemistry, and ionizing radiation.[6,7] Recently, $CO_3^{\bullet-}$ has been suggested to be the more biologically relevant one-electron oxidizer based on studies evaluating the kinetics of Fenton chemistry, where in the presence of bicarbonate, $CO_3^{\bullet-}$ was formed and not $HO^{\bullet}$.[8] Conditions of oxidative stress and inflammation are common means that lead to increased amounts of RONS in cells.

Of the four nucleobases, the guanine (G) base has the lowest reduction potential (1.29V vs. NHE) making G most susceptible to oxidation and producing a wide range of guanine lesions. One of the most extensively studied guanine lesions is 8-oxo-7,8-dihydroguanine (OG).[9] OG in its *syn* conformer is capable of mispairing with adenine (A) as the addition of an oxo group on C8 and a hydrogen on N7 mimics the hydrogen bonding face of thymine (T). OG also has an even lower reduction potential than G (0.74V vs. NHE) making it susceptible to further oxidation to form the hydantoin lesions, guanidinohydantoin (Gh) and spiroiminodihydantoin (Sp) (Figure 1.1A).[9] These non-planar and helix distorting hydantoin lesions are replication and transcription blocks,[10] and in cases where replications occurs, are completely miscoding, ultimately leading to G-to-T transversion and G-to-C transition mutations.[11] RONS can also produce modifications to other bases, including the common oxidative modifications to purine bases such as 8-oxo-7,8-dihydroadenine (OA), and the ring open formamidopyrimidines, 2,6-diamino-4-hydroxy-5-formamidopyrimidine (FapyG) and 4,6-diamino-5-formamidopyrimidine (FapyA).[12] Oxidation products of cytosine can produce a broad spectrum of C-derived lesions, such as 5-hydroxycytosine (5-OHC) and cytosine glycol (Cg), and can be further deaminated to 5-hydroxyuracil (5-OHU) and uracil glycol (Ug) (Figure 1.1A).[13] Deaminated oxidation products of cytosine (C) are highly mutagenic as they possess the same hydrogen bonding face as T. Oxidation

of the thymine also leads to a variety of base lesions, including thymine glycol (Tg), which is a potent replication and transcription block.[14]

Alkylation: The electron rich heterocycles of the DNA nucleobases have numerous nucleophilic sites to readily react with electrophiles.[1,15,16] All nitrogen and oxygen atoms are susceptible to alkylation, but in double stranded DNA, the relative reactivity with S_N2-type electrophiles follows the general trend of G(N7)>A(N3)>>A(N1)>C(N3) and is dependent on the accessibility of the nucleophilic atom (Figure 1.1B).[15,16] Many DNA alkylating agents are environmental carcinogens that may be transformed into the electrophilic species by oxidative metabolic processing by cytochrome P450 (CYP) enzymes primarily in the liver.[17] For example, CYP-mediated oxidation of polycyclic aromatic hydrocarbons (PAHs), including benzo[*a*]pyrene and aflatoxin B1, introduce a strained, epoxide ring that is highly reactive with DNA base nucleophiles (Figure 1.1B).[18] In the cell, methyl transferases can purposefully transfer a methyl group to adenine or cytosine from S-adenosyl methionine (SAM) as the methyl donor generating N^6-methyladenine, N^4-methylcytosine, and 5-methylcytosine, which can serve important roles in epigenetic regulation.[19] Many of the products of DNA base alkylation are more prone to depurination or depyrimidination as a result of weakening the *N*-glycosidic bond between the base and sugar.

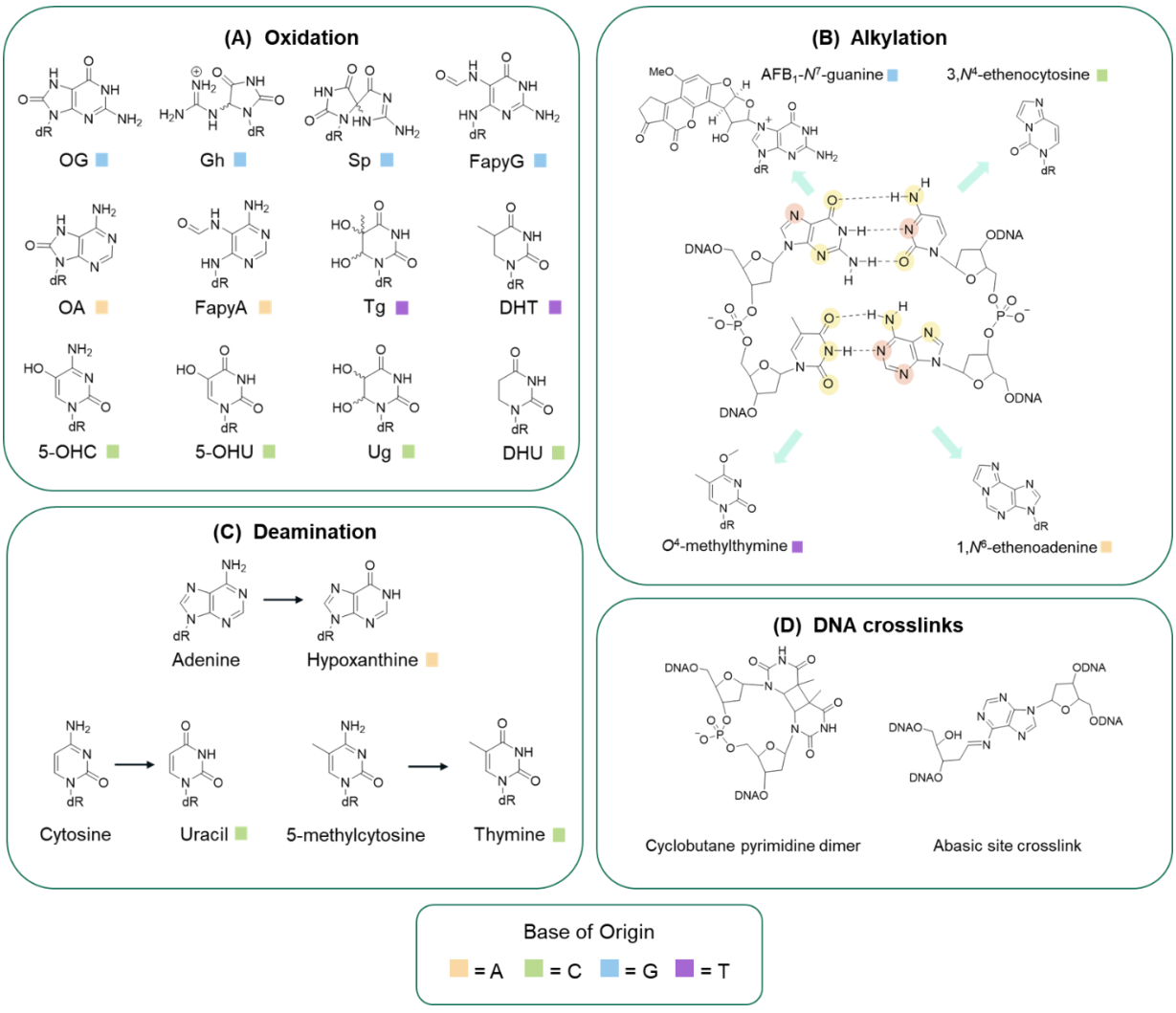

Figure 1.1: Modifications to DNA nucleobase.

(A) Oxidation alters the structure of all four nucleobases producing a wide array of DNA damage. OG: 8-oxo-7,8-dihydroguanine, Gh: guanidinohydantoin, Sp: spiroiminodihydantoin, FapyG: 2,6-diamino-4-hydroxy-5-formamidopyrimidine, OA: 8-oxo-7,8-dihydroadenine, FapyA: 4,6-diamino-5-formamidopyrimidine, Tg: thymine glycol, DHT: dihydrothymine, 5-OHC: 5-hydroxycytosine, 5-OHU: 5-hydroxyuracil, Ug: uracil glycol, DHU: dihydrouracil. (B) All positions highlighted are susceptible to alkylation. Nitrogen atoms highlighted in red are the most nucleophilic atoms on the four nucleobases with common products of alkylation shown. (C) Deamination of adenine, cytosine, and 5-methylcytosine produces hypoxanthine, uracil, and thymine causing mismatches, that lead to mutations within the genome. (D) DNA crosslinks arise from UV radiation (e.g. cyclobutane pyrimidine dimers) or via endogenous production of abasic sites (e.g. AP-A crosslinks). Figure adapted from Hang 2023.

Deamination and DNA mismatches: The exocyclic amines of cytosine, adenine, and guanine are susceptible to deamination under physiological conditions or by enzymatic processing. Conversion of the canonical bases by deamination can change the hydrogen bonding and coding properties of the base.[1] For example, the deamination of cytosine produces uracil (U), a base that is normally confined to RNA. The lack of a methyl group on C5 distinguishes U from T for repair; however, when 5-methylcytosine (5-mC) is deaminated, thymine is produced in DNA and can only be distinguished by its presence paired with G in a T:G mismatch (Figure 1.1C).[20] Additional types of mismatches also arise from alkylation and oxidation events. For example, many oxidation products of G, including OG, Gh, and Sp can all mispair with A and subsequent replication can lead to G:C to T:A transversion mutations.[11]

DNA Crosslinks: Intra- and inter-strand DNA crosslinks are highly toxic forms of DNA damage arising from UV radiation, chemotherapeutics, and endogenously between AP sites and exocyclic amines of purine bases.[21–24] The presence of DNA crosslinks inhibit DNA replication and transcription, mediating cell death, and pose a challenge for DNA repair. UV radiation can produce cyclobutane pyrimidine dimers (CPD) through the reaction of C5-C6 double bonds of adjacent pyrimidines.[21] Cisplatin and nitrogen mustards engage with the highly reactive N7 on guanine to produce intra- and inter-strand crosslinks and are used as clinical chemotherapeutics.[22] Endogenous DNA crosslinks can be formed between the exocyclic amines of A and G and the reactive aldehyde of an AP site. AP site inter-strand crosslinks are reversible but are long lived due to features of the base amine (Figure 1.1D).[24,25]

DNA repair

Several DNA repair pathways exist to mitigate the myriad of DNA modifications that compromise genome integrity. The five primary pathways are direct repair, double strand break,

nucleotide excision repair, mismatch repair, and base excision repair. Between these repair pathways there is some overlap and redundancy to allow for the recognition and repair of the wide range of DNA damage. Briefly, direct DNA repair enzymes removes the modification through chemical reversion of the damage reaction and does not require a DNA template, phosphodiester backbone breaking, or DNA synthesis. CPD photolyases, O6-alkylguanine-DNA alkyltransferase (MGMT), and AlkB family of enzymes all perform such reactions to repair cyclobutane pyrimidine dimers, O^6-methyl guanine, and N^1-methyladenine and N^3-methylcytosine, respectively.[26–28] Double-strand breaks and inter-strand crosslinks can be repaired via homologous recombination (HR) or nonhomologous end joining (NHEJ). Repair of the damaged region by HR requires a template from a homologous undamaged DNA molecule.[29] On the other hand, NHEJ does not require a template for repair and the broken ends are ligated together; unfortunately, repair via this pathway can lead to deletions.[30] Nucleotide excision repair (NER) is responsible for the removal of a wide range of modifications that are often large and/or helix distorting. Recognition of helical distortion initiates the excision of a short fragment containing the base modification and filling of the short gap.[31] Mismatch repair is a strand-specific method responsible for the recognition and repair the undamaged, misincorporated base in the newly synthesized strand arising from DNA replication or recombination.[32] Finally, base excision repair (BER) is a highly conserved repair mechanism for the repair of many modifications and mismatches that arise from oxidation, deamination, and alkylation reactions.[33,34] This pathway will be discussed in detail in the next section.

DNA glycosylases and base excision repair

Base excision repair is initiated by DNA glycosylases that recognize and excise the modified base by hydrolyzing the *N*-glycosidic bond between the base and the sugar (Figure 1.2A).

The resulting AP site is processed by an AP endonuclease (APE1, APE2) to hydrolyze the phosphodiester backbone when the base is excised by a monofunctional glycosylase. Some glycosylases are bi-functional with lyase activity to catalyze either β-elimination or β, δ-elimination reaction at the AP site to produce a 3'-α, β-unsaturated aldehyde and 5'-phosphate termini or 3'- and 5'-phosphate termini, respectively (Figure 1.2B).[35] The gap for cleavage of the phosphodiester backbone is then processed by either short patch or long patch BER. In short patch BER, the DNA backbone was cleaved by the AP endonuclease followed by single nucleotide insertion by DNA polymerase beta (Pol β) and ligation by DNA ligase 1 (Lig1). Long patch BER is initiated by many bifunctional glycosylases that process AP site. The DNA polymerase extends a longer fragment generating a flap that must be removed by flap endonuclease 1 (FEN1) prior to ligation (Figure 1.2C).[36]

Several superfamilies have evolved for recognition and repair of a specific modified base or a set of related modifications (Table 1.1). The diversity of DNA modifications, often in low cellular abundance, make DNA glycosylases remarkable in their ability to find and excise the aberrant nucleobase. The UDG superfamily primarily responsible for the removal the products of deamination, uracil and hypoxanthine, thymine, or 5-fluoro-uracil. TDG, a member of the UDG family, can excise the further oxidized products of the epigenetic modification 5mC. The helix-turn-helix superfamily is more diverse with several subfamilies excising a wide range of oxidation and alkylation products, including OGG1 for the for the removal of OG across from C, MutY/MUTYH for the misincorporated A across from OG, Mig and MBD4 for the removal the mutagenetic T in G:T mismatches, EndoIII and its mammalian homologs, NTHL, for removal of many oxidized pyrimidines, and the AlkA family for the excision of methylated bases. The methylpurine glycosylase is responsible for the removal of alkylated purines in addition to the

HEAT like repeat glycosylase family (AlkC/AlkD). Finally, the Fpg/Nei super family consists of the formamidopyrimidine-DNA-glycosylase (Fpg) and endonucleaseVII (Nei) and their mammalian homologs, NEIL1, 2, and 3, are capable of excising a remarkably wide range of oxidized bases including Gh, Tg, 5-OHU, and FapyA/G in a variety of substrate contexts.

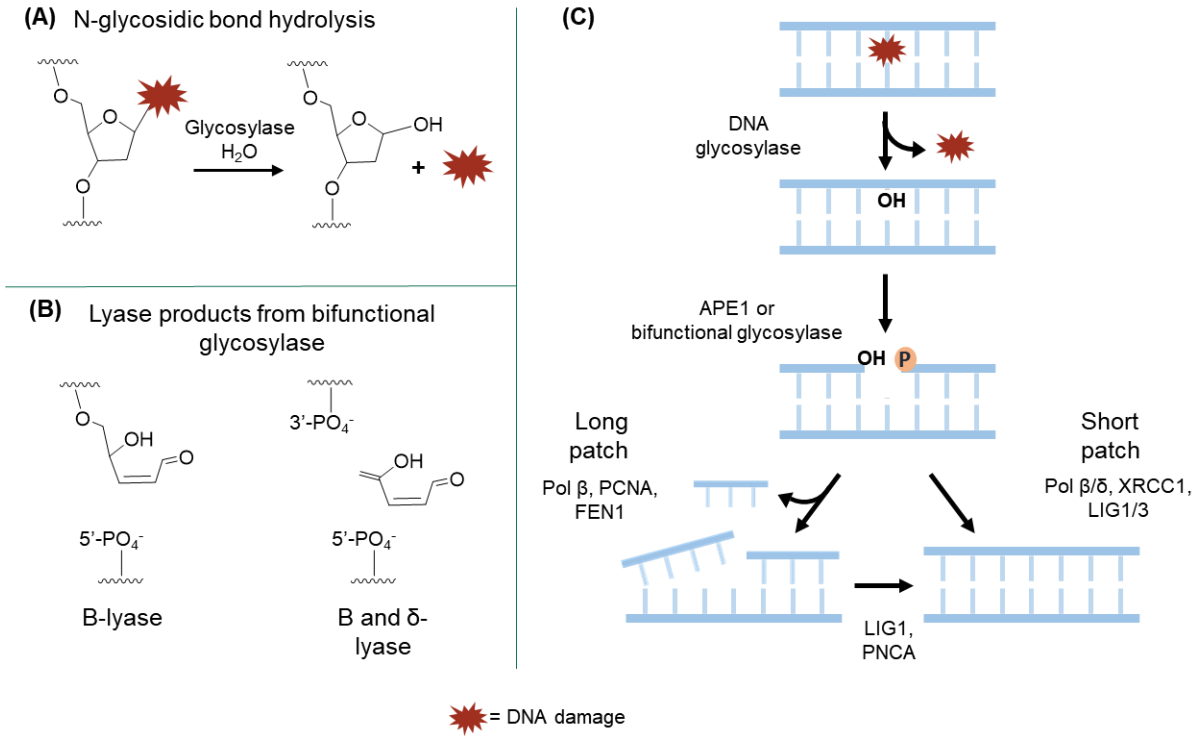

Figure 1.2: DNA glycosylases initiate the base excision repair pathway.

(A) DNA glycosylases hydrolyze the *N*-glycosidic between the modified/misplaced base and deoxyribose sugar. (B) Bifunctional glycosylases also have lyase activity causing a break in the phosphodiester backbone. (C) Downstream base excision repair enzymes restore the proper base after lesion removal by the DNA glycosylase. AP endonuclease (APE1), polymerase beta (Pol β), polymerase delta (Pol δ), DNA ligase 1 and 3 alpha (Lig1 and 3α), X-ray repair cross-complementing protein 1 (XRCC1), and proliferating cell nuclear antigen (PNCA).

Table 1.1: DNA glycosylase superfamilies, DNA glycosylases belonging to each family and their substrates.

DNA Glycosylase Superfamily	DNA Glycosylase	Substrate
UDG	Uracil DNA Glycosylase (UNG)	U
	Single-stranded Monofunctional Uracil DNA Glycosylase (SMUG)	U in ssDNA and duplex, 5-OHU, 5-fluorouracil
	Thymine DNA Glycosylase (TDG)	U, T in G:T mismatch, 5-caC, and 5-fC
Helix-hairpin-helix	Endonuclease III (nth/NTH1)	Oxidized purines including Tg, 5-OHU
	8-OxoG DNA Glycosylase 1 (OGG1)	OG
	MutY/MUTYH	A in G/OG mispairs
	Methyl-CpG Binding Domain Protein 4 (MBD4)	U or 5-fluorouracil
	AlkA	Alkylated purines
MPG	Methylpurine DNA Glycosylase	Alkylated purines
Heat-like repeat	AlkC/AlkD	Alkylated purines
Fpg/Nei	Nei-like glycosylase 1 (NEIL1)	Gh, Sp, FapyA, FapyG, oxidized pyrimidines, alkylated FapyA/G, psoralen crosslinks
	Nei-like glycosylase 2 (NEIL2)	Oxidized pyrimidines and AP sites
	Nei-like glycosylase 3 (NEIL3)	Gh, Sp, abasic site crosslink
	Formamidopyrimidine-DNA-glycosylase (Fpg)	OG, Gh, Sp, FapyA, FapyG, oxidized pyrimidines

Fpg/Nei family of DNA glycosylases

The Fpg/Nei family of DNA glycosylases includes the mammalian homologs, NEIL1, 2, and 3 of Fpg and Nei, and these glycosylases are capable of excising many oxidation and alkylation products from a wide variety of DNA contexts including duplex, single strand, replication forks and G-quadruplex (G4) DNA. The overlapping substrate scope and reactivities of NEIL1, 2, and 3 is a product of structural similarities between the glycosylases. All three glycosylases have a helix-two-turn-helix (H2TH) DNA binding motif in the glycosylase domain and conserved N-terminus with key critical residues for excision.[37,38] NEIL1 has an N-terminal sequence of MPEGPEL, NEIL2 has an N-terminal sequence of MPEGPLV, and NEIL3 varies the most with an N-terminal sequence of MVEGPGC.[38,39] In all cases, there is either a N-terminal proline or valine at position 2 and glutamic acid at position 3. Pro2 is important for the lyase activity of NEIL1 allowing for Schiff base formation between the AP site and the proline. A similar activity is proposed for Pro2 and Val2 for NEIL2 and NEIL3 respectively.[38] Glu3 is in close proximity to O4' of the ribose sugar, and mutations at this position indicate Glu3 is an important residue for catalysis.[40–43]

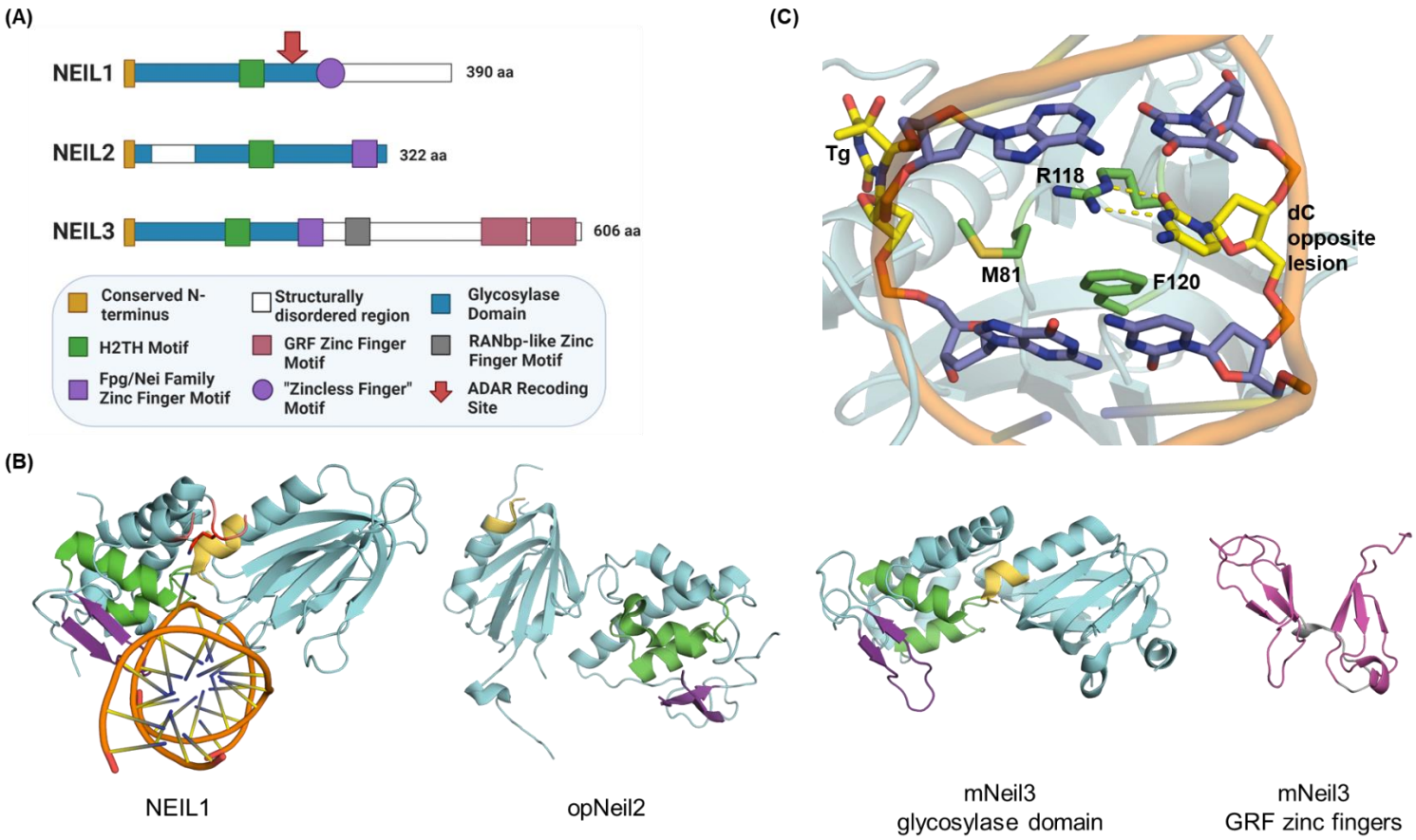

Figure 1.3: Structural features of NEIL family of glycosylases.

(A) Structural representations of the three NEIL glycosylases. Figure adapted from Liu *et al.* 2010. (B) Crystal structures of human NEIL1 (PDB: 5ITX), opossum Neil2 (opNeil2, PDB:6VJI), mouse Neil3 (mNeil3) glycosylase domain (PDB: 3W0F) and GRF zinc fingers (PDB: 7JL5) highlight structural features, including conserved N-terminus (yellow), H2TH motif (green), Fpg/Nei zinc finger or zincless finger (purple), glycosylase domain (cyan), the lesion recognition loop and ADAR1 recoding site of NEIL1 (red), and GRF zinc fingers (magenta) and linker region (light gray) of mNeil3. (C) Probing residues NEIL1 (PDB:5ITX). Met81, Arg118, and Phe120 shown in green, and lesion Tg and the base opposite lesion, dC, are shown in yellow. NEIL2 and NEIL3 lack similar Arg118 and Phe120 probing residues that coordinate with base opposite lesion and scanning residue, respectively.

The NEIL glycosylases also vary in many features that differentiate them in their activity. NEIL3 is the largest of the glycosylases with a total of 606 amino acids (aa) in length followed by NEIL1 (390 aa) and NEIL2 (332 aa) (Figure 1.3A and B).[39,44] All three glycosylases have intrinsically disordered domains that are sites of many protein interactions and regulatory features. NEIL1 and NEIL3 have their C-terminal domains (CTD) disordered, while NEIL2 has two disordered regions in the N-terminus.[38] For example, NEIL1 CTD facilitates the formation of a "BERosome" repair complex with multiple replication-associated proteins, and in the absence of its CTD, NEIL1 loses its association to chromatin and replication foci in S-phase cells.[45] Additionally, NEIL1 has a "zincless" finger motif that is critical for binding of DNA where as NEIL2 and NEIL3 have similar domains containing zinc ions.[46] The NEIL3 C-terminal domain contains many additional zinc finger motifs, including two GRF zinc finger motifs and a RANbp-like zinc finger motif. The GRF zinc finger motifs have an autoinhibitory effect regulating the activity of the glycosylase domain.[47] The NEIL2 N-terminal disordered regions are highly flexible allowing for proper engagement of the enzyme on DNA substrates and are likely sites of protein interacts that are still being determined.[48]

NEIL1, NEIL2 and NEIL3 also differ in key probing residues for the detection of DNA repair. NEIL1 has residues Met81, Arg118, and Phe120 for scanning through the vast amounts of DNA and extrude a damaged base into the catalytic site on the enzyme (Figure 1.3C).[37] Met81 occupies the position of the extruded base entering through the minor groove. Phe120 is wedged between the base opposite the lesion causing unstacking of the bases and leading to severe kinking in DNA. Phe120 is also important in the scanning mechanism as it wedges into the DNA to search for non-planar bases such as Gh and Sp. Arg118 forms H-bonds with the opposite base to the DNA lesion and can discriminate between the four canonical bases to regulate NEIL1 activity.[37,46,49]

NEIL2 and NEIL3 do not have the equivalent Arg118 and Phe120, and the lack of these residues is proposed for NEIL2 and NEIL3's preference for single stranded substrates compared to duplex.[37] Of the three glycosylases, NEIL1 has been the most comprehensively studied, but new work is emerging for NEIL2 and NEIL3 highlighting unique features of their biological roles. Each NEIL glycosylase displays slightly different preferences in regard to DNA context and lesion specificity that are often a reflection of their role in BER.

NEIL1: The substrate scope of NEIL1 has been extensive studied, and the NEIL1 glycosylase has the remarkable ability to excise a wide array of oxidized purines and pyrimidines.[50] Known substrates for NEIL1 include the hydantoin lesions, Gh and Sp, Tg, 5-OHC, 5-OHU, DHT, DHU, FapyG and FapyA (Figure 1.1A).[51–55] NEIL1 can also excise some larger alkylation products, such as methyl-FapyG, 8,9-dihydro-8-(2,6-diamino-4-oxo-3,4-dihydropyrimid-5-yl-formamido)-9-hydroxyaflatoxin B_1 (AFB_1-FapyG), and psoralen induced crosslinks.[56] Notably, OG is not excised by NEIL1 despite conflicting reports in the literature.[52] On the other hand, the further oxidation products of OG, Gh and Sp, are among the best documented substrates of NEIL1.[52] NEIL1 is able to excise damage from a diverse range of structures, including duplex, SS DNA, bubble, and bulge DNA structures, and G-quadruplexes, and has been found to associate with replication forks.[9,52] Additionally, NEIL1 has also been implicated in epigenetic gene regulation via interactions with further oxidized products of 5-mC, 5-formylcytosine (5-fC) and 5-carboxycytosine (5-caC) from pulldown assays, yet these have not been fully verified.[57–59] NEIL1's ability to recognize a wide range of substrates is due its flexible binding pocket of this enzyme; however, due to the planar nature of OG, it is not well excised as it fit poorly into the shallow binding pocket with few hydrogen bonding interactions and greater solvent exposure.[60,61]

Additionally, two isoforms of NEIL1 exist due to RNA editing of the NEIL1 pre-mRNA by the adenosine deaminase ADAR1.[62–64] ADAR1 catalyzes the deamination of adenosine (A) to inosine (I), and such editing events are responsible for altering splice sites or codon changes.[65] Studies evaluating the whole transcriptome sequence analysis from human tissues identified possible A to I editing sites, including the pre-mRNA of the NEIL1.[63] The Beal laboratory identified that ADAR1 is responsible for an editing event causing a single codon change in the transcript.[64] For NEIL1 pre-mRNA, the A at position 725 is converted to I by ADAR1.[64] Since inosine codes as guanosine during translation, the edited mRNA codes for an arginine at position 242 in NEIL1 rather than the lysine coded in the unedited mRNA. The original NEIL1 cDNA sequence identified the edited isoform from a cell population where the mRNA contained the codon code for arginine at position 242,[46,66] and as a result, most of the biochemical substrate analysis was only performed on the edited isoform prior to the landmark paper by the David and Beal laboratories.[64] The David laboratory identified that this single codon change introduces dramatic alterations in lesion removal activity between the unedited (UE, Lys242) and edited (Ed, Arg242) NEIL1 isoforms.[64] UE NEIL1 removes Tg in duplex DNA about ~30-40 fold faster than Ed NEIL1, while the edited isoform excises Gh ~3fold faster.[64] Electrophoretic mobility shift assays 2'-fluorothymidine glycol (2'-F-Tg) and 2'-fluoro-guanidinohydantoin (2'-F-Gh) have shown similar affinity by the two isoforms suggesting that the observed differences in rate are related to a kinetic step rather than lesion binding affinity.[67,68]

Structural studies by Yi and co-workers of Ed and UE NEIL1 bound to a Tg duplex and QM/MM calculations showed that residue 242 plays a critical role in the mechanism of NEIL1 (Figure 1.4A) and is responsible for differences in excision. Lys or Arg 242 side chain lies within the lesion recognition loop of NEIL1, and upon binding with lesion containing DNA, residue 242

directly interacts with the Tg base.[69] Engagement by NEIL1 with the Tg base can promote tautomerization of the lactam to the lactim and allow for protonation of N3 by residue 242 (Figure 1.4B). Differences in excision were attributed to pK_a of Lys (pK_a ~ 10.5) and Arg (pK_a ~ 12.5). The more acidic lysine allowed for greater extent of proton donation with UE NEIL1 to promote Tg tautomerization and facilitate faster excision.[69] The influence of 242 side chain acidity was the most dramatic with Tg, but this does not explain trends observed with other lesions, such as Gh and Sp. Recent structures with additional lesions by Yi and coworkers have also shown that NEIL1 can capture lesions in alternative non-catalytically competent conformations. In the active conformation, residue 242 directly engages with damaged base, while in the non-catalytically active, Tyr244 can stack with lesion keeping the base in a "quarantine" state (Figure 1.4C).[70] Rearrangement of the lesion recognition loop will allow for re-engagement of residue 242 with the lesion and enzyme activity.

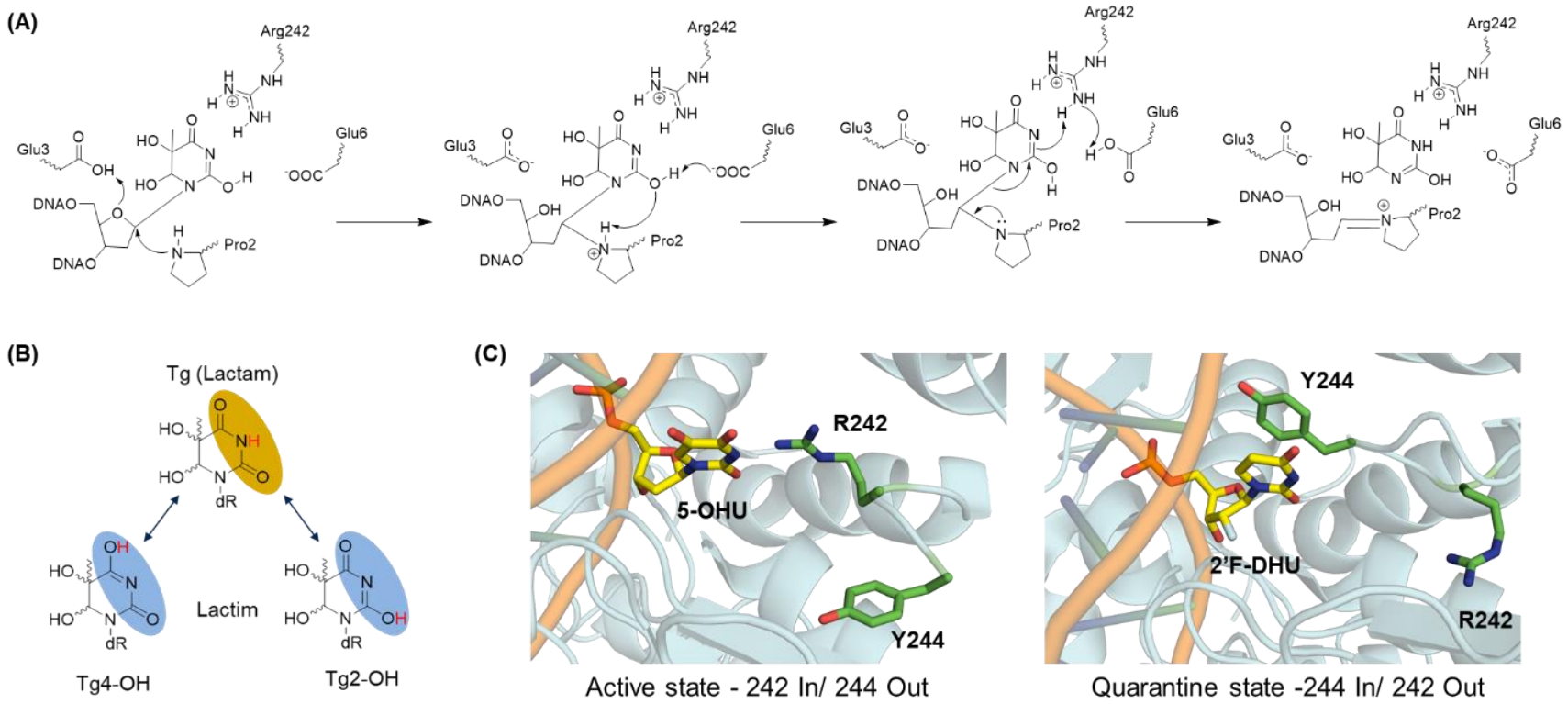

Figure 1.4: Engagement by NEIL1 promotes lesion tautomerization in active conformation.

(A) Proposed mechanism for NEIL1 based on structural studies and QM/MM calculations. Residue 242 engages with lesion tautomer and protonation by residue 242 is critical to the lesion mechanism.[69] (B) Lactim and lactam tautomers of thymine glycol. Figure adapted from Zhu *et al.* 2016. (C) Active state of NEIL1 has engagement by residue 242 with lesion (PDB: 6LWB and 6LWL).

While these structural studies have provided insight into NEIL1 activity and distinguishing the role of residue 242 in NEIL1 base excision, the biological role of having two isoforms of NEIL1 is still unclear. From a single gene, the editing event by ADAR1 produces two forms of NEIL1 with altered substrate specificities. A balance may be needed between the two isoforms for the efficient recognition and repair for all NEIL1 substrates under different cellular conditions, and the lack of the unedited isoform may allow for lesions to persist leading to mutation and strand breaks. In cases of multiple myeloma, the overexpression of Ed NEIL1 had greater cellular proliferation cells and higher level of unrepaired double-strand breaks.[71] Additionally, ADAR1 overexpression and transcriptome hyperediting are associated with cancer, and ADAR1 is expression is up-regulated under conditions associated with inflammation, which is a notable feature of cancer progression.[71–73] In cases of lung cancer and multiple myeloma, the NEIL1 mRNA was completely edited.[72,73]

In addition to cancer connected to RNA editing, NEIL1 is associated with a wide range of disease phenotypes. Loss of NEIL1 is associated with immune deficiencies, loss of olfactory function associated Alzheimer's disease,[74] Werner syndrome,[75] impaired memory retention and increased brain damage.[76] *Neil1-/-* mice exhibit phenotypes of metabolic syndromes[77,78] and anxiety behavior.[79] The link between these phenotypes and loss of NEIL1 activity is not well understood. The diversity of biological consequences is likely a product of NEIL1's broad substrate specificity and the several DNA contexts in which it can function. NEIL1 is most highly expressed in the liver, pancreas, and thymus with moderate expression in brain, spleen, prostate, and ovary.[80] This expression is highest during S-phase, and NEIL1 is found to localize to human condensed chromosomes and centrosomes during mitosis suggesting a link between NEIL1 and replication.[80,81]

NEIL1 associates with enzymes involved in short patch BER, Pol β, X-ray repair cross-complementing protein 1 (XRCC1), and DNA ligase1 and 3α (Lig1 and 3α), and long patch BER, polymerase delta (Pol δ), proliferating cell nuclear antigen (PNCA), FEN-1, and Lig1.[82] Notably, NEIL1 acts in an APE-independent pathway as NEIL1 can perform strand scission due to its highly coupled glycosylase and lyase activities.[82] NEIL1 has also been observed to interact with the DNA replication proteins, PCNA, FEN1, replication protein A (RPA), replication factor C, Pol δ, and DNA ligase 1 acting as a "cowcatcher" in replication forks.[45] NEIL1 stalls Pol δ along the replication fork for pre-replicative repair, which is required to maintain genomic integrity, and suggests a role of NEIL1 in replication associated repair.[45] Additional protein partners of NEIL1 include the DNA glycosylases OGG1 and TDG, where NEIL1 has been found to stimulate the turnover of OGG1 and TDG. For both of these DNA glycosylases, NEIL1 processes the abasic site resulting from OGG1 or TDG glycosylase activity.[59,83] NEIL1 can replace APE1 in the hand off of the processed AP site and facilitate in the turnover of TDG and OGG1. A notable interaction with NEIL1 is the Werner syndrome helicase (WRN) that has been identify to unfold G4 structures.[84] WRN and FEN-1 localize in telomeric regions which are known to have G4, and NEIL1 is capable of excising the hydantoin lesions from G4 structures.[85]

NEIL2: NEIL2 is bifunctional glycosylase with a catalytic Pro2 similar to that of NEIL1. NEIL1 and NEIL2 have overlapping substrate specificity excising Tg, 5-OHU, DHU, Gh and Sp.[50,80,86] AP sites are very efficiently processed by NEIL2 and to a greater extent than oxidized purine and pyrimidine substrates, suggesting that NEIL2 is a more efficient lyase than glycosylase.[48] Unlike NEIL1, NEIL2 displays a preference for damage with in single-stranded and bubble DNA and is capable of initiating repair in D- and R- loops.[53,87]

Similarly to NEIL1, NEIL2 associates with Pol β, XRCC1, and Lig3α.[88] However, unlike NEIL1, NEIL2 expression levels are cell cycle independent and likely does not participate in replication associated repair.[80] NEIL2's context specific repair and association with RNA polymerase II (RNA pol II), Cockayne Syndrome Protein B, which assists RNA pol II with chromatin remodeling, and the transcriptional regulator, heterogeneous nuclear ribonucleoprotein-U (hnRNP-U), suggest a role for NEIL2 in transcription coupled repair.[89] Y-box binding protein, which also associated with transcription, was found to interact with NEIL2 and stimulate glycosylase activity.[90]

The loss of NEIL2 also has many disease phenotypes including increased susceptibility to age-related cataracts,[91] polycystic ovarian syndrome,[92] and decreased cognitive performance.[93] NEIL2 does not have clear cancer phenotype yet established; however, recently identified single nucleotide polymorphisms (SNP) in the *NEIL2* gene shows a significant association between NEIL2 and BRCA2 mutation carriers and breast cancer risk.[94] Further analysis of this SNP showed increased expression of NEIL2 and in BRCA2 mutation carriers, elevated NEIL2 levels correlated with increased oxidative DNA damage.[95] Biochemical assays of possible NEIL2 cancer variants show diminished substrate processing compared to wildtype.[48]

NEIL3: NEIL3 excises similar substrates to both NEIL1 and NEIL2 as previously discussed. NEIL3 is considered a bifunctional glycosylase; however, its lyase activity is diminished compared to NEIL1 and NEIL2. NEIL3 has an N-terminal Val where NEIL1 and NEIL2 have a Pro, and the presence of the valine is proposed to be responsible for the difference in lyase activity.[39,44] NEIL3 is still an efficient glycosylase, but the glycosylase activity can vary between all three NEILs depending on the substrate and DNA context. NEIL3 has a preference for excising damage from SS DNA and G4 contexts compared to duplex due to additional negatively

charged residues that would make contact with the opposite DNA strand.[43] A unique substrate to NEIL3 are AP-site crosslinks, where NEIL3 can "unhook" the linkage between the exocyclic amine of adenine and the AP site.[24,25] These crosslinks are proposed to form at replication forks suggesting that NEIL3 also has a role in replication associated BER.

Similar to NEIL1, NEIL3 expression is increased during S phase. The ERK-MAP kinase pathway induces expression with NEIL3 expression peaking in G2 phase and found to localize at telomeres. NEIL3 is recruited to the telomere by TRF1, which enhances the enzymatic activity of NEIL3.[96] At telomeres, NEIL3 interacts with APE1, PCNA, and FEN1 for targeted repair of oxidative DNA damage.[96] Additionally, NEIL3 has been proposed to possibly assist in pre-replicative repair due to its ability to excise from single stranded DNA and interaction with RPA, and this is further supported by the ability of NEIL3 to unhook inter-strand crosslinks at replication forks.[24,25] Like NEIL1 and NEIL2, NEIL3 has many disease phenotypes including implications with lipid metabolism and preventing atherosclerosis,[97] and loss of NEIL3 is associated with cognitive deficiencies,[98] and atherogenesis.[99] The connections between NEIL3 deficit and disease are still being explored.

Interplay between BER, regulation, and signaling

Emerging data has shown that both DNA modifications traditionally considered to be damage and DNA glycosylases can participate in roles beyond base excision and maintaining genomic integrity. Many BER glycosylases participate in these additional mechanisms and have related activity or association with a NEIL glycosylase. The TDG DNA glycosylase has been implicated to play roles in epigenetic gene regulation as TDG can excise the oxidized products of 5-mC.[100,101] Oxidation of 5-mC by Ten-Eleven-Translocation (TET) family of proteins produces 5-hydroxymethylcytosine (5-hmC), 5-fC and 5-caC as intermediates in demethylation and as gene

regulation elements.[57] TDG is capable of removing 5-fC and 5-caC,[100,101] and NEIL1 has been shown to stimulate TDG turnover.[58,59] NEIL1 was identified in pull-down assays from cells using DNA containing 5-hmC, 5-fC, and 5-caC.[57] The removal of 5-fC and 5-caC by TDG suggests a role for the glycosylase as a "reader" of epigenetic base modifications with support from NEIL1.

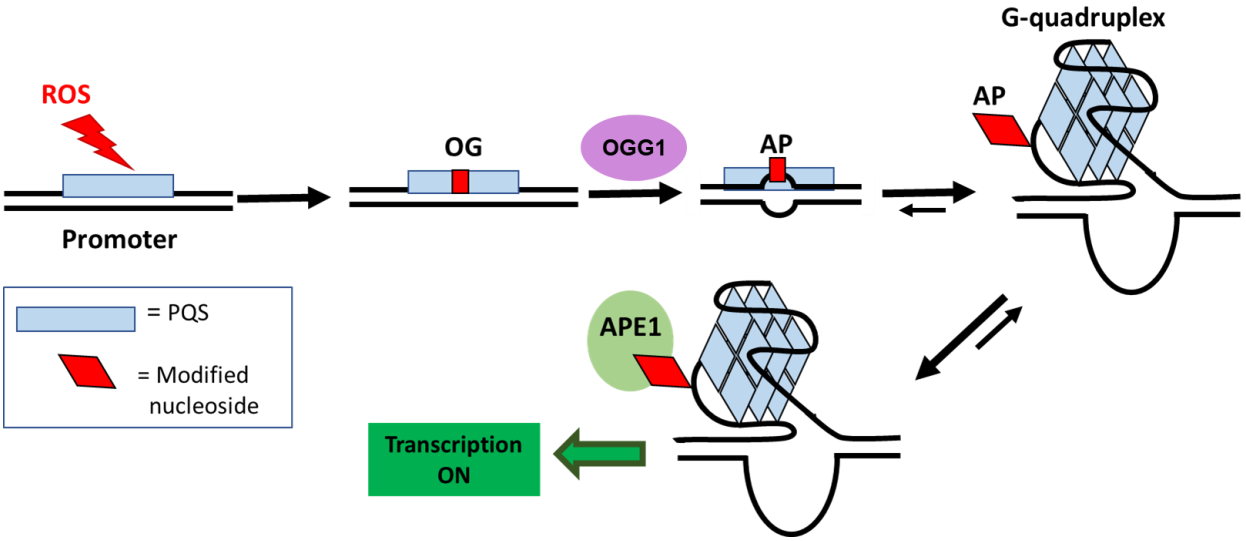

Figure 1.5: Initiation of gene transcription by DNA damage in potential quadruplex forming sequence (PQS).

Removal of OG by OGG1 leaves an AP site encouraging the formation G-quadruplex (G4). Subsequent binding by APE1 can recruit transcription factors to initiate transcription. Figure adapted from Fleming *et al.* 2017.

Recent work by the Burrows laboratory has proposed that the OG modification is not simply a mutagenic form of DNA damage but also epigenetic when forming in a potential quadruplex forming sequence (PQS) (Figure 1.5).[102] Many gene promoters contain sequences that have the potential to form G4s.[103] G4s have been found to form in cells and are of interest as a therapeutic target in modulating regulation. These G-rich sequences are highly susceptible to oxidation resulting in the formation OG in a PQS. Removal of OG by OGG1 produces an AP site and promotes G4 formation. APE1 is then recruited to the G4, and binding of APE1 to G4 produces an increase in gene expression levels.[102] Here, the initiation of base excision repair alters gene

expression. NEIL1 and NEIL3 are capable of excising Gh and Sp from G4 and may also interact with this process.[85] Additionally, the *NEIL1* and *NEIL3* genes contain G4 forming sequences in their promoters, and the formation of oxidative damage in the *NEIL3* promoter can increase NEIL3 expression suggesting a dynamic relationship between the formation of damage and glycosylases responsible for repair.[104]

Finally, the existence of two isoforms of NEIL1 due to RNA editing suggests a regulatory role on repair. As discussed previously, this editing event alters the substrate specificity of NEIL1 glycosylase. Conditions of inflammation can lead to increased oxidative stress and expression of NEIL1, but also inflammation can increase ADAR1 expression suggesting important regulatory feature between RNA editing and DNA repair.[49,64]

Thesis outline

The research in this dissertation aims to probe the influence of DNA base modification and substrate context on recognition and excision by the NEIL family of glycosylases. In chapter 2, I focus on the altered substrate specificities of NEIL1 due to RNA editing of NEIL1 transcript. Previous work has established the single amino acid difference changes NEIL1 activity on the oxidized pyrimidine, Tg. Here, I expand the substrate scope to explore substrates never evaluated with the unedited isoforms. Biochemical analysis paired with calculations in the gas phase elucidated properties of the lesion that influence removal by both forms of NEIL1.

In chapter 3, I evaluate the ability of NEIL1 and mNeil3 to remove Gh from G4 structures from the *VEGF*, *RAD17,*and *KRAS* promoter regions. Damage was introduced at various positions within the sequence to examine the impact of lesion position on the sequences. Additionally, I probed if the addition of the 5-track assisted in lesion removal by NEIL1 and mNeil3. These studies

show that the greatest variable influencing Gh removal from G4 was G4 sequence. The sequence of the quadruplex can influence G4 stability and topology influencing the excision by NEIL1.

Finally, in chapter 4, I discuss preliminary efforts to probe the repair of NEIL substrates in various human cell lines. A reporter plasmid was designed for the incorporation of transcriptionally blocking lesions to study NEIL1 mediated repair in cells. This reporter was first validated in MEFs, and then used in human cell lines to monitor repair of various lesions showing that the human cancer cell lines, HeLa and U87, demonstrated diminished repair of the substrates.

Chapter 2 RNA editing alters lesion specific activity of the DNA glycosylase NEIL1

Contributions of others: Dr. Jongchan Yeo performed the glycosylase assays for 5-OHU, 5-hmU, and DHT and determined the binding affinity of Tg and 5-OHU. Dr. Brittany Anderson-Steele evaluated the activity of NEIL1 the epigenetic modification 5-mC, 5-hmCm 5-fC, and 5-caC and determined the binding affinity of Ug by both isoforms of NEIL1. Dr. JohnPatrick Rogers completed the synthesis and characterization the Ug phosphoramidite and oligonucleotide. 5-hmC, 5-fC, and 5-caC containing oligonucleotides were provided by Dr. Chuan He from the University of Chicago. Dr. Amelia Manlove conducted the synthesis and characterization the OI phosphonamidite and oligonucleotide. Savannah Conlon ran the qualitative gel in Figure 2.3. Dr. Allison Krajeski and Lanxin Zhang of the Jeehiun Lee laboratory performed the calculation on base acidity and proton affinity.

The work presented in this chapter was published as cited below and reprinted with permission of the authors and the journals:

"NEIL1 Recoding Due to RNA Editing Impacts Lesion-Specific Recognition and Excision," Lotsof, E. R.; Krajewski, A. E.; Anderson-Steele, B.; Rogers, J.; Zhang, L.; Yeo, J.; Conlon, S. G.; Manlove, A. H.; Lee, J. K.; David, S. S., J. Am. Chem. Soc. 2022, 144 (32), 14578–1458.

"RNA Editing of the Human DNA Glycosylase NEIL1 Alters Its Removal of 5-Hydroxyuracil Lesions in DNA." Yeo, J.; Lotsof, E. R.; Anderson-Steele, B. M.; David, S. S., Biochemistry 2021, 60 (19), 1485–149.

Introduction

NEIL1 is unique from all other DNA glycosylases as two isoforms exist due to RNA editing. The adenosine deaminase ADAR1 is responsible for the deamination of adenosine (A) to inosine (I) at position 725 in the NEIL1 pre-mRNA.[62–64] During translation, inosine codes for a guanosine (G), and the edited mRNA (AIA) codes for an arginine (R) at position 242 in NEIL1 rather than the lysine (K) in the unedited mRNA (AAA) (Figure 2.1A). Until the identification of the unedited isoform of NEIL1 by the David and Beal laboratories, the only isoform known and studied had an arginine at position 242.[64]

This editing event, producing a single amino acid change from Lys242 (unedited, UE) to Arg242 (edited, Ed), has resulted in dramatic changes in base excision activity between various lesions. For thymine glycol (Tg), UE NEIL1 removes the lesion in duplex DNA ~30-40 fold faster than the Ed NEIL1 isoform.[64] While the oxidized purine lesion, guanidinohydantoin (Gh), the rate of excision by the edited isoform is ~3 fold greater.[64] Despite the difference in the observed rates, the two isoforms exhibited similar affinity in electrophoretic mobility shift assays (EMSA) to duplex DNA containing non-cleavable synthetic analogs, 2'-fluorothymidine glycol (2'-F-Tg) and 2'-fluoro-guanidinohydantoin (2'-F-Gh).[67,68] The binding affinity results suggested that the difference in lesion processing is related to a kinetic step. However, the biological implications of NEIL1 recoding are not fully understood. Multiple myeloma cells overexpressing Ed NEIL1 proliferated at significantly higher rates and presented hallmark signatures associated with unrepaired double-strand breaks.[71]

Based on the alignments of the bacterial homolog Fpg, residue 242 was proposed to be within the lesion recognition loop of NEIL1 and a critical residue for lesion excision.[105] X-crystal structures of Ed and UE NEIL1 bound to Tg containing oligonucleotide confirmed that residue

242 makes contact with the oxidized base for lesion removal.[69] The structure paired with QM/MM calculations proposed a ribose protonated pathway with Lys/Arg242 serving as the proton donor for N3 of Tg in this excision mechanism.[69] The difference in pK_a of Lys versus Arg is suggested to be responsible for the ~30-40 fold difference in the rate of excision of Tg by the two isoforms.[71]

The DNA glycosylase NEIL1 is responsible for the excision for a wide range of DNA modifications to purine and pyrimidine bases. Known substrates include the hydantoin lesions, guanidinohydantoin and spiroiminodihydantoin (Sp), thymine glycol (Tg), 5-hydroxycytosine (5-OHC), 5-hydroxyuracil (5-OHU), dihydrothymine (DHT), and the formamidopyridines (FapyG and FapyA) (Figure 2.1B).[52,54,55,106–108]

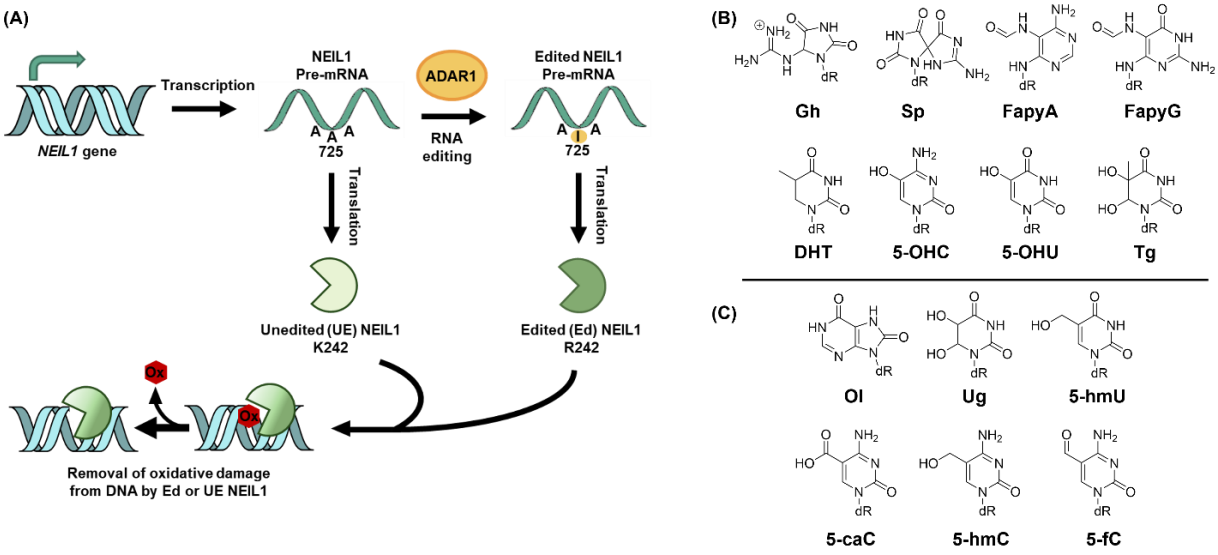

Figure 2.1: RNA editing produces two forms of NEIL1 that excise a wide range of base lesions

(A) *NEIL1* gene encodes for a lysine at position 242 in the enzyme's lesions recognition loop. NEIL1 pre-mRNA is a substrate for ADAR1, which deaminates adenosine 725 to inosine in the pre-mRNA, and this editing event results the encoding of an arginine at position 242 of the NEIL1 enzyme. Both Lys242 and Arg242 containing NEIL1 are active and remove oxidative damage from DNA. **(**B) Known substrates for edited NEIL1: Gh, guanidinohydantoin; Sp, spiroiminodihydantoin; FapyA, 4,6-diamino-5-formamidopyrimidine; FapyG, 2,6-diamino-4-hydroxy-5-formamidopyrimidine; DHT, dihydrothymine; 5-OHC, 5-hydroxycytosine; 5-OHU, 5-hydroxyuracil; Tg, thymine glycol. (C) Additional lesions tested as potential substrates for edited and unedited NEIL1 in this work**:** OI, 8-oxoinosine; Ug, uracil glycol; 5-hmU, 5-hydroxymethyluracil; 5-caC, 5-carboxycytosine; 5-hmC, 5-hydroxymethylcytosine; 5-fC, 5-formylcytosine. Figure published in Lotsof *et al.* 2022.

To probe the role on RNA editing on NEIL1 response to a variety of DNA modifications, we examined the glycosylase activity of both isoforms of NEIL1 on substrates previously examined with only Ed NEIL1 and new potential substrates (Figure 2.1 B and 2.1C). The pyrimidine lesions, 5-OHC, 5-OHU, DHT and the epigenetic lesions, 5-formylcytosine (5-fC), 5-hydroxymethylcytosine (5-hmC), and 5-carboxycytosine (5-caC), which have been previously evaluated with the edited isoform, were also examined with the unedited isoform. We also examined uracil glycol (Ug) as a potential substrate. Ug is structurally similar to Tg and a common oxidation product from the oxidation and deamination of cytosine (C) leading to C→T transversion mutations.[13,109,110] We also evaluated removal of a modified version of 8-oxo-7,8-dihydroguanine (OG), lacking the 2-amino group (8-oxoinosine, OI) by NEIL1 to illuminate the impact of structural modifications on isoform-specific excision. OG is not considered a substrate for NEIL1 as its large planar structure does not fit into the shallow binding pocket.[105]

Results and Discussion

Evaluation of substrates for both isoforms of NEIL1

The glycosylase activity of the NEIL1 isoforms was analyzed with DNA duplexes containing a variety of modified bases (Figure 2.1) to reveal potential differences in activity as a result RNA editing and the resulting amino acid change. As mentioned previously, the analyses of lesion removal were only completed by the edited isoform until the discovery of the unedited isoform by the David and Beal laboratories.[46,50,64] We explored additional modifications with both isoforms of NEIL1 to see if similar patterns arose between the two isoforms as we have previously observed with Tg and Gh. The pyrimidine modifications, U, 5-OHU, 5-hmU, 5-OHC, 5-hmC, 5-fC, 5-caC, and DHT, and purine modifications, I, OI, and OG, were examined in this study.

The glycosylase activity of UE and Ed NEIL1 on lesion containing duplexes in the most likely biological context were initially surveyed by incubating with enzymes in excess for 60 minutes. In this assay, several modifications that were potential substrates and previously considered a substrate were not removed (Figure 2.2). U and I were not substrates and OG, 5-fC, 5-caC and 5-hmC were removed at *extremely* low levels by both isoforms (<10%) (Figure 2.2 and Figure 2.3A). The lesions 5-hmU, 5-OHC, OI, DHT and 5-OHU were found to be excised to differing extents by the NEIL1 isoforms (Figure 2.3B). Identity of the opposite base influenced excision of several lesions. Minimal excision of 5-hmU was observed when paired with G (<10%), however, in a duplex positioned across from C, 5-hmU was removed to a significant extent by UE NEIL1 (Figure 2.3B). Similarly, 5-OHC was removed to a small extent by both NEIL1 isoforms (<10%) in a duplex context opposite G but was found to be completely removed when paired with C. Both isoforms removed OI opposite C to similar extents under these conditions. In studies with 5-OHU, and both isoforms of NEIL1, the greatest excision was seen with lesions paired with C and reduced excision with those paired with A.[49] DHT:A, 5-OHU:C, 5-OHC:C substrates were processed almost completely by Ed and UE NEIL1 in the 60-minute incubation period (Figure 2.3). Based on these observed results, full time-course, single-turnover analyses were performed to reveal potential isoform and lesion-specific activity differences (Table 2.1).

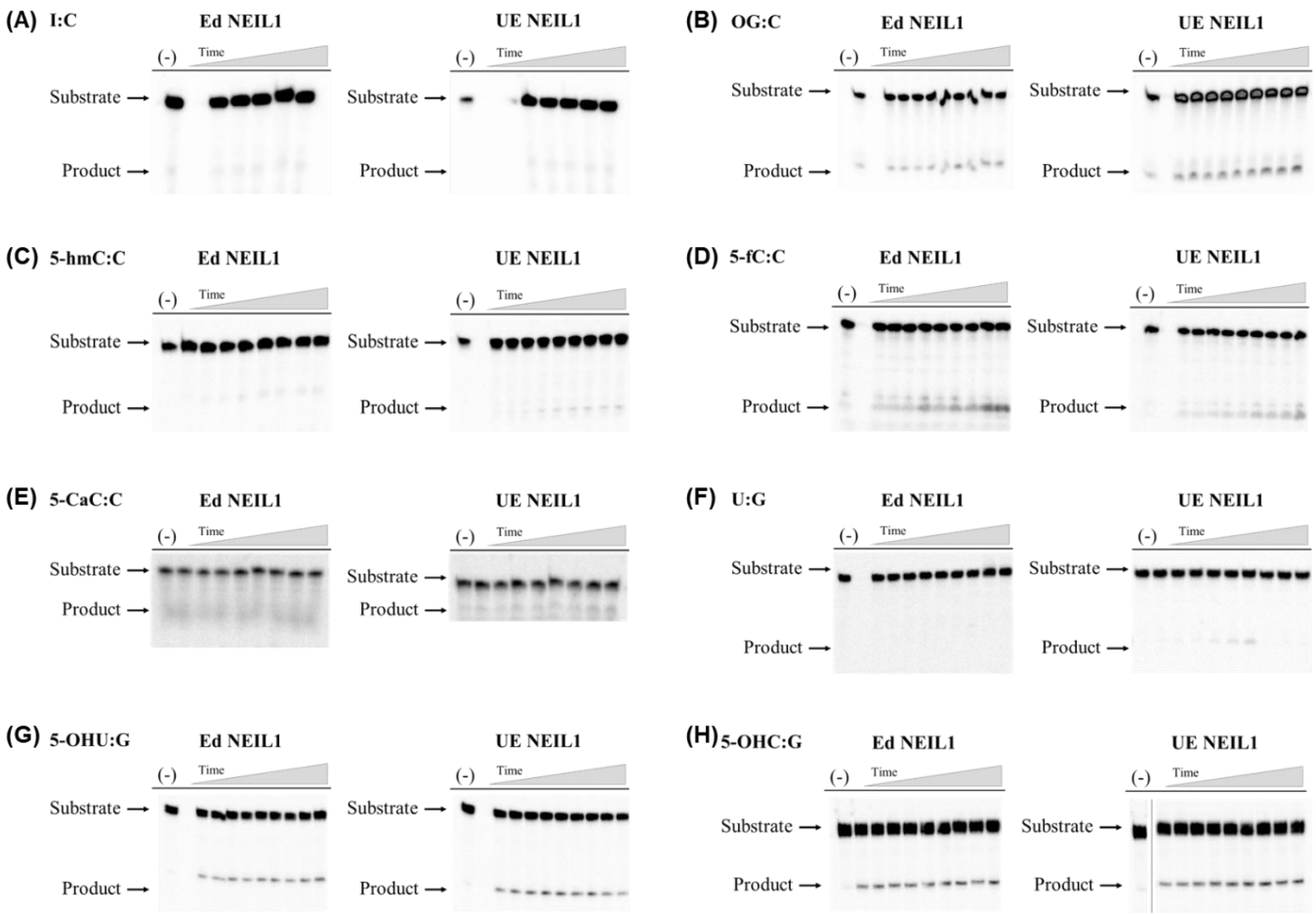

Figure 2.2: Representative storage phosphor autoradiograms of various lesions and epigenetic modifications excised by Edited (Ed, R242) and Unedited (UE, K242) NEIL1 from duplex DNA.

(A) Inosine (I), (B) 8-oxo-7,8-dihydroguanine (OG), (C) 5-hydroxylmethylcytosine (5-hmC) (D) 5-formylcytosine (5-fC) (E) 5-carboxycytosine (5-caC), (F) Uracil (U), (G) 5-hydroxyuracil (5-OHU), and (H) 5-hydroxycytosine (5-OHC). [γ-^{32}P]ATP-labeled duplex DNA containing a central lesion was incubated with enzyme under single turnover conditions (200 nM enzyme, 20 nM DNA) at 37 °C with 150 mM NaCl. Reactions were quenched at time points between 20 sec and 60 min. Figure published in Lotsof *et al.* 2022.

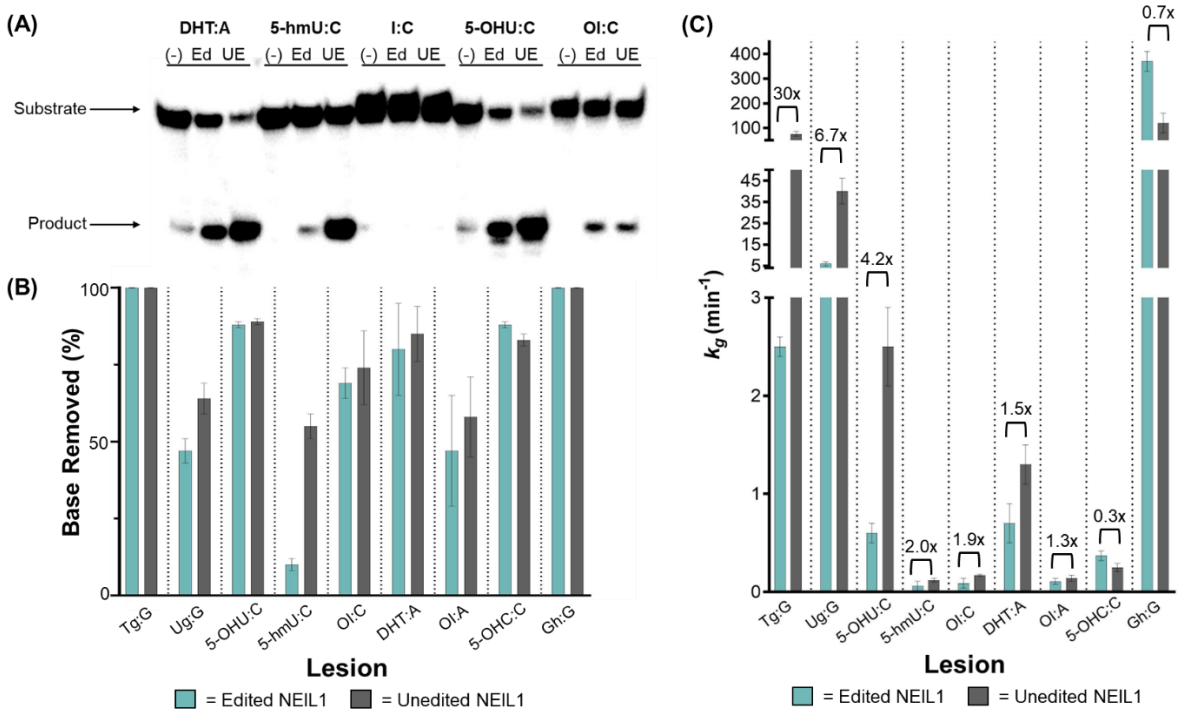

Figure 2.3: Lesion specific removal by edited (Ed) and unedited (UE) NEIL1.

(A) Representative storage phosphor autoradiogram of extent of glycosylase activity of Ed and UE NEIL1 (200 nM) with DHT:A, 5-hmU:C, I:C, 5-OHU:C, OI:C-containing 30-bp duplexes (1•2, 20 nM) at 60 minutes at 37 °C. (B) Overall extent of base removed (%) by NEIL1 isoforms with various lesions (values listed in Table 2.1). The lesion containing DNA duplex substrate (20 nM) was incubated with excess Ed or UE NEIL1 (200 nM) at 37 °C in pH 7.6 buffer containing 150 mM NaCl. The maximal base removed (%) was calculated by dividing the concentration of product produced after a 1 hr reaction by the total concentration of the substrate quantified via gel densitometry and multiplying by 100. Error bars are the standard deviation for the end point across three trials. (C) Differences in lesion excision rates (k_g) measured under single-turnover conditions with Ed and UE NEIL1 (values listed in Table 2.1). Values above bar represent the ratio of UE/Ed NEIL1 excision for each lesion. Figure published in Lotsof *et al.* 2022.

Table 2.1: Comparison of lesion removal activity from duplex DNA by edited (Ed) and unedited (UE) NEIL1.

Lesion	Edited k_g, min^{-1} (%completion)[a,b]	Unedited k_g, min^{-1} (% completion)[a,b]	k_g UE/k_g Ed
Tg:G[d]	2.5 ± 0.1	76 ± 10	30
Ug:G	6 ± 1(47%)	40 ± 6 (64%)	6.7
5-OHU:C	0.6 ± 0.1 (80%)	2.5 ± 0.4 (83%)	4.2
5-hmU:C	0.06 ± 0.05 (<10%)[c]	0.12 ± 0.02 (55%)	2.0
OI:C	0.09± 0.01 (69%)	0.17 ± 0.05 (74%)	1.9
DHT:A	0.7 ± 0.2 (81%)	1.3 ± 0.2 (84%)	1.5
OI:T	0.11± 0.03 (47%)	0.14 ± 0.03 (58%)	1.3
5-OHC:C	0.37 ± 0.05 (89%)	0.25 ± 0.04 (88%)	0.7
Gh:G[d]	370 ± 40	120 ± 40	0.3

[a]Rate constants of base removal were measured under single-turnover conditions (20 nM substrate, 200 nM enzyme) at 37 °C (see methods for details of assay conditions). Data were fit to a single exponential equation, $[P]_t = A_0[1 - \exp(-k_g t)]$. A_0 is the associated amplitude of k_g. [b]The percent completion of reactions that did not go to 100% are reported in parenthesis. [c]The overall extent of product formation was very low such that the fitting is likely an overestimate of the rate constant. [d]These data were previously reported in reference 64. Values presented in Lotsof *et al.* 2022.

Scheme 2.1: Minimal kinetic scheme of NEIL glycosylase activity

$$\text{NEIL} + \text{DNA}_s \underset{}{\overset{K_D}{\rightleftharpoons}} \text{NEIL-DNA}_s \xrightarrow{k_g} \text{NEIL-DNA}_p \xrightarrow{k_r} \text{NEIL} + \text{DNA}_p$$

Enzyme specific differences in excision of the pyrimidine lesions

The screening of substrates for NEIL1 demonstrated isoform specific differences in the removal of pyrimidine lesions. Full time course glycosylase assays were performed under single turnover conditions ([NEIL1] > [DNA]) with pyrimidine substrates identified in qualitative assays to isolate the rate constant of glycosidic bond cleavage (k_g). DNA glycosylases, like NEIL1, have been shown to follow burst kinetics due to slow product release compared to the rate of glycosidic bond cleavage, $k_r << k_g$ (Scheme 2.1), and glycosylase assay can be used to measure rate of lesion removal under single turnover single turn over conditions.[52,64] For the pyrimidine lesions, these trends were similar to those that the David laboratory has shown previously with Tg.[64] Tg had a

striking 30-fold difference in favor of UE NEIL1.[64] Other pyrimidine lesions also demonstrated this preference with UE NEIL1. 5-OHU had a greater excision by the unedited isoform, yet these differences were not to the same extent and identity of the opposite base impacted the rate of excision and amount of base excision. 5-OHU had the greatest excision across from C followed by T and G and A had the lowest amount of overall removal (Figure 2.4). In the base pair with C, UE NEIL1 removed 5-OHU four-fold faster (k_g = 2.5 ± 0.3 min^{-1}) than Ed NEIL1 (k_g = 0.6 ± 0.1 min^{-1}) (Figure 2.3, Table 2.1). With the DHT:A substrate duplex, UE NEIL1 removed DHT approximately two-fold faster (k_g =1.3 ± 0.2 min^{-1}) than Ed NEIL1 (k_g = 0.7 ± 0.2 min^{-1}). In addition, DHT removal did not reach completion and the endpoints were similar for both isoforms. In the case of 5-hmU:C duplex, 5-hmU is removed to high levels by UE NEIL1, despite the fact that the observed rate constant (k_g) is significantly smaller than with the DHT, 5-OHU, and Tg substrates (Figure 2.3, Table 2.1).

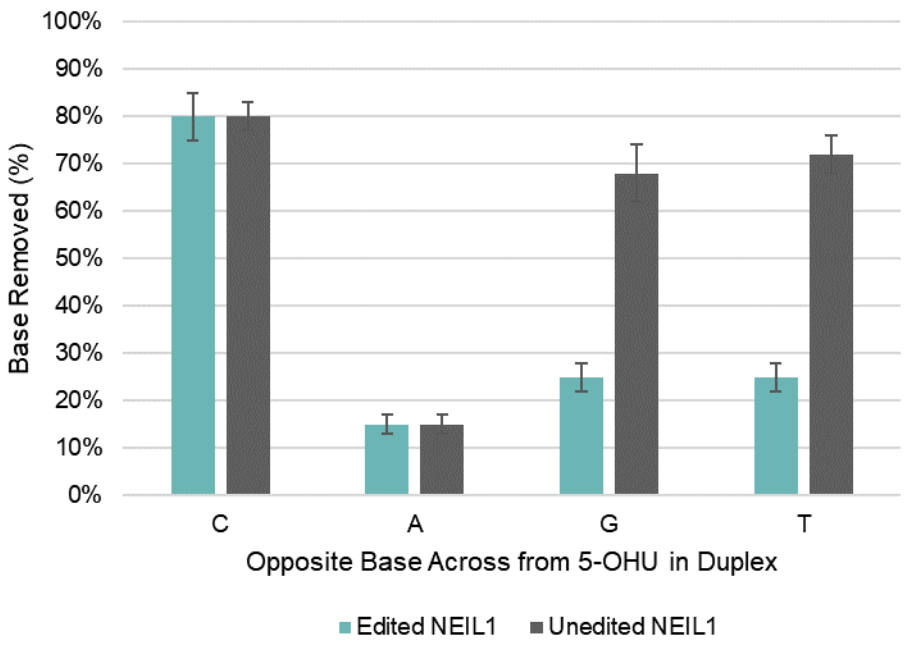

Figure 2.4: Opposite base dependence of 5-OHU removal by edited (Ed) and unedited (UE) NEIL1.

The 5-OHU-containing DNA duplex substrate (20 nM) was incubated with excess Ed or UE NEIL1 (200 nM) at 37 °C in pH 7.6 buffer containing 150 mM NaCl. The maximal percent of 5-OHU removal was calculated by dividing the concentration of product produced after a 1 h reaction by the total concentration of the substrate and multiplying by 100.

5-OHC deviates from our trend for the pyrimidine lesions and is more rapidly excised by Ed NEIL1 opposed to UE NEIL1. This further reinforces that the lesion structure and context impacts NEIL1 isoform activity differences. 5-OHC would be most naturally paired with G, yet minimal removal was observed by NEIL1 in the glycosylase assay (Figure 2.3). When paired with C in duplex DNA, removal of 5-OHC was faster by Ed NEIL1 (k_g = 0.37 ± 0.05 min^{-1}) over UE NEIL1 (k_g = 0.25 ± 0.04 min^{-1}) and reached completion. These results are surprising in light of the MS studies with γ-irradiated calf thymus DNA.[56] In this assay, removal of 5-OHC, and not 5-OHU, was detected with both isoforms of NEIL1, and higher efficiency of removal was seen with Ed NEIL1, which agrees the glycosylase assay results. Using high MW DNA may allow for increased removal of 5-OHC across from G due to the diversity of the lesion sequence context.[56] It is striking

the switch in isoform specificity with 5-OHC relative to the other pyrimidine lesions of U/T identity (i.e. 5-OHU and Tg) and suggest that features of the base may impact isoform specificity.

NEIL1 excises the analog of OG lacking the 2-amino-group.

OG is known be a poor substrate for Ed NEIL1, and our glycosylase assays have confirmed poor removal of OG by UE NEIL1. The lack of NEIL1-mediated removal of OG is likely due to shallow binding pocket that cannot accommodate OG and has increased solvent exposure and fewer hydrogen bond contacts.[105] We used OI to probe features that may influence activity of NEIL1. OI is not a naturally occurring base modification but has provided important structural insights for recognition of OG:A mispairs by the DNA glycosylase MutY.[111] OI was excised by both Ed and UE NEIL1, but UE NEIL1 removed OI more efficiently and to a greater extent compared to the edited isoform. The rate constant (k_g) was 1.5-1.9-fold greater for the UE NEIL1 isoform (Table 2.1). It is striking that OI is a substrate while I and OG are not substrates for NEIL1. NEIL1 maybe recognizing I as a natural base similar to that of G, so the addition of the oxygen on C8 is enough to differentiate it from the natural base. While the lack of the 2-amino group of OG, may allow for the OI lesion to be accommodated and to make the necessary contacts for excision.

Uracil Glycol is a novel substrate for NEIL1

In initial studies with the two isoforms of NEIL1, the Tg lesion exhibited the largest difference in removal by UE relative to Ed NEIL1 (Table 2.1). Ug is structurally similar to Tg, simply lacking the methyl group on C5, and may also be a substrate for NEIL1. Ug arises from the oxidation and deamination of cytosine,[13] and the bacterial homology of NEIL1, Fpg, can excise this damage from duplex DNA.[110] To test Ug as a potential substrate, Ug-containing oligonucleotides were prepared by Dr. JohnPatrick Rogers.[112] Ug removal was first examined under single-turnover conditions with Ed and UE NEIL1. When Ug is paired with G or C, the rates

were too fast to evaluate manually, and rapid quench flow methods were used. Clear isoform specific differences were revealed in the removal of Ug from Ug:G and Ug:C substrates. Again, when the lesion was paired with C, greater rates of excision can be seen with both isoforms NEIL1, but lower overall excision was seen across from G, which would be natural base across Ug. The data were fitted to a single-exponential equation to extract k_g, and compared to results with Tg (Figure 2.3, Table 2.1). For the Ug:G substrate, UE NEIL1 displays a 6-fold faster rate for Ug removal compared to Ed NEIL1. Despite structural similarities between Tg and Ug, UE NEIL1 showed a 30-fold faster rate for the removal of Tg from the corresponding Tg:G duplex than Ed NEIL1.[64] The smaller difference in relative processing between the two forms is a consequence of both an *increased* rate of removal of Ug relative to Tg by Ed NEIL1, and a *decreased* rate of removal of Ug relative to Tg by UE NEIL1. Remarkably, the lack of the single methyl-group in Ug results in more similar processing of this lesion by the two NEIL1 isoforms.

NEIL1 demonstrates biphasic excision of pyrimidine lesions

In our analysis of Ug, Tg, and 5-OHU removal, we found that production curves for all three lesions best to a two-exponential equation ($[P]_t = A_0(1 - \exp(-k_g't)) + B_0(1 - \exp(-k_g''t))$) consistent with two distinct excision processes (Figure 2.5). The kinetic parameters determined using two-exponential fitting provided a larger rate constant (k_g') and an associated amplitude, A, and a smaller rate constant (k_g") with an associated amplitude, B. Similar biphasic trends have been observed in the Wallace group analysis of mimivirus Nei, the viral homolog of NEIL1, with DNA duplex containing Tg.[113]

In examining the excision of Ug to Tg, both isoforms display lower level of percent base removal with Ug relative to Tg. Comparison of the Ug and Tg excision rate constants and associated amplitudes provide further insight into the influence of the lesion and NEIL1 isoform.

The rate constants (k_g' and k_g") for Tg and Ug lesion excision were similar for both isoforms of NEIL in all of the base-pairing contexts evaluated (Table 2.2). However, the associated amplitudes of the two rate constants differ significantly between the two isoforms of NEIL1. For UE NEIL1, the majority of Tg and Ug lesion excision is associated with the larger rate constant (k_g') (Figure 2.5, Table 2.2). In contrast with Ed NEIL1, most of the Ug or Tg excision (80-90%) was associated with the smaller rate constant (k_g"). 5-OHU had similar overall excision to Ug; however, the k_g" was smaller for 5-OHU compared to Ug and Tg for both isoforms (Figure 2.5, Table 2.2). The trends of associated amplitudes for 5-OHU also differed from results with Ug and Tg. For both isoforms, a greater proportion of excision is associated with the smaller rate constant (k_g").

We suggest that the two rate constants correspond to two distinct processes where the large rate constant k_g' is associated with lesion removal from the fraction of the lesion bound in a catalytically competent complex, while the smaller rate constant is due to the lesion being positioned in an alternative orientation that requires enzyme/DNA conformational changes for catalysis to take place. The reduced extent of reaction completion with Ug, and several other lesions, suggests a potential third population of lesion that is oriented in a manner that is even less efficiently removed. Recent crystal structures published by Yi and coworkers show a catalytically inactive, or "quarantine", state supporting our hypothesis.[70] Structures of NEIL1 bound to DHU show an active state where Lys242 is engaged for catalysis (Figure 2.6A) and catalytically inactive quarantine state from stacking of Tyr244 over the lesion (Figure 2.6B).[70] The quarantine conformation was only found with Ed NEIL1 and not UE NEIL1. Our observation of more efficient processing by UE NEIL1 suggests that the UE enzyme can better align the target nucleotide for hydrolysis of the glycosidic bond.

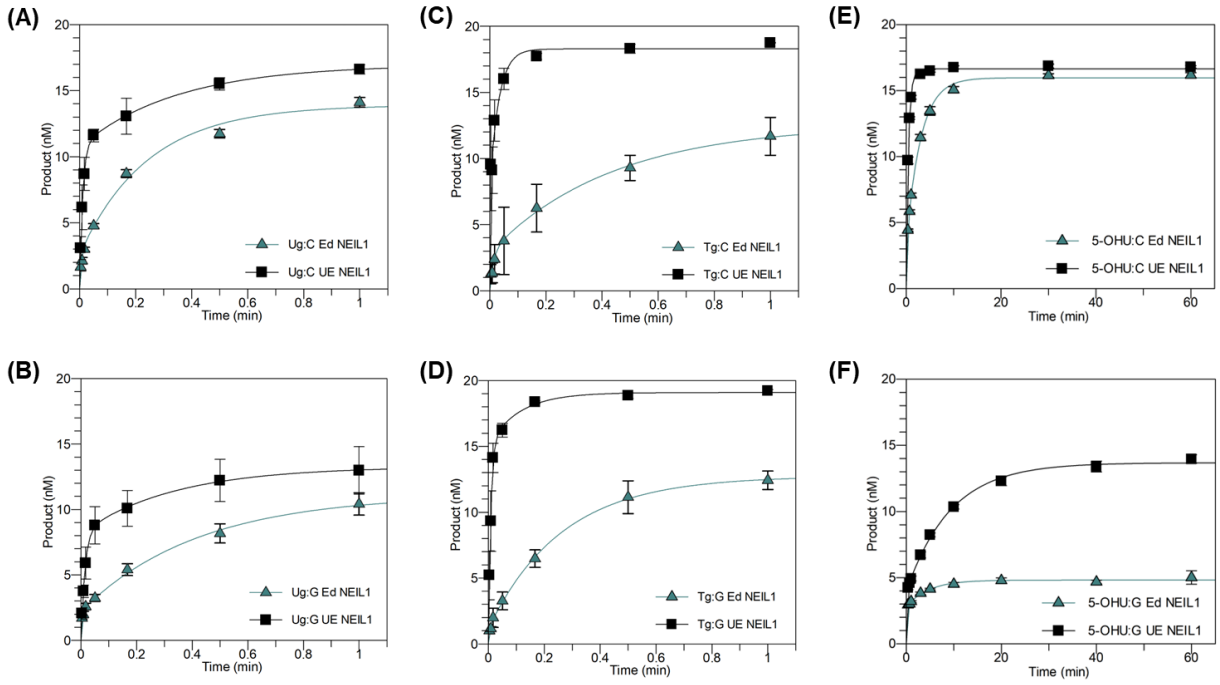

Figure 2.5: Lesion specific removal of uracil glycol, thymine glycol, and 5-hydroxyluracil demonstrate that small differences in lesion structure dramatically impact base excision by NEIL1 isoforms.

Removal and affinity of edited (Ed) and unedited (UE) NEIL1 to duplexes (1•2) containing Ug or Tg was evaluated using rapid quench flow methods with Ed (blue) and UE (black) NEIL1 (200nM) with a DNA duplex (20 nM) containing (A) Ug:C (B) Ug:G (C) Tg:C, and (D) Tg:G. 5-OHU was evaluated via manual methods at the same conditions (E) 5-OHU:C, and (F) 5-OHU:C at 37 °C with 150 mM NaCl Data were fit to a two-exponential equation ($[P]_t = A_0(1 - \exp(-k_g't)) + B_0(1 - \exp(-k_g''t))$).

Table 2.2: Kinetic parameters from two-exponential fitting of Ug, Tg, and 5-OHU removal from duplex DNA by Ed and UE NEIL1.

Duplex	Edited (Ed)				Unedited (UE)		
	Rate Constant (min^{-1})[a]		Amplitude (nM)[b]	Completion (%)[c]	Rate Constant (min^{-1})[a]	Amplitude (nM)[b]	Completion (%)[c]
Ug:C	k_g'	380 ± 200	2.2 ± 0.4	70 ± 6	120 ± 10	10.6 ± 1.0	85 ± 3
	k_g"	3.6 ± 1.0	11.5 ± 0.7		3.9 ± 1.5	6.1 ± 0.6	
Ug:G	k_g'	330 ± 85	2.2 ± 0.1	55 ± 5	68 ± 10	8.8 ± 1.1	73 ± 8
	k_g"	2.3 ± 0.2	9.0 ± 0.9		2.8 ± 1.0	5.8 ± 0.9	
Tg:C	k_g'	>500	1.2 ± 0.6	58 ± 3	161 ± 60	12.0 ± 2.1	93 ± 5
	k_g"	2.9 ± 0.3	11.2 ± 1.2		10 ± 2	5.7 ± 1.0	
Tg:G	k_g'	>500	1.3 ± 0.4	62 ± 5	126 ± 30	15.5 ± 1.1	95 ± 4
	k_g"	3.6 ± 0.1	11.6 ± 0.2		7.4 ± 2	3.6 ± 1.1	
5-OHU:C	k_g'	>2	3.3 ± 0.4	80 ± 5	>2	4.2 ± 0.2	83 ± 3
	k_g"	0.33 ± 0.1	13 ± 1		1.8 ± 0.2	12 ± 0.2	
5-OHU:G	k_g'	>2	2.8 ± 0.4	24 ± 3	>2	4.0 ± 0.4	68 ± 6
	k_g"	0.22 ± 0.1	2.0 ± 0.2		0.11 ± 0.04	9.7 ± 0.3	

[a]Data for Ug and Tg removal by Ed and UE NEIL1 fit to a two-exponential equation $[P]_t = A_0(1 - \exp(-k_g't)) + B_0(1 - \exp(-k_g''t))$. 20nM of substrate was incubated with 200nM enzyme at 37 °C using a Kintek RQF-3 Rapid-Quench for Ug and Tg. 5-OHU was evaluated using manual methods. [b]Amplitude (nM) of A_0 and B_0 relates to the associated amplitude and amount of substrate processed with k_g' and k_g" respectively. [c]The overall extent of reaction completion (%) = [(A_0 + B_0)/20 X 100]. Values presented in Lotsof *et al*. 2022 and Yeo *et al*. 2021.

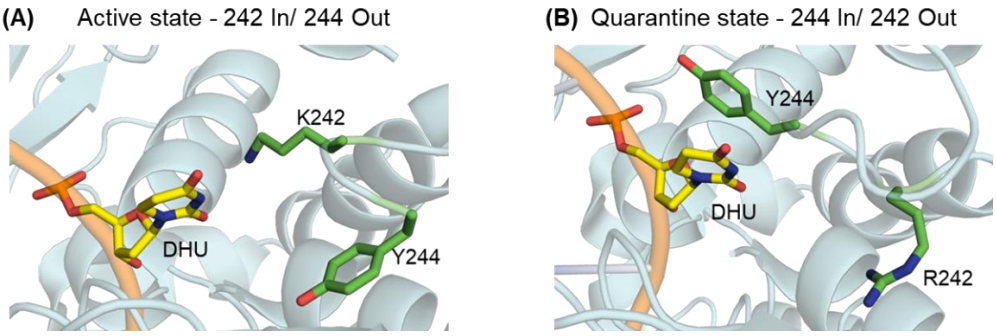

Figure 2.6: Alternative conformations of residues 242 and 244 of NEIL1 isoforms with dihydrouracil (DHU).

(A) X-ray structures of UE (K242, PDB ID: 6LWJ) NEIL1 show residue 242 engaged with DHU lesion in an active conformation. (B) X-ray structures of Ed (R242, PDB ID: 6LWK) NEIL1 show residue 242 away from with DHU lesion and Tyr 242 in a proposed quarantine state. Figure adapted from Lotsof *et al.* 2022.

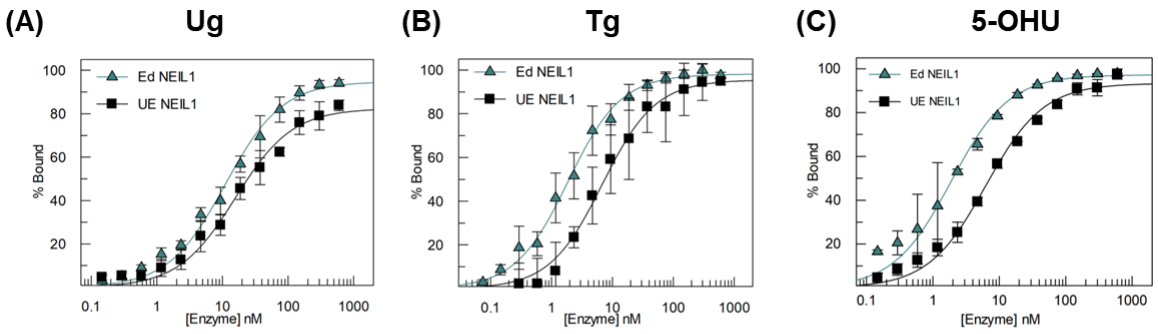

(D)

Lesion	Edited (nM)	Unedited (nM)
Ug:G	11 ± 1	16 ± 3
Tg:G	1.7 ± 0.5	6.5 ± 2.2
5-OHU:G	1.8 ± 0.6	6.3 ± 0.2

Figure 2.7: Edited (Ed) NEIL1 binds to Ug, Tg, and 5-OHU containing DNA similarly and slightly tighter than the unedited (UE) isoform.

Plot of percent bound enzyme, either Δ56 K54L Ed NEIL1 or Δ56 K54L UE NEIL1, versus total enzyme concentrations ([Etotal] = ~[Efree]) for 30-nt duplexes (1•2) containing (A) Ug:G, (B) Tg:G, or (C) 5-OHU:G measured by electrophoretic mobility shift assays (EMSA). D) Reports the values from EMSA and shown in plots (A), (B), and (C). Data were obtained at 25 °C and 150 mM NaCl with 10 pM substrate and enzyme concentrations ranging from 1000 to 0.2 nM. Data were fit to the equation: $C[E]^n/((K_d)^n + [E]^n)$, Hill coefficient = 1. Figure adapted from Lotsof *et al.* 2022.

NEIL1 isoforms differentially recognize uracil glycol and 5-hydroxyuracil in duplex DNA

Electrophoretic mobility shifts assays (EMSA) were used to measure relative dissociation constants (K_d) for the two NEIL1 isoforms to Ug, Tg, and 5-OHU containing duplex DNA (Figure 2.7). EMSA was performed with K54L variant and truncated form of NEIL1 (Δ56 K54L Ed NEIL1 and Δ56 K54L UE NEIL1).[42,46,49] Mutation of Lys54 to Leu inactivates the NEIL1 glycosylase activity while still allowing lesion-duplex affinity.[42] Truncation of 56 residues from the disordered C terminal domain of NEIL1 improves the quality of the EMSA and ability to resolve and quantify bands,[49,68] and previous work has shown that this truncation does not significantly impact the activity of the enzyme.[46] Both Ed and UE Δ56 K54L NEIL1 tightly bind to Ug, with Ed NEIL1 binding slightly tighter (11 ± 1 nM) than the unedited isoform (16 ± 3 nM). The binding affinity of Tg:G is higher relative to Ug:G, but in a similar fashion the Ed isoform (1.7± 0.5 nM) binds more tightly compared to UE NEIL1 (6.5 ± 2.2 nM) for Tg:G. The values and trends for Tg:G are similar to that of 5-OHU:G where Ed Δ56 K54L NEIL1 exhibits ~4-fold greater affinity (1.8 ± 0.6 nM) than the unedited enzyme (6.3 ± 0.2 nM) to a 5-OHU:G duplex (Figure 2.7C). Remarkably, affinity is *inversely* correlated with substrate processing, where despite being more efficient at lesion removal, the UE NEIL1 isoform binds more weakly to Ug, Tg, and 5-OHU than Ed NEIL1 (Figure 2.7). This trend suggests that the differences in excision due to the catalytic steps rather than earlier steps related to lesion recognition.

UE NEIL1 preferentially removes pyrimidine lesions

UE NEIL1 excises pyrimidine lesions to a faster and greater extent than Ed NEIL1. For UE NEIL1, the following trend was observed in the rates: Gh > Tg > Ug > 5-OHU > DHT > 5-OHC > OI ≈ 5-hmU, and a similar trend was seen with Ed NEIL1: Gh >> Ug > Tg > DHT ≈ 5-OHU > 5-OHC > OI ≈ 5-hmU. When we examine the ratio the rate constants of the unedited

isoform to the edited, we observe the following trend Tg > Ug > 5-OHU > 5-hmU ≈ OI:C ≥ DHT ≈ OI:T > 5-OHC > Gh. As previously published, Tg has the greatest differences in the rate constants between the two isoforms, and 5-OHC and Gh are more rapidly excised by the edited isoform.

From the structural studies of NEIL1 bound to Tg containing duplex and QM/MM calculations, the Yi group proposed that Lys/Arg242 of UE/Ed NEIL1 makes a hydrogen bond with N3 of the Tg lactim tautomer.[69] Residue 242 serves as a proton donor in their mechanism of base excision, and thus the relative differences in the pK_a between UE (K242, pK_a ~ 10.5) and Ed (R242, pK_a ~ 12. 5) allow for UE NEIL1 to be better proton donor and faster in the excision of Tg (Figure 2.8). However, the mechanism and pK_a differences do not fully explain the differences observed in our biochemical trends with other pyrimidine lesions. Even with Ug, a modification very similar to Tg, the difference in the rate constants is only ~6 fold difference, and this difference between UE and Ed NEIL1 excision only decreases through the series. Residue 242 plays a critical role in the observed differences in excision, but other properties of the modified pyrimidine likely influencing this difference further.

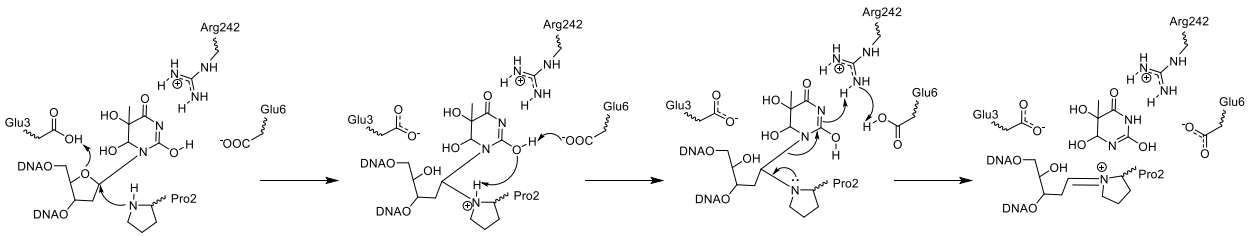

Figure 2.8: Proposed reaction mechanism for Ed and UE NEIL1.

Zhu *et al.* (2016) used X-ray crystal structures and QM/MM calculations to propose this ribose protonated reaction mechanism for the removal of Tg. Of note, Arg242 or Lys242 engages with the tautomer of Tg, and residue is responsible for the protonation of Tg at N3 as a critical step in base excision.[69]

Gas-phase calculations provide insights on features of the base that influence excision.

We conducted gas-phase calculations on the pyrimidine lesions, Tg, Ug, 5-OHU, 5-hmU, DHT, 5-OHC, and purine lesions, OI and Gh, using B3LYP/6-31+G(d) to uncover features of the base and the mechanism that influence Ed and UE NEIL1 activity. Prior work has established that gas-phase calculations can well correlate to the activity of glycosylase.[114–119] Assuming that DNA glycosylases provide a hydrophobic environment for base excision for the breaking of the N1-C1' bond, the trends for the gas phase acidities have been shown to track with the trends in rate of excision.[114,116,117,119] Tautomerization of modified base is important for the excision mechanism of pyrimidine lesion by NEIL1 and is considered in our analysis. Tg, Ug, 5-OHU, 5-hmU, and DHT can all adopt lactim and lactam structures, while 5-OHC is different from other lesions as it does not have a carbonyl at C4. In the gas phase, the most stable tautomer is the lactam, over the lactim, for Tg, Ug, 5-OHU, 5-hmU, and DHT (Figure 2.9, Table 2.3). In terms of the relative stabilities among the lactim tautomers, for Tg, Ug, and 5-OHU, the 2-hydroxy lactim (2-OH lactim) is preferred energetically. For 5-hmU and DHT, the 4-hydroxy lactim (4-OH lactim) is more stable (Figure 2.9, Table 2.3). The calculations for Tg agree with those previously reported, where Tg 2-OH lactim had a lower relative energy than the Tg 4-OH lactim tautomer.[69]

Table 2.3: Relative enthalpy of lactam and lactim tautomers for NEIL1 substrates.

Substrate	Lactam	2-OH Lactim[a]	4-OH Lactim[b]
Tg	0.0	17.8/26.8	21.9/22.7
Ug	0.0	17.8/26.8	22.0/23.2
5-OHU	0.0	16.0/26.1	17.0/23.7
5-hmU	0.0	19.0/29.4	14.9/19.5
DHT	0.0	20.2/29.8	19.7/27.6

All values are ΔH (kcal/mol) at 298 K, calculated using B3LYP/6-31+G(d); [a] The first value is for the rotamer where the 2-OH proton is oriented toward the N3; the second value is for the proton oriented toward the N1; [b] The first value is for the 4-OH proton oriented toward the N3; the second value is for the proton oriented toward the C5. Values presented in Lotsof *et al*. 2022.

The N1-H acidity (ΔH_{acid}, kcal/mol) of the neutral more stable lactam substrates were evaluated to examine if there is a correlation with experimental trends of k_g (UE/Ed) and the lability of the N1-C1' bond to ascertain the correlation with the experimental trends for enzyme excision (Figure 2.6). We find that the calculated N1-H acidity trend for the lactam structures is 5-hmU (325.9 kcal/mol) > 5-OHU (330.4 kcal/mol) > Ug (341.4 kcal/mol) > Tg (342.0 kcal/mol) > DHT (347.7), which does not track with the trends observed in our experimental results (Table 2.1), either in magnitude of excision rate constants k_g or the UE:Ed NEIL1 excision rate ratio. This lack of alignment between these values underscores the proposed importance of the lactim tautomer, which would engage more favorably with Lys 242 in UE and Arg 242 in the Ed NEIL1.[69]

Considering the importance of the lactim structure in the excision mechanism, the N1-H acidities were calculated with the 2-OH and 4-OH lactims. For both the 2-OH lactims or 4-OH lactims, the N1-H acidity trends did not track with either k_g or the UE:Ed NEIL1 excision ratio (Table 2.1). For example, comparison of the 2-OH lactim tautomers for the N1-H acidity of Tg versus 5-OHU shows that 5-OHU (acidity of 314.5 kcal/mol) is much more acidic than Tg (acidity of 323.4 kcal/mol), but Tg has a faster excision rate constant k_g and higher UE:Ed NEIL1 excision rate ratio. Thus, the N1-H acidities of the lactims seem to show no correlation to experimental data.

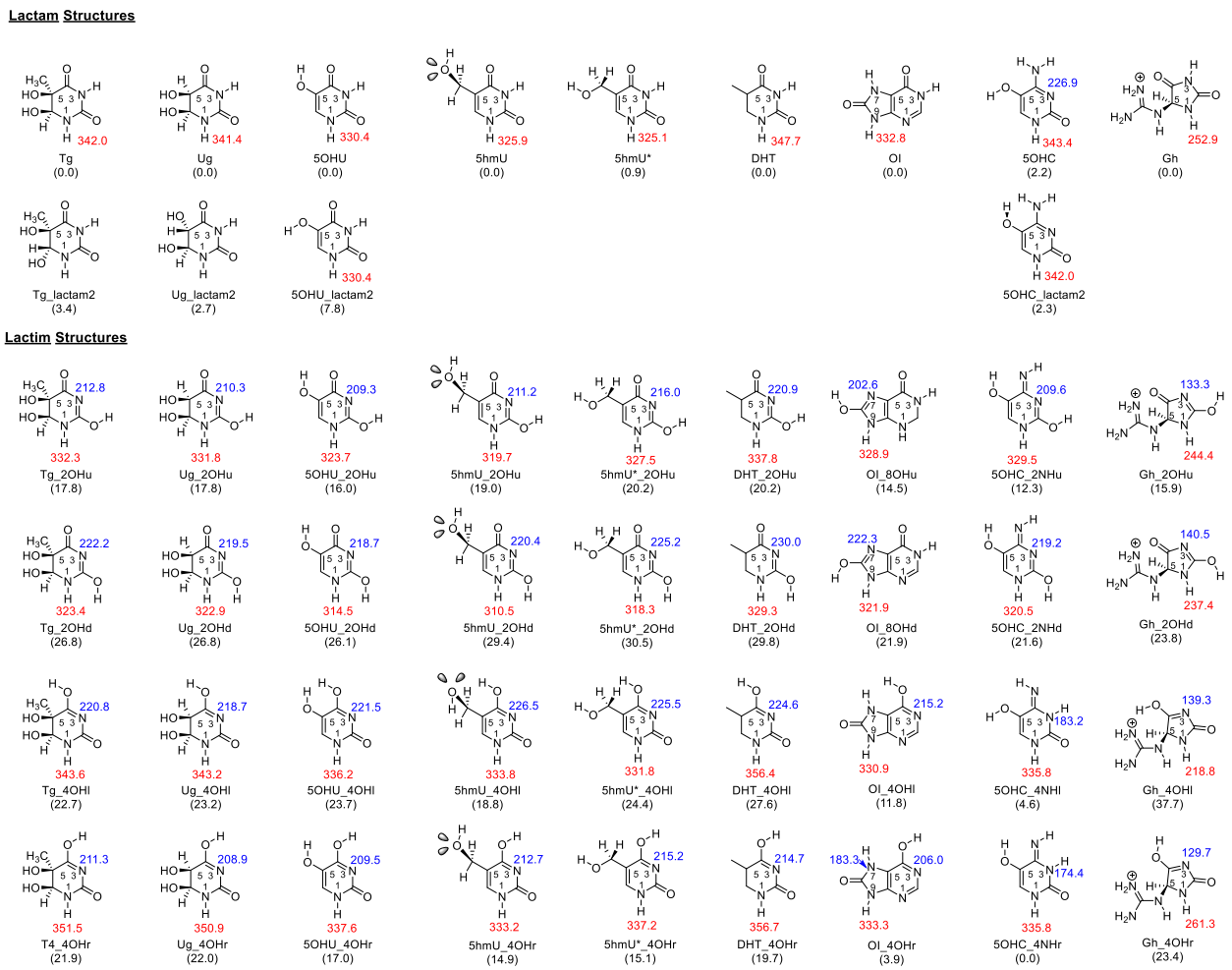

Figure 2.9: Lactam and lactim tautomers for NEIL1 substrates with associated calculated values.

Relative enthalpies of lactam and lactim structures (black), N1-H acidity in ΔH_{acid} (red), and N3 proton affinity (PA) values (blue), Relative stability for each tautomer is indicated in parenthesis. All values are ΔH at 298K, in kcal/mol. U=up, d=down, l=left, and r=right denote the position of the hydrogen in the OH of the tautomer as drawn. Atoms of OI and Gh are numbered in a fashion analogous to pyrimidines for our analysis. Values presented in Lotsof et al. 2022.

N3 proton affinity influences the difference in excision between the two isoforms

In the proposed mechanism for NEIL1, residue 242 engages with N3 of the lactim tautomer of the N3 base. Protonation of N3 is a critical step for the mechanism, so we considered the N3 proton affinity (kcal/mol) in our calculations. Initially, all calculations were performed where the lesion adopt the 2-hydroxy form in the same rotamer as proposed in the mechanism for Tg with NEIL1.[69] The N3 proton affinity trend is: DHT (230.0 kcal/mol, 2-OH lactim) > Tg

(222.2 kcal/mol, 2-OH lactim) > 5-hmU (220.4 kcal/mol, 2-OH lactim) > Ug (219.5 kcal/mol, 2-OH lactim) > 5-OHU (218.7 kcal/mol, 2-OH lactim) (Figure 2.9). This trend is not consistent with the UE:Ed NEIL1 experimental excision ratio; however, this does not take into account previous calculations where 5-hmU and DHT prefer the 4-hydroxy lactim tautomer. When we take into consideration the preferred tautomer, 2-hydroxy lactim for Tg, Ug and 5-OHU, and 4-hydroxy lactim for 5-hmU and DHT, the N3 proton affinity (kcal/mol) matches well with the experimental data: Tg (222.2, 2-OH lactim) > Ug (219.5, 2-OH lactim) > 5-OHU (218.7, 2-OH lactim) > 5-hmU (215.2, 4-OH lactim) > DHT (214.7, 4-OH lactim). This correlation between our calculations and the experimental excision ratio supports the importance of the N3 protonation with the most stable lactim.

We also evaluated three lesions that are structurally different from the lactam/lactim pyrimidines: 5-OHC (a pyrimidine without a carbonyl at O4), Gh (guanidinohydantoin), and OI (a purine) (Figure 2.9). 5-OHC can adopt similar lactam and lactim structures to the other pyrimidine lesions. The most stable of these is the 5-OHC 4-NH lactim where the 4-NH proton oriented toward N3. Unlike the other pyrimidines, this structure has a proton on N3, which is not consistent with hydrogen bonding to the lysine or arginine in position 242. Considering the protonation of N3 in 5-OHC's preferred tautomer, it is reasonable that the edited form of NEIL1 excises 5-OHC at a faster rate than UE NEIL1 since a Arg242 is less acidic to its unedited counterpart. This is supported by the low N3 PA of 5-OHC (174.4 kcal/mol). For Gh, the more stable lactim-like structure is Gh 2-OH lactim (in this structure, the number has been adjusted to be similar to that of the pyrimidines) (Figure 2.9). Gh has a nitrogen that can hydrogen bond to the lysine or arginine 242, but the proton affinity of that N3 is quite low (140.5 kcal/mol), likely because Gh is already protonated, so another protonation would make the substrate doubly charged. The charge on Gh

may allow it to be more quickly excised by both isoforms of NEIL1(Table 2.1), consistent with the higher N1-H acidity (Figure 2.9). Yet, the UE/Ed excision ratio for Gh of 0.3 in favor of the edited isoform and suggests that the more acidic K242 in the UE form does not enhance excision, which is also consistent with the low PA at N3. For OI, the base was also numbered as 6-membered ring like a pyrimidine. There are two possible lactims, with the more stable being the 4-OH lactim, whose PA at N3 is 206.0 kcal/mol. The ability of OI to more closely approximate a U/T lesion structure, is consistent with the modest increased removal by UE over Ed.

Comparing the N3 proton affinity (kcal/mol) of all the substrates for NEIL1 in the substrate's most stable lactam or lactim structure, the trend for all the lesions is as follows: Tg (222.2 kcal/mol, 2-OH lactim) > Ug (219.5 kcal/mol, 2-OH lactim) > 5-OHU (218.7 kcal/mol, 2-OH lactim) > 5-hmU (215.2 kcal/mol, 4-OH lactim) > DHT (214.7 kcal/mol, 4-OH lactim) > OI (206.0 kcal/mol, 4-OH lactim) > 5-OHC (174.4 kcal/mol, 4-NH lactim) > Gh (140.5 kcal/mol, 2-OH lactim) (Figure 2.9). This aligns favorably to trends in UE:Ed excision ratio (Table 2.3). Additionally, the three lesions that are more stable as the 2-hydroxy lactim form (Tg, Ug, and 5-OHU) are the most efficiently removed with the greatest preferential excision by UE over Ed NEIL1. This trend between our calculations and the experimental excision ratio supports the importance of the N3 proton affinity of the most stable lactim.

Structural insights influencing NEIL1 excision

Both our experimental results and calculations show that pyrimidine lesions are preferentially excised by UE NEIL1, with the exception of 5-OHC. Lesions that prefer the 2-OH tautomer (Tg, Ug, and 5-OHU) are more readily protonated by Lys242. Lesions that favor the 4-OH tautomer (5-hmU and DHT) have a reduced N3 proton affinity and likely make the excision of these lesion less sensitive to the inherent differences in pK_a of Lys242 (UE) versus Arg242 (Ed).

Furthermore, the tautomer encountered (2-OH v 4-OH) by NEIL1 may also impact additional contacts made by the enzyme making the base more poised for catalysis or captured quarantine state. The 2-OH tautomers allow for more favorable contacts with the catalytic residue Glu6, while 4-OH tautomers may not provide the preferred alignment of catalytic residues for optimal excision with either isoform (Figure 2.10A and B). Specific features of the lesion may further impact alignment in the active site and interaction residue 242 between an active and quarantine state.

Our studies on Ug not only identified a new substrate for the NEIL1 glycosylase, but also highlight structural features of the modified bases that impact NEIL1 excision. Ug, which lacks the methyl group of Tg on C5, was still preferentially excised by UE of Ed NEIL1, but with a much less striking difference than observed with Tg. The decrease in N3 proton affinity is in alignment with the decrease ratio of UE:Ed NEIL1 (Figure 2.9 and Figure 2.10C). In addition to the reduction in N3 PA, crystal structures of NEIL1 bound to Tg (R242, PDB ID: 5ITY and K242, PDB ID:5ITX) show the C5 methyl of Tg in a hydrophobic pocket. This contact likely assists proper catalytic alignment of Tg, and the lack of the methyl group may impact alignment and excision of Ug. We observe a lower percent removal and slower rate compared of Ug compared to Tg with both isoforms of NEIL1. Additionally, the UE NEIL1 kinetics of Ug showed more substrate excision associated with the faster process than with Ed NEIL1, while the K_d measurements showed that Ed NEIL1 binds Ug DNA with higher affinity than UE NEIL1. These results suggest that Ed NEIL1 may bind more of the Ug lesion tightly in a non-productive conformation. All of these features taken together demonstrate how small differences in the lesions can impact NEIL1 binding and excision.

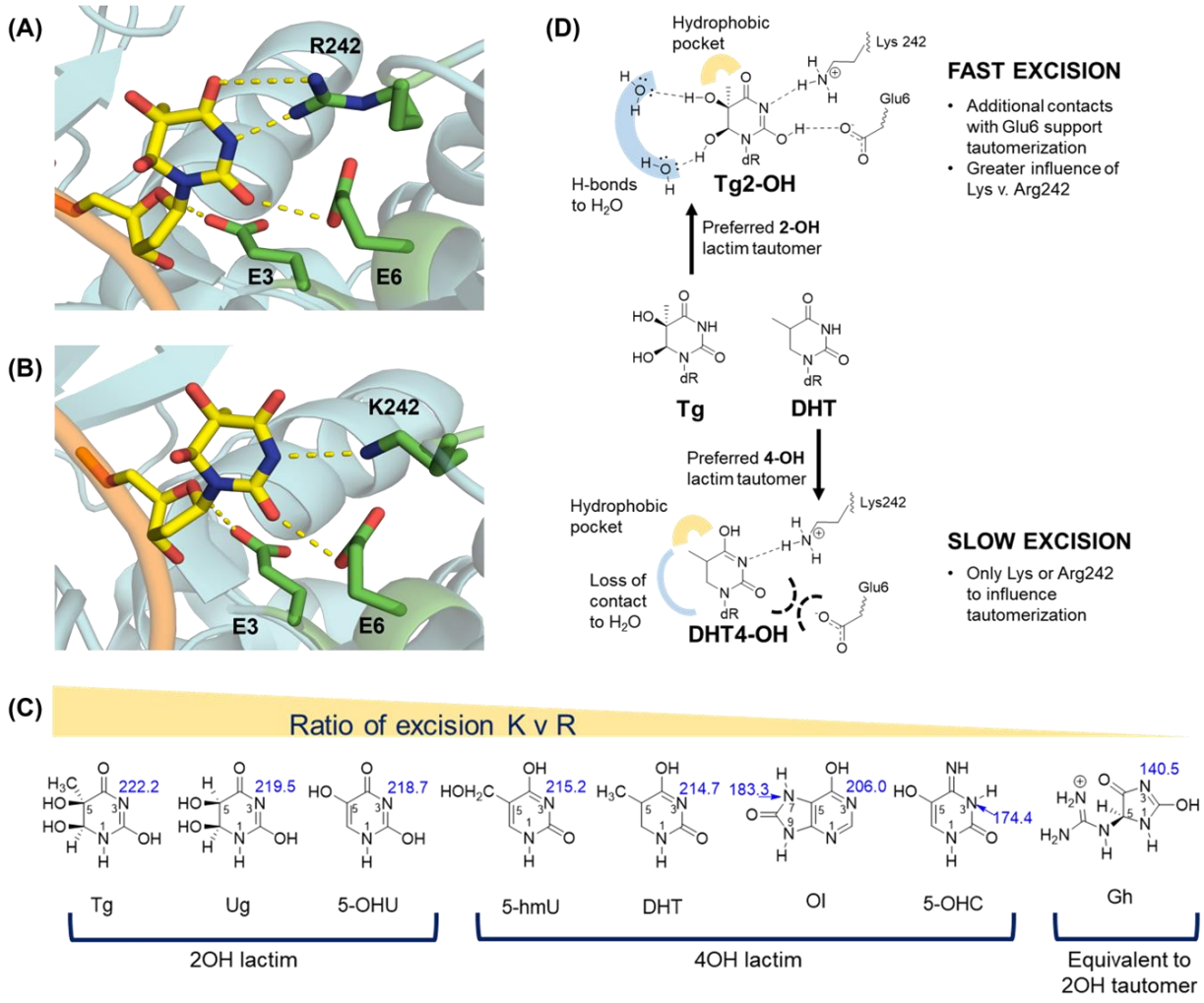

Figure 2.10: Structural features of oxidative damage influence base tautomerization and interaction with NEIL1.

(A, B) X-ray structures of Ed (R242, PDB ID: 5ITY) and UE (K242, PDB ID:5ITX) NEIL1 show Glu3, Glu6, and Arg/Lys242 make key contacts with Tg base. (C) Correlation of ratio of the lesion excision and favored tautomer. Lesions are ordered based on N3 proton affinity (ΔH kcal/mol, blue) Calculations were done on free base, and excision rates were obtained with duplex DNA (Table 2.1). (D) Schematic proposal of the impact of the preferred base tautomer on the rate of excision and isoform differences excision. Figure published in Lotsof *et al*. 2022.

Contacts critical for catalysis

Our results demonstrate an intricate relationship between structural features of the modified base on both isoforms of NEIL1's lesion recognition and base excision. NEIL1 can engage lesions in an active catalytic state or quarantine state as reflected in the crystal structures and our kinetics from the lesions studied.[70] This balance between the quarantine and active states is further modulated by the damaged base encountered by the enzyme, which vary in their preferences for tautomerization, inherent lability, and proton affinity. Both Ed and UE NEIL1 can remove a wide range of lesions, but the efficiency, rate, and preference vary between the two isoforms. Those lesions that are nonplanar such as, Gh, Sp, Tg, Ug, and FapyG, more efficiently excised than those more flat, aromatic lesions such as DHT, OI, 5-OHU, and 5-OHC. Those planar lesions may be more readily captured in the quarantine state by stacking of Tyr244, but lesions capable of solvent mediated interactions and/or charge (Tg and Gh) may also thwart the engagement of the quarantine state (Figure 2.6 and Figure 2.10).

Recognition and excision by UE and Ed NEIL1 are extremely sensitive to features of the base. Engagement with NEIL1 promotes tautomerization and influences the observed differences in excision for the lesion series, Tg, Ug, 5-OHU, and DHT. On the other hand, 5-OHC and Gh are removed more efficiently by Ed NEIL1 and are likely less influenced by tautomerization for removal. 5-OHC most stable tautomer is protonated at N3, which would be repulsive for the protonation step of the mechanism and the more acidic Lys242. Gh is positively charged has greatly lability as reflected in the N1-H acidity, which may explain why Gh is more rapidly excised than Tg by both isoforms. In addition, FapyG is a good substrate for both isoforms, with a slightly greater preference by Ed NEIL1, but the FapyG structure is very different for the lesions evaluated

in this study. These cases, positioning of the lesion in the active site may play a larger role in catalysis than Lys242 or Arg242 protonating the lesion.

Another critical factor that may be influencing excision is the base pair opposite of the lesion. Our analysis with 5-OHU, and other lesions, such as 5-hmU and 5-OHC, showed that the lesions were most efficiently excised when paired with C.[49] Arg118 makes contact the orphaned base the lesion is in the enzyme active site and would make favorable contacts with C (Figure 2.11). Arg118 may help the enzyme identify the opposite base pair and influence if the enzyme engages in an active or non-catalytic fashion. Moreover, in comparing structures of NEIL1 unbound or bound to lesion containing DNA, the lesion recognition loop must undergo a large conformational change to have engagement of either residue 242 or 244. Structural and computational studies of the bacterial homologs Fpg and Nei suggest that the lesions recognition loop's flexibility allow the glycosylase to accommodate a wide range of substrates.[60,61,64,69,105] Further structural and biophysical analyses are needed to sort out the intricate means of NEIL1 recognition and excision by both isoforms.

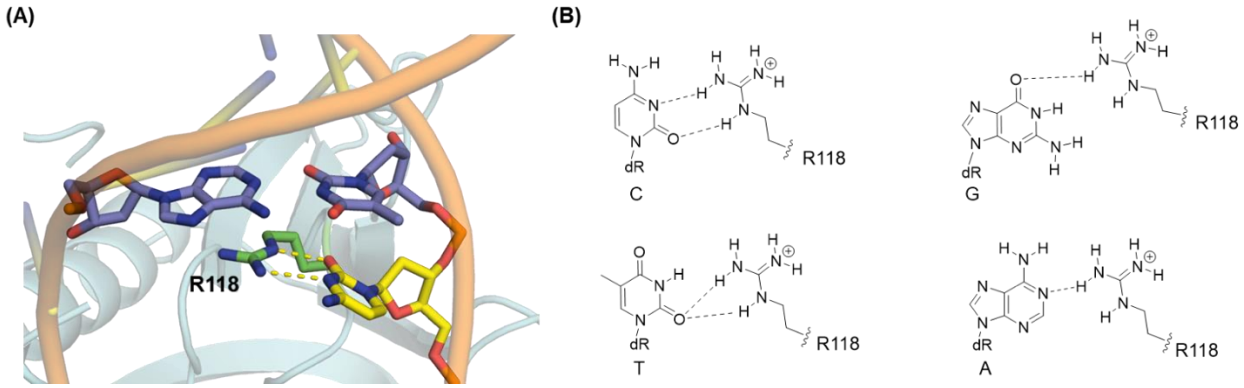

Figure 2.11: Arg118 makes contact with orphan base to lesion.

(A) X-ray crystal structure highlighting contacts of orphan C base to Tg by Arg118 PDB ID: 5ITY. (B) Possible contacts made by Arg118 with on bases. Substrates across from C are most rapidly excised followed by T/G and the worst excision is with A in studies performed with 5-OHU.

Biological implications of RNA editing on NEIL1 transcript

From a single gene, RNA editing gives two isoforms of NEIL1, each with their own distinct substrate specificity. Our work has shown that editing can dramatically impact the function *in vitro*, yet the impacts at a biological level are still unclear. RNA editing may play important regulatory role in responding to DNA damage created in different cellular conditions and may maintain a balance between the two isoforms. Conditions of oxidative stress and inflammation increases the generation of oxidation of lesions like Gh and upregulates ADAR1 expression, likely increasing amounts of Ed NEIL1 to address these lesions. However, ADAR1 overexpression and hyperediting are associated with cancer, and ADAR1 expression is upregulated under conditions associated with inflammation, which is a feature of cancer initiation and progression. In cases of lung cancer and multiple myeloma, NEIL1 mRNA was found to be completely edited in patient cases. These cases emphasize a need for balance between the two isoforms. Aberrant hyper-editing by ADAR1 of the NEIL1 transcript would lead to reduced amounts of UE NEIL1 and may diminish repair of oxidized pyrimidines leading to increased mutations, strand breaks, and overall genomic instability. Genomic instability drives oncogenic transformation, a feature that is also known to be associated with ADAR1 overexpression.[72,120]

Future work

These studies explored a wide substrate scope between the two isoforms of the NEIL1 glycosylase highlighting many subtle features of the lesion that influence excision. Yet the diversity of NEIL1 substrates and DNA contexts in which NEIL1 can act upon leaves many avenues for exploration. We have already identified that in our studies with 5-OHU and lesions evaluated here that NEIL1 have an opposite base preference for C and reduced excision for A. However, one of the best substrates for NEIL1 is Tg, that naturally arises across from A and is

rapidly excised by both isoforms.[64] While another T derived lesion, DHT, has relatively low overall base removal and k_g compared to Tg (Figure 2.3, Table 2.1). Here, the lesion, in addition to the opposite base partner, influence the excision of the base. Further studies with lesions that form across from A or maybe paired with A upon replication warrant further study to examine role of the opposite base. Additionally, our work has focused on the preferences of UE and Ed NEIL1 on the lesion itself, but limited work has been done evaluating the role of sequence. The David laboratory had identified that having adjacent 5' or 3' mismatches to the lesion reduced 5-OHU excision with the 5' being more detrimental and the Ed NEIL1 being more sensitive to mismatches. NEIL1 makes more contacts along the 3' end than 5' relative to the damage base which may influence sequence preference.[49] Further studies evaluating 5' and 3' base pairs to the lesion could highlight additional preferences for the glycosylase. Finally, additional studies exploring alternative DNA structures biologically relevant to NEIL1, such as the replication fork, are warranted. The David laboratory has evaluated the hydantoin lesions and 5-OHU in duplex, SS, bubble and bulge DNA, and the removal of Gh from G-quadruplex structures will be addressed in Chapter 3. NEIL1 is expressed during S phase of the cell cycle and work with replication machinery to catch lesions during replication and further studies with DNA structures during replication offer avenues of further exploration.

Beyond the substrate scope and DNA context, the biological role of NEIL1 recoding is still not well understood. Having a balance of Ed and UE may allow for the efficient removal of a wide range of substrates as evaluated in these studies. In cases of ADAR1 hyperediting in multiple myeloma, the NEIL1 transcript was found to be fully edited, and may lead to poor removal of pyrimidine lesions. Evaluating the impact of NEIL1 editing in a cellular could help to understand the biological function and NEIL1 hyper editing as it relates to disease.

Materials and Methods

General methods and materials. [γ-^{32}P] – ATP used for radiolabeling was purchased from PerkinElmer. T4 polynucleotide kinase was obtained from New England BioLabs. Microspin G-50 columns were obtained from Amersham Pharmacia. All solutions and buffers were prepared using deionized water from a Milli-Q PF System. Storage phosphor autoradiography was performed on a Typhoon 9400 or Typhoon Trio phosphorimager. Nuclear magnetic resonance spectra were obtained on a 300 MHz Mercury Plus spectrometer for ^{31}P NMR and an 800 MHz Bruker Advance III spectrometer for ^{1}H and ^{13}C NMR. MALDI-MS was obtained using a 3-hydroxypicolinic acid matrix on a Bruker UltraFlextreme MALDI TOF/TOF at the University of California, Davis or at the Mass Spectrometry Lab, School of Chemical Sciences, University of Illinois at Urbana-Champaign. High resolution ESI-MS for HRMS was obtained on an Applied Biosystem Qtrap Linear Ion Trap Spectrometer at the University of California, Davis. ImageQuant version 5.4 was used for the analysis of gel electrophoresis, and rate constants and percent completion values were determined using GraFit version 5.0. Prism GraphPad was used for the creation of the bar graphs. All other chemicals and reagents were purchased from VWR, Fisher Scientific, or Sigma and used without further purification.

Synthesis and purification of DNA oligonucleotides. The 8-OI and Ug phosphoramidite was synthesized as previously reported.[121,122] OG and 5-hmU phosphoramidites were purchased from Glen Research and used without further purification. DNA oligonucleotides containing OG, OI, 5-hmU, and Ug, were synthesized at the University of Utah Medical School's DNA/Peptide core facility. Oligonucleotides containing DHT, 5-OHU, U and I were purchased from Midland Reagents, and oligonucleotide containing 5-OHC was purchased from Sigma Aldrich. 5-fC, 5-caC, and 5-hmC containing oligonucleotides were provided by Dr. Chuan He (University of Chicago).

All oligonucleotides were HPLC purified using a Beckman Gold Nouveau or Shimadzu Liquid Chromatography system with a Dionex DNApac100 ion-exchange column using a 30-100% gradient of 90:10 H_2O/acetonitrile with 2M ammonium acetate. Isolated fractions were lyophilized and desalted using with a Waters SEP-PAK C18 column. Masses of oligonucleotides were confirmed by MADLI and ESI-MS, and DNA concentrations were determined using the Abs 260 nm.

The sequences used for glycosylase and electrophoretic mobility shift assays are reported in Table 2.4. The 30-nucleotide (nt) duplex 1•2 contained the I, OI, OG, DHT, 5-OHC, U, 5-OHU, or 5-hmU lesions paired to their likely Watson-Crick partner. The 23-nt duplex 3•4 contained the 5-fC or 5-caC modifications, and the 32-nt duplex 5•6 contained the 5-hmC lesion, all three across from G. The lesion-containing strand was 5' end-labeled with [γ-^{32}P]-ATP via T4 polynucleotide kinase at 37 °C and purified with a Microspin G-50 column. For glycosylase assays, additional unlabeled lesion containing DNA was added to adjust the concentration to approximately 5% labeled DNA. The lesion containing mixture was then annealed to a 20% excess of the unlabeled complementary strand in annealing buffer (20 mM Tris-HCl, pH7.6, 10 mM EDTA, 150 mM NaCl) by heating to 90 °C for 5 min and allowing to cool to 4 °C slowly for >6 hours. For electrophoretic mobility shift assays (EMSA), 100% radiolabeled lesion-containing DNA was added with an upper limit of the concentration estimated by the amount originally labeled; the sample was mixed with an equimolar amount to its complementary strand and annealed as described above.

Table 2.4: DNA sequences used in glycosylase and binding studies.

(1) 5’ – TGTTCATCATGGGTC**X**TCGGTATATCCCAT – 3’
(2) 5’ – ACAAGTAGTACCCAG**N**AGCCATATACCGTA – 3’
(3) 5’ – CCACTGCTCA**Y**GTACAGAGCTGT – 3’
(4) 5’ – ACAGCTCTGTAC**N**TGAGCAGTGG – 3’
(5) 5’ – TAATCCCATCCTC**Z**GGAAGGAGTTCACCAATT – 3’
(6) 5’ – AATTGGTGAACTCCTTCC**N**GAGGATGGGATTA – 3’
X = OG, 5-OHC, DHT, I, OI, U, 5-OHU, 5-hmU; Y = 5-fC, 5-caC; Z = 5-hmC; N = C, A, T, or G

Enzyme Purification. C-terminally His-tagged Ed and UE NEIL1 were expressed in Rosetta (DE3) pLysS cell strains from Novagen using a pET30a plasmid purified as reported previously. Total protein concentration was determined via absorbance at 280 nm. Active enzyme concentrations were determined using a 30-nt duplex containing a central Gh:C lesion as previously reported, and all protein concentrations reflect active enzyme concentrations.[123]

The preparation of C-terminal truncated inactive (Δ56 K54L) were reported previously. Total protein concentration was determined by Bradford assays. As a proxy for active enzyme concentration, the fraction competent at binding was measured using a THF:C-containing duplex to mimic an abasic site, under conditions > Kd, assuming 1:1 binding stoichiometry.

Glycosylase Assay. The glycosylase activity of Ed and UE NEIL1 was evaluated under single-turnover experiments as previously described (Scheme 2.1).[123,124] For experiments in which the reaction was too fast to measure manually, a Kintek RQF-3 Rapid-Quench instrument was utilized as previously reported.[124] Briefly, 20 nM lesion-containing DNA duplex was incubated at 37 °C with 200 nM NEIL1 in glycosylase assay buffer [20 mM Tris-HCl (pH 7.6), 10 mM EDTA, 0.1mg/mL BSA, and 150mM NaCl]. Aliquots were removed from the reaction mixture at various time points and quenched in NaOH (0.1 M) at 90 °C (30 min). Data analysis was performed using ImageQuant version 5.4 for quantification and Grafit version 5.0.2 for fitting. The resulting

production curves were fitted with one-exponential equation, $[P]_t = A_0[1 - \exp(-k_g t)]$, and two-exponential equation, $[P]_t = A_0[1 - \exp(-k_g' t)] + B_0[1 - \exp(-k_g'' t)]$, to determine the relevant rates constants to describe the glycosylase steps (k_g, k_g', and k_g''). A_0 and B_0 are the amplitude of the exponential phase for the associated rate constants. The percent base removed was determined by dividing A_0 by 20, the total DNA concentration of substrate (20nM), and multiplying by 100.

Dissociation Constant Determination. Electrophoretic mobility shift assays (EMSAs) were performed similarly to that previously reported.[49] Various enzyme solutions of inactive K54L Δ56 Ed or UE NEIL1 (1000-0.2nM) prepared at 4 °C were mixed with 10 pM of 100% ^{32}P-labeled duplex DNA (1•2) containing a central lesion of interest for 30 minutes at 25 °C in 20mM Tris-HCl pH 7.6, 150mM NaCl, 1mM EDTA, 1mM DTT, and 10% glycerol. The reactions were run a 6% non-denaturing polyacrylamide gel with 0.5X TBE at 120 V for 2.5 h at 4 °C. Gels were dried and exposed to phosphorimager screens for 72 h. Dissociation constants (K_d) were determined by fitting the percent bound substrate versus enzyme concentration to a one-site binding equation ($C[E]^n/((K_d)^n + [E]^n)$, Hill coefficient = 1).

Chapter 3 Removal of oxidative damage from G-quadruplex structures by NEIL1 and NEIL3

Contribution of others: The Gh-containing G-quadruplex sequences were designed and prepared by Dr. Aaron Fleming and Dr. Judy Zhu. April Averill purified mNeil3 Δ324 used in the glycosylase assay and NEIL3 Δ324 and NTHL1 enzymes used in the qualitative assay. Dr. Brittany Anderson-Steele performed the representative gels with the BER glycosylases Edited and Unedited NEIL1, NEIL3 Δ324, and NTHL1 glycosylases with the VEGF, RAD17, and KRAS G4 and assisted with a replicate of glycosylase assays with NEIL1. Savannah Conlon conducted the glycosylase assays with mNeil3 Δ324 and KRAS containing oligos and assisted in evaluating removal with Gh-containing G4 at various enzyme concentrations. Kelsey Miflin assisted with replicates of glycosylase assay with mNeil3 Δ324 and VEGF G4. Joshua Bumgarner assisted in the replicates of Ed NEIL1 with RAD17 and KRAS G4.

Introduction

G-quadruplexes (G4) are unique DNA structures that arise from regions of the genome with high guanine (G) content.[9,103,125] Guanines from adjacent G runs can Hoogsteen base pairing to form a G-tetrad, and tetrads are further stabilized by stacking with a central monovalent cation, such as K^+ or Na^+ (Figure 3.1A).[103,125] G4 folding in human cells have been demonstrated with immunofluorescence and fluorescent nucleoside probes.[126,127] More than 375,000 potential quadruplex forming sequences (PQS) have been identified via bioinformatic analysis of the whole genome with a greater proportion of PQS within gene promoters.[103] These G4 structures have been implicated in gene regulation and approximately 10,000s PQS have been identified via G4 ChIP-seq with the potential to fold into G4.[125] Several genes, such as *VEGF*,[128] *c-MYC*,[129] *KRAS*,[130] and *SRC*,[131] have been reported to be regulated by a promoter PQS and these sequences have become of therapeutic interest.

The high G content of G4 also make them highly susceptible to oxidative DNA damage.[9] Guanine has the lowest redox potential of all the bases and adjacent G's can increase the likelihood of oxidation.[51,132] One of the most common oxidation products of G is 8-oxo-7,8-dihydroguanine (OG), and OG is susceptible to further oxidation producing the hydantoin lesions, guanidinohydantoin (Gh) and spiroiminodihydantoin (Sp).[9,51] The presence of oxidative damage in the G4 sequence can have profound effects on structure and stability of the G4. Oxidation products, such as OG or Gh, can disrupt Hoogsteen hydrogen bonding, and non-planar lesions, such as Gh, can interrupt π-stacking between the tetrads (Figure 3.1B).[85,133] However, several PQS have been identified to have an additional run of G's, and this additional run of G's, referred to as the 5th track, can replace the lesion containing run of G's to help stabilize the G4 as verified with thermodynamic, spectroscopic, and DNA footprinting studies with the *VEGF* G4 (Figure 3.1C).[134]

Notably, hydantoins are more destabilizing than OG in duplex DNA and therefore would also alter the duplex/G4 equilibrium in greater favor of the G4 if the hydantoin can be placed in a loop position (Figure 3.1D), which is not detrimental to the G4 stability.[135]

In addition to impacting the structure of G4, oxidative damage in PQS can impact G4 formation and gene regulation due to the activity of BER enzymes. Studies by the Burrows group using luciferase reporter construct containing *VEGF* PQS in the reporter promoter observed increased expression of luciferase when OG was synthetically installed into the PQS. Removal of OG by the BER glycosylase, OGG1, promotes G4 formation and recruitment of APE1 to the abasic site in the G4 to mediate increased luciferase gene transcription.[102] Formation of oxidized bases, such as Gh, that are likely to form in G-rich promoter regions, and removal of these oxidized bases by BER glycosylases may similarly impact gene transcription.

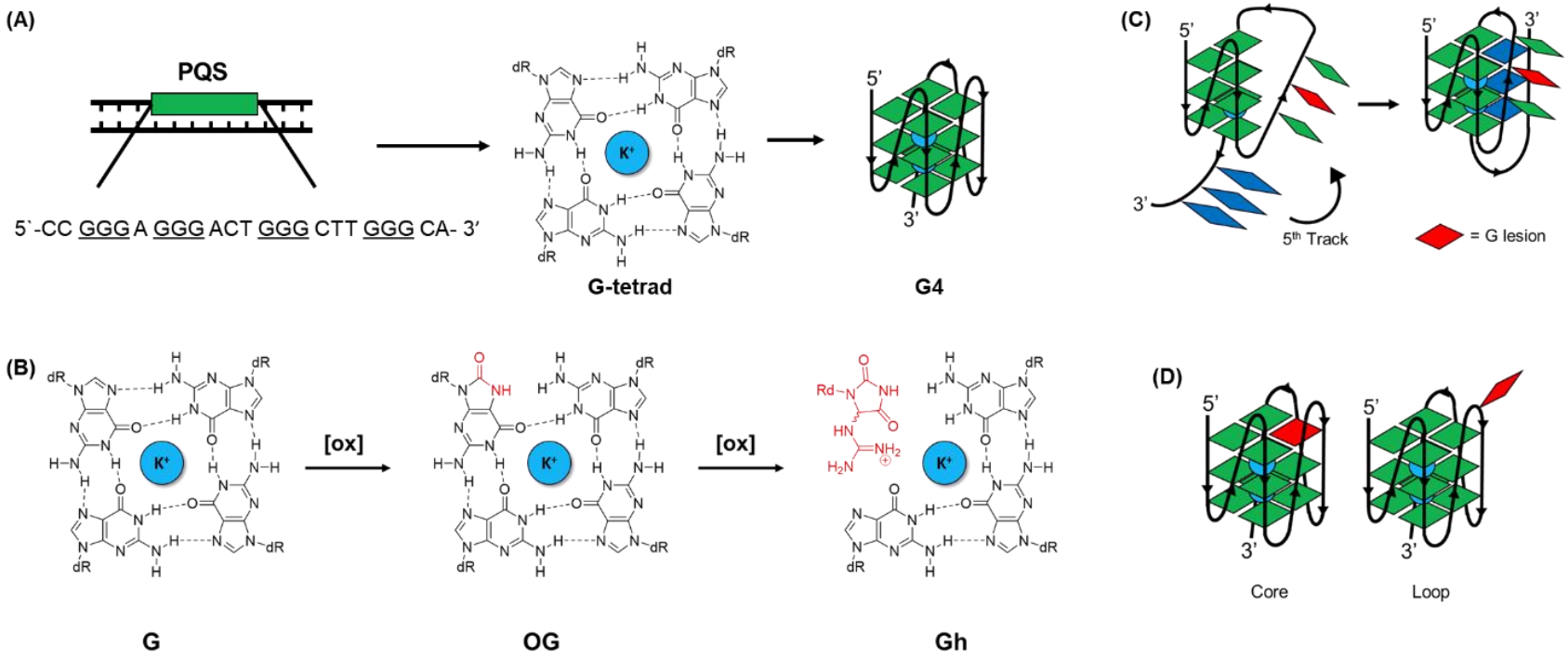

Figure 3.1: G-quadruplex structures and the impacts of oxidation.

(A) G-quadruplex (G4) arise from G-rich potential quadruplex forming sequences (PQS) and stacking of G-tetrads stabilized by a potassium ion (K^+). (B) The introduction of the of 8-oxo-7,8-dihydroguanine (OG) and guanidinohydantoin (Gh) lesions can be destabilizing to G-tetrad and G4 by the loss of hydrogen bonds and π-stacking. (C) Fifth track of G (blue) proposed to serve as a "spare tire" to replace damage containing G-track and stabilize the G4. (D) Representation of the position of core versus loop modifications in a G4 structure.

The BER glycosylases, NEIL1, NEIL2, NEIL3, and NTHL1 are likely candidates for recognition and removal of Gh from G4 structures. The NEIL glycosylases have been shown to excise Gh from a wide range of structures including duplex, single-stranded, and G4 DNA contexts. NEIL1 and NEIL3 have also been shown to excise oxidized lesions, such as Gh, within *VEGF* and hTelo G4 structures.[85] Additionally, during S phase, NEIL3 has been found to localize at the telomeres, which are abundant in G4 structure. Here, we examine the ability of NEIL1 and mNeil3 glycosylase's ability to excise Gh from a variety of G4 sequences varying the position of damage within the G4. PQS sequences from the *VEGF*, *RAD17*, and *KRAS* from the each of the gene's promoters were used in this study. In each sequence, the position of damage was either in the G-tetrad (core) or in a loop outside of the G-tetrad (Figure 3.1D). Additionally, we characterized mNeil3 Δ324 and NEIL3 Δ324 in duplex and single stranded DNA contexts with the Gh lesion as this has not well defined in the literature.

Results

Excision of Gh by Edited and Unedited NEIL1 from VEGF G4s

Previous work showed that edited (Ed) NEIL1 is able to excise Gh from the VEGF G4, but the unedited enzyme had not been evaluated.[85] In duplex, both isoforms of NEIL1 efficiently excise Gh to completion.[136] We evaluated the glycosylase activity of Ed and UE NEIL1 with Gh-containing *VEGF* G-quadruplex sequences where the Gh lesion was positioned in either a core or loop position within the G4, analogous to previous studies (Table 3.1).[134,137,138] Briefly, all Gh containing G4 oligo nucleotides were made via selective oxidation of OG containing oligonucleotides to Gh containing oligonucleotide with K_2IrBr_6. Gh containing sequences were separated from unreacted OG containing oligonucleotides via HPLC and confirmed via ESI-MS. In the presence of KCl, G4 sequences will adopt a G4 structure and have been previously

characterized.[85,134] Similar to non-quadruplex forming sequences, *VEGF* oligonucleotides were 5' end labelled with [γ-^{32}P]-ATP and annealed in buffer containing KCl to form the G4.[85] The Gh base excision activity by Ed and UE NEIL1 was monitored with enzyme in excess at 37 °C for 60 min.

Both Ed NEIL1 and UE NEIL1 exhibited low levels of excision of Gh at both the core and loop position in the 4-track *VEGF* sequence (Figure 3.2), consistent with previous results seen with the edited isoform.[135] Excision of Gh in the 5-track *VEGF* G4s was increased with both Ed and UE NEIL1; however, the overall extent of Gh removed by both isoforms of NEIL1 on 4- and 5-track *VEGF* G4 are incomplete (~12%-48% at 60 min), despite enzyme being in excess (Figure 3.2 and Table 3.1). In duplex and single stranded DNA context, both Ed and UE NEIL1 have excised Gh to completion and are known to be good substrates for NEIL1.[52,136]

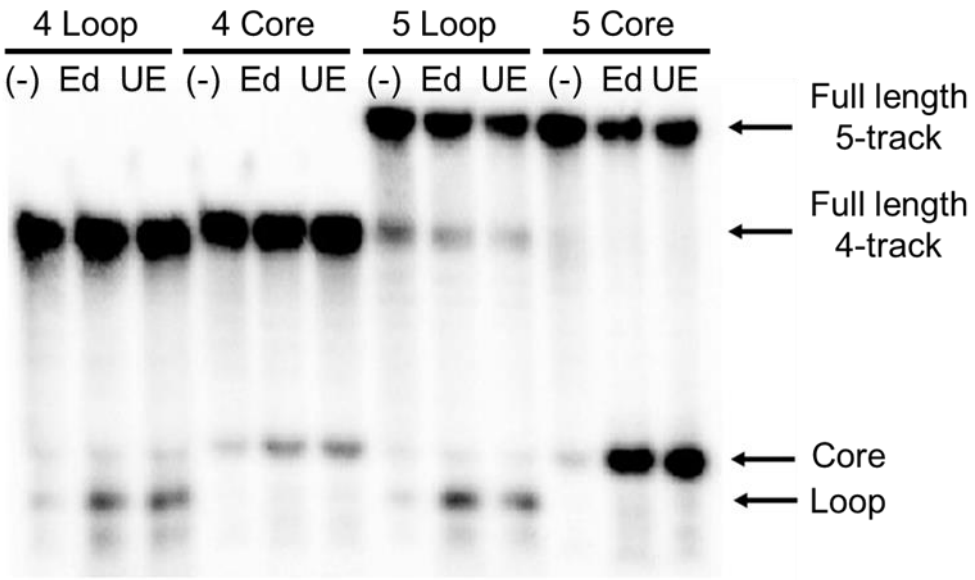

Figure 3.2: Representative storage phosphor autoradiogram of the removal of Gh by edited (Ed) and unedited (UE) NEIL1 from *VEGF* G4s.

Experiments were conducted with 200 nM enzyme and 20 nM Gh-containing G4 DNA at 37 °C, pH 7.6 , and 100 mM KCl at 60 min incubation.

NEIL1 demonstrates biphasic excision of Gh from VEGF G4

A full-time course of the glycosylase activity of Ed and UE NEIL1 under single-turnover (STO) conditions ([enzyme] > [DNA]) was monitored to further reveal features of Gh lesion processing by both isoforms on *VEGF* G4s. We found that the data best fit to a two-exponential equation $[P]_t = A_0(1-\exp(-k_g't)) + B_0(1-\exp(-k_g''t))$. The kinetic parameters determined using two-exponential fitting provided a larger rate constant (k_g') and an associated amplitude, A, and a smaller rate constant (k_g") with an associated amplitude, B. As discussed in Chapter 2, biphasic production curves have been observed with 5-OHU, Tg, and Ug, and the two phases are consistent with distinct excision processes, an active, a quarantine state, and a transition from quarantine to active.[49,113,139] However, we had previously observed that the excision of Gh in duplex DNA fits well to a single-exponential curve with a single rate constant,[136] so here G4 structure impacts excision of Gh by NEIL1.

Kinetic analysis shows that the rates of glycosidic bond cleavage from the *VEGF* G4s are similar for both Ed and UE NEIL1 (Table 3.1 and Figure 3.3). Across all of the *VEGF* G4s, the associated amplitude for each rate constant (A_0 and B_0) are approximately equal (Figure 3.4B, dark blue (A_0) and light blue (B_0)), with the exception of the *VEGF* 5-track core sequence. Differences were observed for the rate constant k_g" associated where more efficient excision was observed with NEIL1 for Gh from a core position versus a loop position for the 4-track *VEGF* Gh (k_g" = 0.45 ± 0.33 min^{-1} versus 0.12 ± 0.1 min^{-1}). In the 5-track *VEGF* sequence, NEIL1 excised Gh with similar efficiency at both core and loop positions (k_g" = 0.1 ± 0.1 min^{-1} and k_g" = 0.1 ± 0.2 min^{-1}, respectively) (Table 3.1). These data also confirm differences observed in the qualitative analysis of minimal overall excision of Gh by both NEIL1 isoforms from *VEGF* G4 contexts (Figure 3.3). Maximal NEIL1 excision of Gh located within the loop of 4 and 5-track *VEGF* G4s was 20%.

Notably, significantly more efficient (large amplitude for k_g') and overall % based removed of Gh located in the core of the 5-track G4 (48% ± 8%) versus 4-track G4 (16% ± 5%) was observed. These results indicate that the presence of the "spare tire" provides a higher fraction of Gh that can be efficiently removed by both NEIL1 isoforms (Figure 3.4). However, we did not observe much difference in the rate constants between the two isoforms of NEIL1 despite previously reported ~3-fold difference in favor of the Ed isoform in duplex.[136] Due to this lack of difference, we proceeded to use only Ed NEIL1 for the remainder of analysis with other G4 sequences.

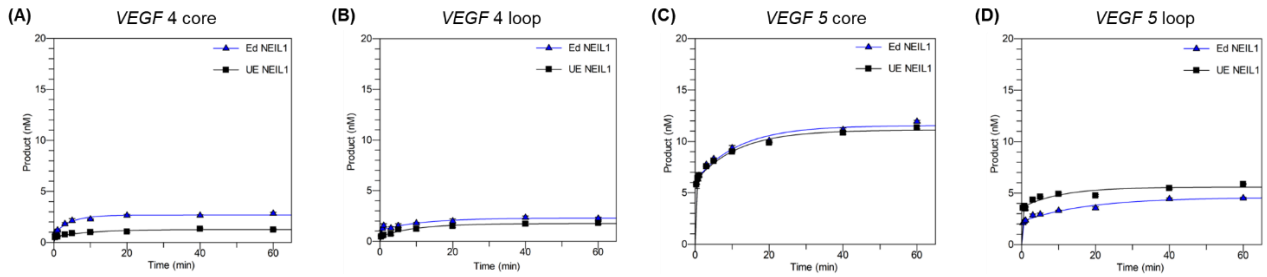

Figure 3.3: Time-course of removal of Gh from *VEGF* promoter G4 by Edited (Ed) and Unedited (UE) NEIL1.

(A) *VEGF* 4-core, (B) *VEGF* 4-loop, (C) *VEGF* 5-core, and (D) *VEGF* 5-loop. Experiments were conducted with 200 nM enzyme and 20 nM Gh-containing G4 DNA at 37 °C, pH 7.6 , and 100 mM KCl. Data is fit to a two-exponential equation, $[P]_t = A_0(1\text{-}\exp(\text{-}k_g't)) + B_0(1\text{-}\exp(\text{-}k_g''t))$ and reported in Table 3.1.

Table 3.1: Kinetic parameters of Gh removal from *VEGF* promoter G4 by Edited (Ed) and Unedited (UE) NEIL1.

		VEGF 4 core	*VEGF* 4 loop	*VEGF* 5 core	*VEGF* 5 loop
Ed NEIL1	k_g' min^{-1} (A – nM)[a,b]	>2 (0.8 ± 0.3)	>2 (1 ± 0.7)	>2 (4.3 ± 1.5)	>2 (1.2 ±0.8)
	k_g'' min^{-1} (B – nM) [a,b]	0.45 ± 0.33 (1.5 ± 0.4)	0.12 ± 0.1 (2.5 ± 1.6)	0.1±0.1 (5.3 ± 1)	0.2 ± 0.2 (2.1 ± 0.8)
	% base removed[c]	12 ± 2	17 ± 6	48 ± 8	16 ± 5
		VEGF 4 core	*VEGF* 4 loop	*VEGF* 5 core	*VEGF* 5 loop
UE NEIL1	k_g' min^{-1} (A – nM)[a,b]	>2 (0.5±0.1)	>2 (0.4±0.1)	>2 (6.1±0.2)	>2 (3.6±0.3)
	k_g'' min^{-1} (B – nM) [a,b]	0.12±0.03 (0.7±0.1)	0.13±0.04 (1.3±0.2)	0.09±0.01 (5.0±0.1)	0.09±0.04 (2.6±0.4)
	% base removed[c]	6.3±0.5	9.0±0.7	56.7±0.7	30.7±1.4

[a] k_g' and k_g'' are the observed rates of base removal. The associated amplitude of each rate constant (capacity) in nM, and percent base removal of reaction after 60 min incubation. [Enzyme]= 200 nM, [DNA] = 20 nM, pH 7.6, 37 ºC, [KCl]=100mM, fit to a two-exponential equation, $[P]_t = A_0(1-\exp(-k_g't)) + B_0(1-\exp(-k_g''t))$. [b] A_0 and B_0 are the associated amplitudes of k_g' and k_g'' respectively. [c] % base removed = $((A_0+B_0)/20)*100$.

Excision of Gh by mNeil3 Δ324 from VEGF G4s

We also examined the removal of Gh by NEIL3 from the *VEGF* G4 sequences as NEIL3 is a prime candidate for the removal of oxidative damage from G4s. A truncated version of the highly homologous mouse Neil3 (mNeil3 Δ324) was used for these assays as the human and full length glycosylase are difficult to purify, and mNeil3 Δ324 has been shown to exhibit similar glycosylase activity to the human NEIL3 in SS DNA.[140] Similar to NEIL1, excision of Gh from

VEGF G4 by mNeil3 Δ324 was inefficient and low for all contexts (Figure 3.4B). The percent base removed observed from the 4-track *VEGF* at loop and core position was around 20% of the total, while in the 5-track *VEGF* G4 excision was around 30% (Figure 3.4B).

The data for mNeil3 Δ324 also best fit to a two-exponential like that of NEIL1. In all *VEGF* G4 substrates, k_g' was >2 min^{-1} with a very small associated amplitude (A), and most of the excision (B) was associated with the smaller k_g" (0.03-0.06 min^{-1}) (Table 3.2). Like NEIL1, the overall extent of cleavage of Gh by mNeil3 Δ324 around 25% for all *VEGF* G4, yet there is no observed preference for core substrates over loop substrates like with NEIL1. mNeil3 Δ324 exhibited similar biphasic removal of Gh from the G4, indicative of distinct excision processes that are impact by G4 structure. Analysis with additional G4 sequences and DNA contexts may help to define this trend in lesion processing and will be discussed in later sections.

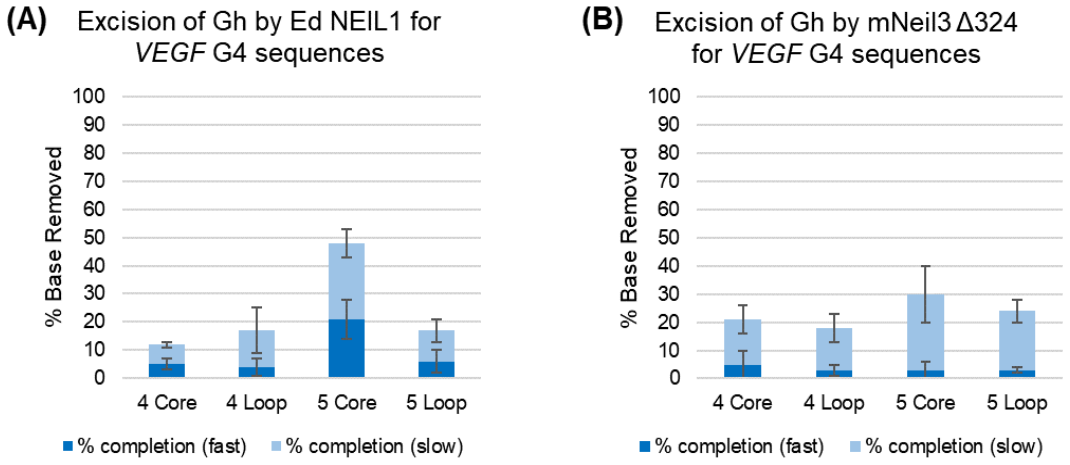

Figure 3.4: Excision of Gh from *VEGF* G4 by edited (Ed) NEIL1 and mNeil3 Δ324.

Percentage of base removed from *VEGF* G4s by (A)Ed NEIL1 and (B) mNeil3 Δ324. The dark blue portion of the bar graph depicts the portion excised under the fast rate (k_g') of the total damage removed and the light blue similarly depicts the portion excised at the slow rate (k_g"). Experiments were conducted with 200 nM enzyme and 20 nM Gh-containing G4 DNA at 37 °C, pH 7.6 , and 100 mM KCl.

Table 3.2: Kinetic parameters of Gh removal from *VEGF*, *RAD17*, and *KRAS* G4s by mNeil3 Δ324.

	VEGF 4 core	*VEGF* 4 loop	*VEGF* 5 core	*VEGF* 5 loop
k_g' min^{-1} (A – nM)[a,b]	>2 (1.0±0.3)	>2 (0.6±0.2)	>2 (0.6±0.2)	>2 (0.6±0.1)
k_g'' min^{-1} (B – nM) [a,b]	0.07±0.01 (3.3±0.3)	0.07±0.01 (3.1±0.8)	0.03±0.02 (5.33±0.7)	0.06±0.01 (4.2±0.2)
% base removed[c]	22±3	20±2	23±2	24±1
	RAD17 4 core	*RAD17* 4 loop	*RAD17* 5 core	*RAD17* 5 loop
k_g' min^{-1} (A – nM)[a,b]	>2 (1.1±0.2)	>2 (1.5±0.3)	>2 (0.7±0.1)	>2 (1.0±0.1)
k_g'' min^{-1} (B – nM) [a,b]	0.38±0.04 (12±1)	0.14±0.01 (11±1)	0.20±0.1 (7.7±0.3)	0.11±0.01 (7.7±0.2)
% base removed[c]	71±1	63±2	45±1	45±2
	KRAS 4 core	*KRAS* 4 loop	*KRAS* 5 core	*KRAS* 5 loop
k_g' min^{-1} (A – nM)[a,b]	>2 (1.5±0.3)	>2 (1.4±0.1)	>2 (1.5±0.2)	>2 (8.1±0.1)
k_g'' min^{-1} (B – nM) [a,b]	0.42±0.02 (12±1)	0.14±0.01 (12±1)	0.21±0.02 (11±1)	0.16±0.01 (5.3±0.1)
% base removed[c]	69±2	68±1	68±1	63±1

[a] k_g' and k_g'' are the observed rates of base removal. The associated amplitude of each rate constant (capacity) in nM, and percent base removal of reaction after 60 min incubation. [Enzyme]= 200 nM, [DNA] = 20 nM, pH 7.6, 37 ºC, [KCl]=100mM, fit to a two-exponential equation, $[P]_t = A_0(1-\exp(-k_g't)) + B_0(1-\exp(-k_g''t))$. [b] A_0 and B_0 are the associated amplitudes of k_g' and k_g'' respectively. [c] % base removed = $((A_0+B_0)/20)*100$.

Excision of Gh by BER Glycosylases from RAD17 and KRAS G4s

An abundance of G4 PQS can be found in the promoter regions of many genes, and the sequences of PQS can greatly vary, which can impact G4 topology and thermal stability.[141] Moreover, variations in sequence and structure may alter the impact of oxidative damage on the G4 and the interactions with BER glycosylases. NEIL glycosylases have been previously able to excise Gh and Sp from hTelo G4, which has distinct sequence and structural differences compared to *VEGF* G4.[85,142] Examining additional G4 sequences from other promoters with varied positions of damage (core versus loop) would further highlight these differences and provide insights to preferences by the BER glycosylase. We evaluated the removal of Gh by Ed and UE NEIL1, NEIL3, and NTHL1 from the *RAD17* and *KRAS* promoter G4s with damage located at core or loop positions and in the presence or absence of a fifth G-track. Each respective enzyme was incubated in excess with a given G4 at 37 °C and 100 mM KCl for 60 min (Figure 3.5). For NTHL1, Gh in *RAD17* and *KRAS* G4s are poor substrates as seen in the representative gel assays (Figure 3.5). This is unsurprising as NTHL1 does have a preference for duplex DNA and oxidized pyrimidines over Gh.[85,133] The NEIL glycosylases was found to excise Gh from the *RAD17* and *KRAS* G4 differently than trends observed with the *VEGF* G4. Upon visual inspection, Gh is removed from 5-track G4s to a lower extent than from the 4-track G4s by all enzymes from *RAD17* G4s. Additionally, greater Gh excision by NEIL1 was observed from a core relative to loop position in *RAD17* and *KRAS* G4s Notably, more quantitative analysis is warranted to further delineate potential differences in excision. The glycosylase activity is similar for Ed and UE NEIL1 as was observed with the *VEGF* G4s. Due to the low Gh glycosylase activity of NTHL1 in the G4 context and similar behavior of edited and unedited NEIL1, we proceeded with only edited NEIL1 and mNeil3 Δ324 for a more detailed kinetic inspection with these G4s.

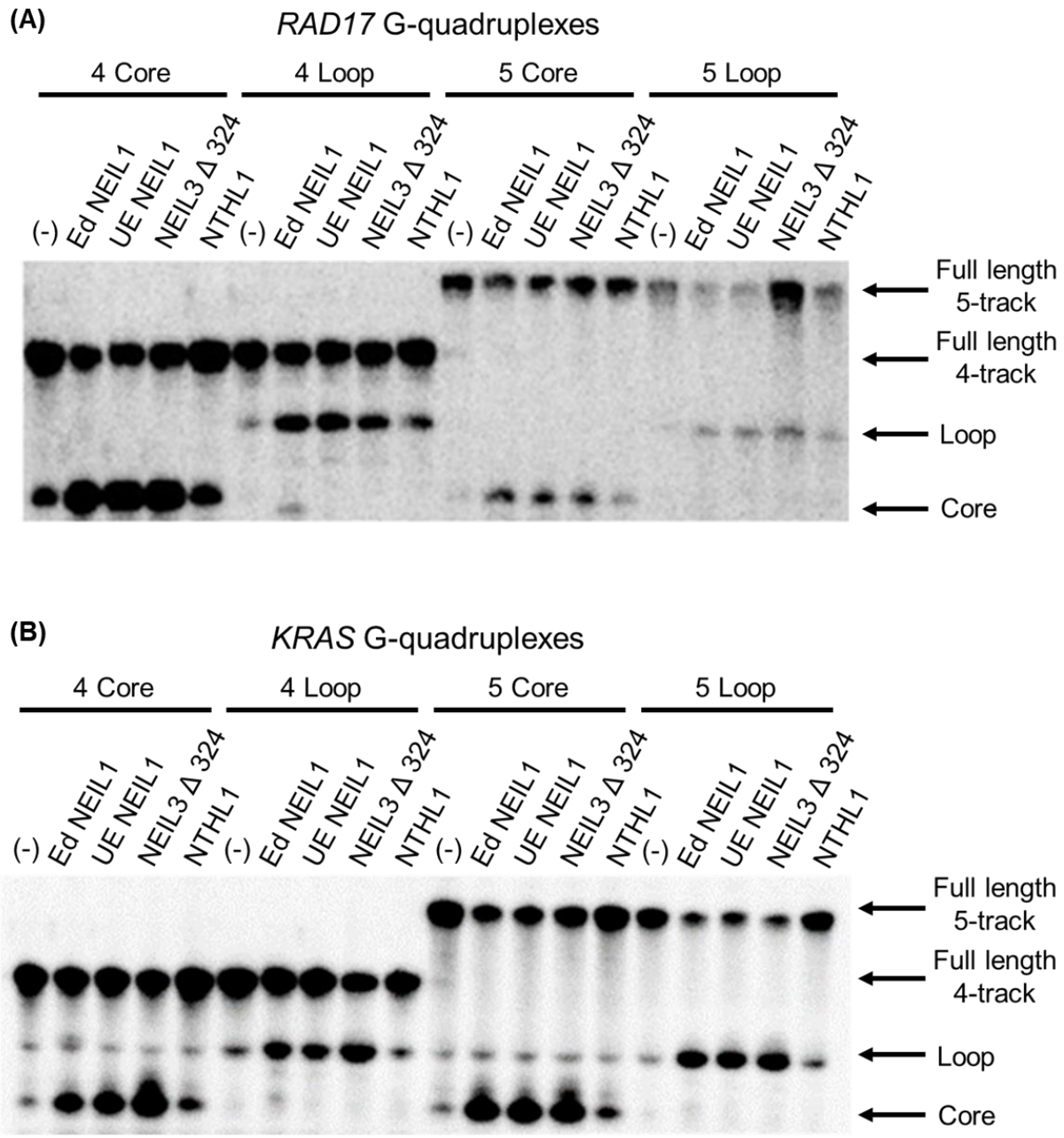

Figure 3.5: Representative storage phosphor autoradiogram of the excision of Gh from (A) *RAD17* and (B) *KRAS* G4s by BER glycosylases.

20nM G4s were incubated with 200 nM Edited (Ed) NEIL1, Unedited (UE) NEIL1, NEIL3 Δ324, or NTHL1 for 60 min at 37 C and 100 mM KCl. Negative control lanes represent G4 with no enzyme added. G4s were either 4 or 5 G-tracks in length, and Gh was excised from either a core or loop position.

Biphasic excision of Gh by NEIL glycosylases from RAD17 and KRAS G4

Similar to the excision of Gh from *VEGF* G4s, the data from the excision *RAD17* and *KRAS* G4s fit best to a two-exponential equation for Ed NEIL1 and mNeil3 Δ324. The total amount of Gh excised is greater when in the core position in all G4s (Figure 3.6, Figure 3.8). For Ed NEIL1, Gh lesions located at core position in 4-track *RAD17* G4 (72% ± 2%) had higher % base removed than loop positions (34% ± 8%). Similarly, when Gh was located at a core position and loop position with the 5-track *RAD17* G4, the % base removed was higher in the core position compared to loop. Overall base removal was lower in 5-track G4 compared to the 4-track in the *RAD17* sequence Additionally, a similar reduction in rate (k_g*')* can be observed in the excision of Gh from 4- and 5-track G4. k_g" for Ed NEIL1 mediated removal of core position Gh in 4-track *RAD17* G4 is 0.23 ± 0.03 min^{-1} but is reduced to 0.05 ± 0.02 min^{-1} in the corresponding position in the 5^{th} track, and these rates are further reduced when damage is in the loop position (Table 3.3). With the *KRAS* G4s, greater excision by Ed NEIL1 was seen from the core position and from 5-track compared to the loop position and 4-track G4 respectively (Table 3.3, Figure 3.6, Figure 3.8A). The k_g*"* for Ed NEIL1 excision of *KRAS* G4s were all around 0.2 min^{-1}, except for Gh located within the core of the 4-track G4, which was slightly larger at 0.48 ± 0.45 min^{-1}. Notably, the amplitudes associated with the two rates with the *RAD17* and *KRAS* G4s varied significantly due to Gh position and sequence (Figure 3.6, Figure 3.8A).

Table 3.3: Kinetic parameters from two-exponential fitting experiments with Edited NEIL1 and *RAD17* and *KRAS* G4s.

	RAD17 4 core	*RAD17* 4 loop	*RAD17* 5 core	*RAD17* 5 loop
k_g' min^{-1} (A – nM)[a,b]	>2 (9.5 ± 1.0)	>2 (2.9 ± 0.8)	>2 (1.9 ± 0.6)	>2 (1.9 ± 0.8)
k_g'' min^{-1} (B – nM) [a,b]	0.23 ± 0.03 (4.8±1.2)	0.11 ± 0.09 (4.0 ± 1.6)	0.05 ± 0.02 (7.0 ± 0.5)	0.17 ± 0.06 (3.7 ± 1.1)
% base removed[c]	72 ± 2	35 ± 8	45 ± 5	28 ± 3
	KRAS 4 core	*KRAS* 4 loop	*KRAS* 5 core	*KRAS* 5 loop
k_g' min^{-1} (A – nM)[a,b]	>2 (3.2 ± 0.8)	>2 (1.4 ± 0.4)	>2 (0.5 ± 0.4)	>2 (4.9 ± 1.5)
k_g'' min^{-1} (B – nM) [a,b]	0.48 ± 0.45 (6.5 ± 1.9)	0.13 ± 0.12 (3.9 ± 1.7)	0.016±0.003 (15 ± 1)	0.25 ± 0.09 (6.4 ± 0.9)
% base removed[c]	48 ± 11	26 ± 9	80 ± 7	57 ± 7

[a] k_g' and k_g'' are the observed rates of base removal. The associated amplitude of each rate constant (capacity) in nM, and percent base removal of reaction after 60 min incubation. [Enzyme]= 200 nM, [DNA] = 20 nM, pH 7.6, 37 ºC, [KCl]=100mM, fit to a two-exponential equation, $[P]_t = A_0(1-\exp(-k_g't)) + B_0(1-\exp(-k_g''t))$. [b] A_0 and B_0 are the associated amplitudes of k_g' and k_g'' respectively. [c] % base removed = $((A_0+B_0)/20)*100$.

Gh excision by mNeil3 Δ324 from 4-track *RAD17* G4 at core and loop positions were similar in overall percent base removed (65%). Notably the presence of the 5th track resulted in overall reduction in percent of Gh removed to ~50%. Gh localized within a core position was excised faster (k_g'' - 0.38 ± 0.13 min^{-1}) than within the loop (k_g'' - 0.14 ± 0.03 min^{-1}) of *RAD17* 4 track G4 by mNeil3 Δ324. The 5-track *RAD17* containing Gh at the core and loop positions was excised with a k_g'' of 0.20 ± 0.28 min^{-1} and 0.11 ± 0.03 min^{-1}, respectively (Table 3.2, Figure 3.7, Figure 3.8). For all *KRAS* G4s, Gh was excised by mNeil3 Δ324 to the same extent of about 65%. The k_g'' for Gh removal from all *KRAS* G4s was 0.2 min^{-1}, except for within the core of the 4-track

G4, which was slightly increased at 0.42 ± 0.05 min^{-1}. Notably, a comparison of the amplitudes associated with the two rates shows that most of the Gh removed from *KRAS* and *RAD17* G4 contexts is associated with the slower rate. The exception was observed for Gh at the loop position within the *KRAS* G4 containing the 5th track, where mNeil3 Δ324 excision was most efficient.

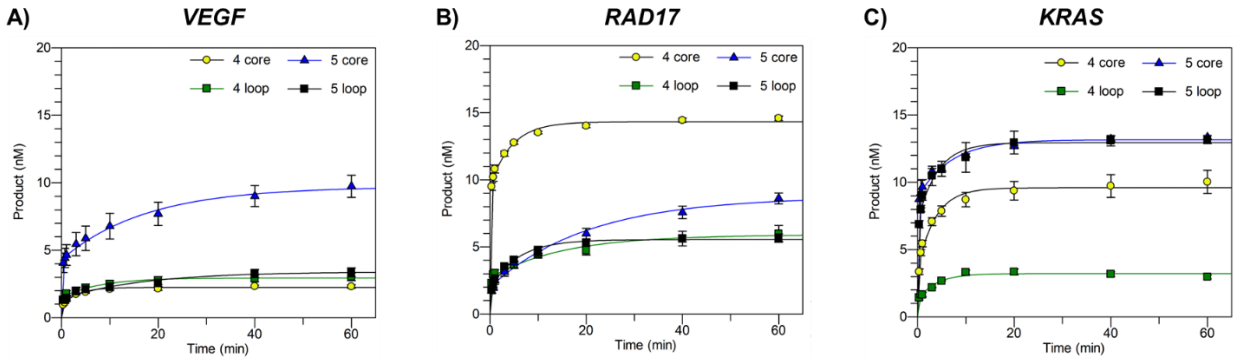

Figure 3.6: Removal of Gh from *VEGF*, *RAD17*, and *KRAS* promoter G4 by Edited (Ed) NEIL1.

20 nM of Gh containing (A) *VEGF*, (B) *RAD17*, or (C) *KRAS* G4 was incubated with 200nM Ed NEIL1 at 37°C, pH 7.6 in the presence of 100 mM KCl. Data is fit to a two-exponential equation, $[P]_t = A_0(1-\exp(-k_g't)) + B_0(1-\exp(-k_g''t))$. Values are reported in Table 3.1 and Table 3.3.

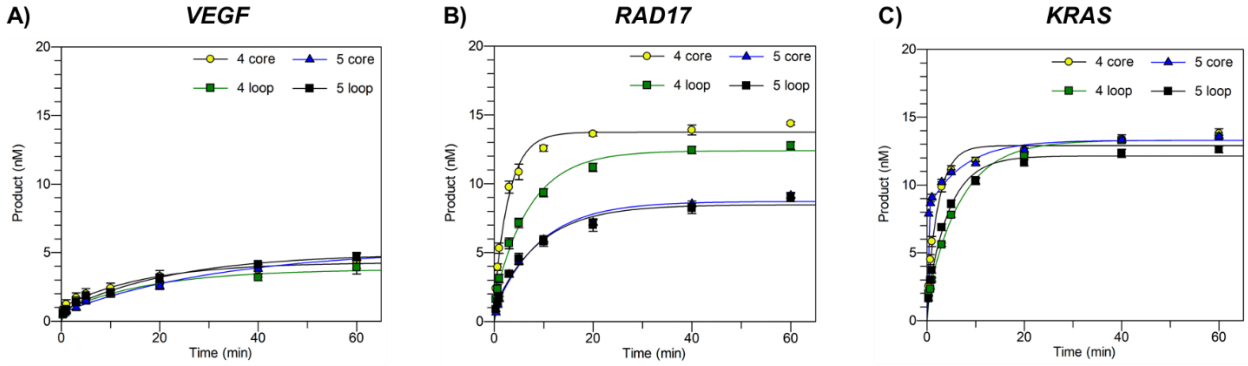

Figure 3.7: Removal of Gh from *VEGF*, *RAD17*, and *KRAS* promoter G4 by mNeil3 Δ324.

20 nM of Gh containing (A) *VEGF*, (B) *RAD17*, or (C) *KRAS* G4 was incubated with 200nM mNeil3 Δ324 at 37°C, pH 7.6 in the presence of 100 mM KCl. Data is fit to a two-exponential equation, $[P]_t = A_0(1-\exp(-k_g't)) + B_0(1-\exp(-k_g''t))$. Values are reported in Table 3.2.

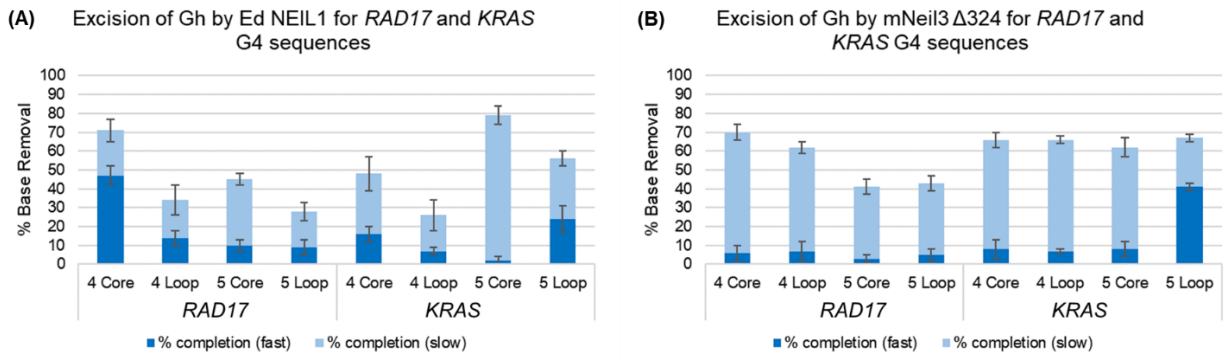

Figure 3.8: Percentage Gh removed by (A) Edited (Ed) NEIL1 and (B) mNeil3 Δ324 from the *RAD17* and *KRAS* G4s.

20 nM G4 was incubated with 200 nM enzyme for 60 min at 37 C and 100 mM KCl. Dark blue = % Gh removed with k_g'; light blue = % Gh removed associated with k_g". Values reported in Tables 3.2 and 3.3.

Comparison of Gh removal in SS, duplex and G4 DNA by Ed NEIL1 and mNeil3.

Each glycosylase is proposed to have different DNA context preferences. For example, NEIL1 has been previously shown to efficiently excise from duplex over SS DNA, while mNeil3 has a preference for SS DNA due to the additional negatively charged residues that would make an electrostatic clash with opposite strand in duplex.[44] Here, we evaluated the role of context on removal of Gh by Ed NEIL1 and mNeil3 Δ324 with the *RAD17* 4-track core sequence. G4s was directly compared to the corresponding duplex and single-stranded Gh-containing substrates. Excess enzyme (200 nM) was incubated with G4 (20 nM) in 100 mM KCl, single-stranded G4 in 100 mM LiCl, or duplex G4 annealed to its corresponding complement in 100 mM KCl. In the case of Ed NEIL1, Gh is removed most efficiently from the duplex context, as expected based on previous work by our laboratory and others. Upon visual inspection of representative storage phosphor autoradiograms (Figure 3.9), NEIL1 excised Gh the best from duplex, while mNeil3 excises Gh better from SS and G4 DNA contexts.

To explore these trends more fully, we performed full time courses to evaluate the excision of Gh from *RAD17* in SS, duplex and G4 DNA. NEIL1 excises Gh from single stranded DNA to a comparable extent for G4 (72% ± 2%) and single strand (72% ± 2%) DNA, and also with similar rates when fit to a 2-expontential equation (Table 3.4). However, with mNeil3 Δ324, Gh is removed more efficiently from G4 DNA context (71% ± 1%) followed by single stranded DNA (63% ± 1%) and with the least amount of excision out of duplex (50% ± 3%) (Table 3.4). For mNeil3, Gh is excised to a greater extent out of G4 context, but k_g'' is greater in a SS context followed by duplex compared to G4 (Table 3.4).

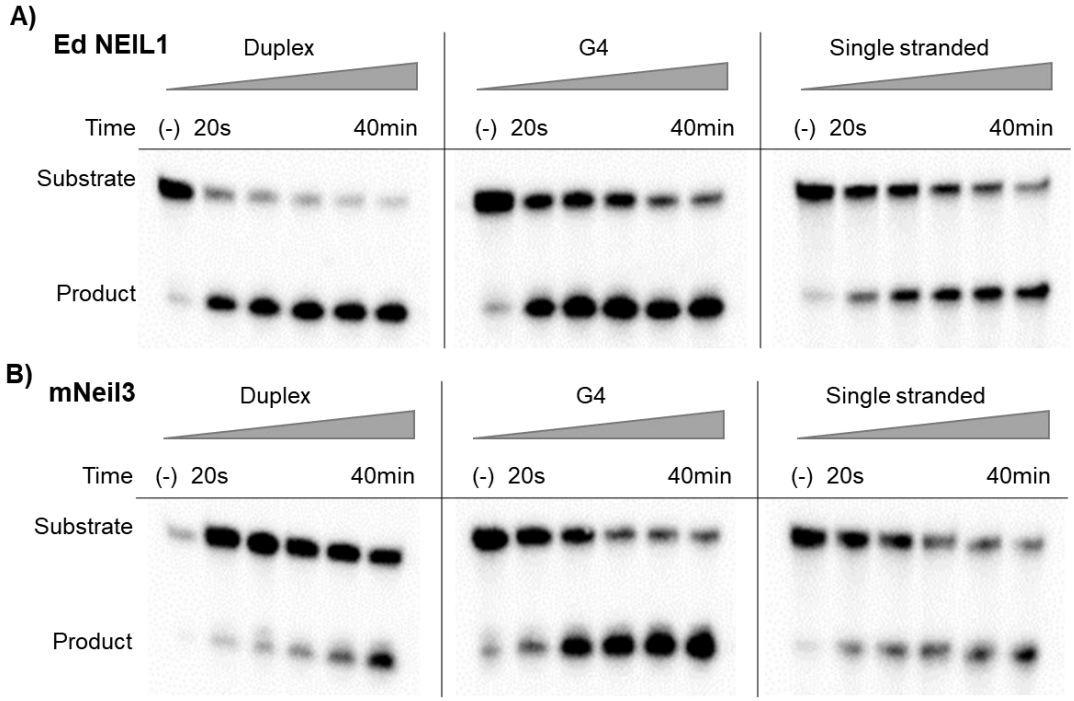

Figure 3.9: The removal of Gh from *RAD17* 4-core in single-stranded (SS), G-quadruplex, and duplex forms by (A) Edited (Ed) NEIL1 (B) mNeil3 Δ324.

For these representative storage phosphor autoradiograms, 200nM enzyme was incubated with G4 in 100mM KCl, SS G4 in 100mM LiCl, or duplex G4 annealed to its corresponding complement in 100mM KCl at 37 °C. Samples were quenched with NaOH at 20 s, 1 min, 5 min, 15 min, and 40 min. (-) represents the no enzyme control.

Table 3.4: Rates and excision completion of Edited (Ed) NEIL1 and mNeil3 Δ324 with *RAD17* 4-track core in duplex, G4, and single stranded contexts.

Ed NEIL1	Duplex	G4	Single Stranded
k_g' min^{-1} (A – nM)[a,b]	>2 (8.6 ± 0.8)	>2 (9.5 ± 1.0)	>2 (11 ± 1)
k_g'' min^{-1} (B – nM) [a,b]	0.28 ± 0.3 (3.02 ± 0.3)	0.23 ± 0.03 (4.8±1.2)	0.18 ± 0.05 (3.2 ± 0.4)
% base removed[c]	85 ± 3	72 ± 2	72 ± 2
	Duplex	G4	Single Stranded
k_g' min^{-1} (A – nM)[a,b]	>2 (1.9 ± 1.1)	>2 (1.1±0.2)	>2 (2.4 ± 1.4)
k_g'' min^{-1} (B – nM) [a,b]	0.6 ± 0.3 (8.7 ± 1.4)	0.38±0.04 (12±1)	0.82 ± 0.24 (11 ± 1)
% base removed[c]	51 ± 1	71±1	63 ± 1

[a] k_g' and k_g'' are the observed rates of base removal. The associated amplitude of each rate constant (capacity) in nM, and percent base removed of reaction after 60 min incubation. [Enzyme]= 200 nM, [DNA] = 20 nM, pH 7.6, 37 ºC, [KCl]=100mM, fit to a two-exponential equation, $[P]_t = A_0(1\text{-}\exp(\text{-}k_g\text{'}t)) + B_0(1\text{-}\exp(\text{-}k_g\text{''}t))$. [b] A_0 and B_0 are the associated amplitudes of k_g' and k_g'' respectively. [c] % base removed = $((A_0+B_0)/20)*100$.

Excision of Gh by mNeil3 from SS and duplex DNA by mNeil3 and NEIL3

We previously characterized the removal of Gh by NEIL1 in both single stranded (SS) and duplex DNA contexts.[136] However, similar analysis has not been performed with mNeil3 Δ324 or NEIL3 Δ324 to establish a base line for activity with these more traditional DNA contexts. The removal of Gh by mNeil3 Δ324 and NEIL3 Δ324 were evaluated with a non-G4 forming sequence (H30) using rapid quench flow methods. The data were fit to a one-exponential equation ($[P]_t = A[1 – \exp(\text{-}k_g t)]$) with these substrates similar to NEIL1 and compared to the values

obtained for Ed NEIL1. The percent base removed shown are obtained from the endpoint value (2 min) on quench flow methods unless stated otherwise. In agreement with previously reported values, mNeil3 Δ324 had a higher base removal for Gh in SS DNA (55% ± 7%) compared to duplex (29% ± 15%) (Table 3.5). However, the rate of excision is almost 2-fold greater in duplex than the SS DNA substrate (Table 3.5), which is surprising when mNeil3 is predicted to interact more favorably with SS DNA due to its many negatively charged amino acids that would destabilize interactions with duplex.[44] At 60 min time point, the percent base removed by mNeil3 Δ324 was more comparable for SS (83%) and duplex DNA (73%). Additionally, we were able to purify the human homolog, NEIL3 Δ324, and characterize its activity on Gh containing oligonucleotides in a SS or duplex DNA context. Like the mouse homolog, NEIL3 Δ324 removed Gh from a context (35% ± 7%) to a greater extent than duplex (< 10%), and we observed a higher k_g from duplex. However, due to the low amount of base removed in this assay, the k_g for NEIL3 Δ324 is likely an over estimation of the rate constant.

Table 3.5: Rate constants (k_g) and percent completion of base removal of Gh in H30 sequence in SS and duplex contexts by Ed NEIL1 and mNeil3 Δ324.

Substrate Context	Ed NEIL1, k_g, min^{-1} (% base removed)[a,b]	mNeil3 Δ324, k_g, min^{-1} (% base removed)[a,b]	NEIL3 Δ324 k_g, min^{-1} (% base removed)[a,b]
Gh SS	2.4 ±0.1 (<100)[d]	12±2 (55±7)	6.2±2 (35±7)
Gh:C duplex	104 ± 14 (100)[d]	20±6 (29±15)	112±20 (<10)[c]

[a]Rate constants of base removal were measured under single-turnover conditions (20 nM substrate, 200 nM enzyme) at 37 °C using a Kintek RQF-3 Rapid-Quench. Data were fit to a single exponential equation, $[P]_t = A_0[1 - \exp(-k_g t)]$. [b]The % base removed of reactions reflect the endpoint value (2 min) on quench flow methods . [c]The overall extent of product formation was very low such that the fitting is likely an overestimate of the rate. [d]Values for Ed NEIL1 have been reported previously in Yeo *et al.* 2010.

Effect of varied enzyme and G4 concentration on G4 excision.

In all of our Gh containing G4 sequences, we observe less than 70% total base removed by NEIL1 and mNeil3 Δ324 despite 10-fold excess enzyme present in the reaction. We explored the impact of DNA/enzyme ratio in the Gh removal reaction by varying both enzyme and DNA concentrations. First, the glycosylase was increased to 40-fold over DNA compared to previous work that used 10-fold enzyme compared to DNA. We selected three representative G4s to test the excision of Gh with increased enzyme: 4-track *RAD17* core damage, 4-track *KRAS* loop damage, and 5-track *VEGF* core damage. Notably, with 40-fold excess enzyme, we observed minimal change in rate or extent of base removal by Ed NEIL1 or mNeil3 Δ324 with all three G4s (Table 3.6).

Similarly, we also varied the concentration of the G4 to determine if G4 DNA concentration would alter the extent of Gh removed. A representative glycosylase assay was performed with Ed NEIL1 or mNeil3 Δ324 at 200 nM with either 1, 10, 50, 100, or 200 nM G4 DNA with the same three representative G4s, 4-track *RAD17* core damage, 4-track *VEGF* core damage, and 5-track *VEGF* core damage. Regardless of the DNA concentration and G4 sequence, Ed NEIL1 and mNeil3 Δ324 excised Gh to the same percent base removal as the original glycosylase assay conditions (20 nM G4 DNA and 200 nM enzyme). For *RAD17* 4 track core damage, total percent base removal was about 75% and 70% for Ed NEIL1 and mNeil3 Δ324 respectively (Figure 3.10A and B). With 4- and 5-track *VEGF* core damage, no change in total Gh base removal was observed either (Figure 3.10 C-F). Here, we see that varying the DNA and enzyme concentration does not alter processing of Gh by NEIL1 and mNeil3 Δ324, and likely engagement of the enzyme with G4 has a greater influence on excision.

Table 3.6: Percent base removal by Edited (Ed) NEIL1 and mNeil3 Δ324 from representative G4s (20nM) with 200nM versus 800nM enzyme.

Ed NEIL1	% base removed[a] 200nM enzyme	% base removed[b] 800 nM enzyme
4-track *RAD17* core Gh	73	77
4-track *KRAS* loop Gh	26	39
5-track *VEGF* core Gh	48	40
mNeil3 Δ324	% base removed[a] 200nM enzyme	% base removed[b] 800 nM enzyme
4-track *RAD17* core Gh	69	68
4-track *KRAS* loop Gh	67	73
5-track *VEGF* core Gh	23	39

[a]Percent base removed of reaction after 60 min incubation [Enzyme]= 200 nM or 800nM, [DNA] = 20 nM, pH 7.6, 37 ºC, [KCl]=100mM.

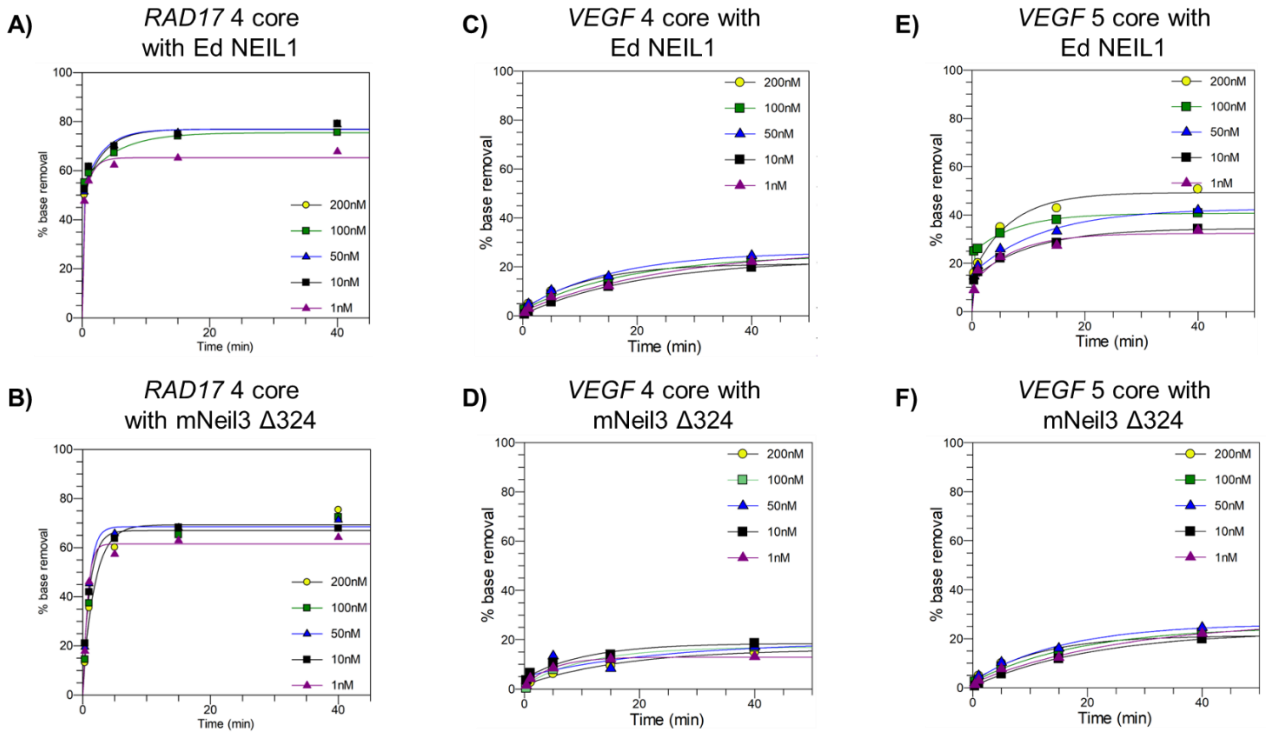

Figure 3.10: Representative plots of percent base removal of Gh from *RAD17* and *VEGF* at various concentrations of G4 with Edited (Ed) NEIL1 or mNeil3 Δ324.

G4s were incubated with 200nM enzyme at 37 °C and 100mM KCl. Reactions were quenched with NaOH at 20 s, 1 min, 5 min, 15 min, and 40 min before separation via denaturing PAGE.

Discussion

Differences in NEIL1 and mNeil3 influences Gh excision for G4

The work presented herein revealed distinct features for the removal of the oxidized guanine lesion, Gh, by NEIL1 and mNeil3 Δ324 from three distinct G4 sequences with Gh located at core and loop positions. We also evaluated the impact of the presence of a 5th G-track on Gh removal by NEIL1 or mNeil3 Δ324. Taken together, these results show that both NEIL1 and mNeil3 Δ324 can excise the damaged Gh base from several G4 sequences, but with distinct differences in efficiency and overall extent of lesion removed (Figure 3.11A).

A feature that emerged in our analysis of the kinetics of Gh removal by NEIL1 and mNeil3 Δ324 from G4s was better fitting of the data with a two-exponential equation, with two distinct rates and associated amplitudes. These two rates are likely due to the ability of the NEILs to capture Gh in productive and non-productive conformations for excision.[70] As discussed in chapter 2, stacking of Y244 on the lesion by NEIL1 can stall excision. However, crystal structures with Ed or UE NEIL1 bound to Gh containing DNA show both enzymes only in a productive state.[70] This is unsurprising as Gh is observed to be one of the best lesion substrates for both glycosylases.[39,124] For NEIL1, the preferred context is duplex DNA; NEIL1 can remove Gh across from C with a k_g of 104 ± 14 min^{-1}![124] NEIL1 can also efficiently excise Gh from single stranded DNA but at a slower observed rate (2.4 ±0.1 min^{-1}).[136] The two-exponential fit of the data from our G4 studies with NEIL1 give an initial faster rate (k_g') of >2 min^{-1} and on average a slower rate (k_g'') of 0.15 ± 0.05 min^{-1}. The associated "faster" and "slower" G4 rate constants are similar to that of the observed rate constants of Gh excision from duplex and single stranded DNA by NEIL1, respectively. The initial excision of Gh from G4s (characterized by k_g') is fast, similar to NEIL1's excision from duplex, while the second process, k_g" is much smaller indicating slower processing

and is in the same order of magnitude for the excision of Gh from single stranded DNA. The associated amplitudes of the two rates for Gh removed by NEIL1 are nearly equal. We suggest that the alternative G4 structure may allow for some of the Gh to be removed in a manner similar to that in duplex DNA, while the rest of the Gh in the G4 is in a structure more similar to SS DNA that requires more extensive remodeling for excision.

Where NEIL1 and mNeil3 differ is in their preferred substrate context. The data for mNeil3 Δ324 also best fit to a two-exponential equation with a k_g' of >2 min^{-1} and an average k_g'' of 0.16± 0.04 min^{-1} across all G4. The associated amplitudes to the rate show that a great population of Gh is excised at the smaller rate (k_g'') by mNeil3. Notably, mNeil3 excises Gh in single stranded DNA to a greater extent more readily than Gh from duplex yet at a faster rate from duplex (Table 3.4). Interestingly, the mNeil3 Δ324 crystal structure reveals that the enzyme has several negatively charged residues along the region that would interacting with the opposite strand of duplex DNA as compared to the structure of Fpg.[44] This electrostatic repulsion provides a rationale for poor interaction of mNeil3 with duplex.[44] However, in our studies of Gh excision from *RAD17* G4 in multiple substrate contexts, mNeil3 Δ324 has highest extent of base removal from G4 (71%) followed by single stranded (63%) DNA demonstrating a preference for the G4 context (Table 3.4). Yet, the k_g for mNeil3 Δ324 from a single stranded context is twice that of G4, and the best substrate context of mNeil3 are both G4 and SS DNA.

We did observe that both the non-G4 forming sequence and *RAD17* 4-track core damage have comparable rates of excision between SS and duplex DNA contexts. NEIL3 is predicted to have a preference for SS DNA, and we see that preference in the % base removal but with comparable rates of excision in both contexts. It is worth noting that the truncated form of the NEIL3 proteins was used in these assays, as the full-length protein can be difficult to purify due

to the highly disordered C-terminus.[44] However, this truncation removes NEIL3's two GRF zinc fingers, which have been shown to preferentially bind to SS DNA and splayed replication fork. These zinc fingers have been found regulate the activity of the NEIL3 glycosylase domain in biochemical assays with SS DNA and splayed replication forks.[47] The absence of this domain may allow for some of the similarity in the observed rates better duplex and SS DNA.

G4 stability aligns Gh excision by NEIL1 and mNeil3

The kinetics of Gh removal by NEIL1 and mNeil3 in the three different G4s revealed that the sequence of the G4 had the largest impact on Gh removal activity. For both NEIL1 and mNeil3, the greatest extents of Gh removal were observed from the *RAD17* and *KRAS* G4 structures. The extents of Gh removal from the *VEGF* G4 was particularly low, especially for mNeil3. The observed sequence dependence suggests that features of the G4 structure impacts the ability of NEIL glycosylases to mediate Gh excision. The sequence of the G4 also influences the type of G4 structure adopted (Figure 3.11B), as well as its overall stability. Table 3.7 shows the reported topologies and thermal stabilities of the *VEGF* and *RAD17* G4. The *KRAS* topology is still being evaluated and the thermal stabilities are preliminary values provided by Dr. Aaron Fleming from the University of Utah. In the presence of KCL, all G4 sequences adopt G4 structures as verified on native page (data not shown). Of note, each G4 was evaluated with different lesions (*VEGF* - Gh, *RAD17*-OG, and *KRAS* - abasic site analog, THF). The lesion present will further vary the stability of the G4, but a small decrease in stability was seen between similar *VEGF* G4 containing OG versus Gh. These values provide insight into features of the G4 structure and stability related to the G4 sequence.

The *VEGF* G4 has the highest thermal stability of the three G4 sequences evaluated. Moreover, introduction of Gh into the *VEGF* 4-track and 5-track G4 in most cases resulted in

minimal reduction of stability (Table 3.7). The notable exception is with Gh introduction into 4-track *VEGF* in a core position (ΔTm ~ -20 °C). In contrast, *RAD17* and *KRAS* 4- and 5-track G4s have generally lower T_m's (ΔTm ~ -10-20 °C).[137] Our NEIL glycosylase assays show higher levels of Gh removal from G4s with lower T_m's. The higher stability of the *VEGF* G4s may limit the access and ability of the glycosylases to flip Gh into the active site with the proper alignment to promote glycosidic bond hydrolysis.

Table 3.7: Topology and thermostability of undamaged and lesion containing *VEGF* and *RAD17* G4.

VEGF G4	4 WT	4 Core (Gh)	4 Loop (Gh)	5 WT	5 Core (Gh)	5 Loop (Gh)
Topology	Parallel	Triplex	Parallel	Parallel/ Hybrid mix	Parallel/ Hybrid mix	Parallel/ Hybrid mix
T_m (℃)	85.6	63.4	85.5	79.1	80.5	83
RAD17 G4	4 WT	4 Core (OG)	4 Loop (OG)	5 WT	5 Core (OG)	5 Loop (OG)
Topology	Hybrid	Triplex	Anti-parallel	Mix of topologies	Parallel	Parallel
T_m (℃)	69.5	40.9	63.8	68.6	63.9	65.4
KRAS G4[a]	4 WT	4 Core (THF)	4 Loop (THF)	5 WT	5 Core (THF)	5 Loop (THF)
Topology	*?*	*?*	*?*	Parallel	*?*	*?*
T_m (℃)	50	43	57	50	50	60

Values *VEGF* G4 are reported in Zhou *et al.* 2015 and *RAD17* G4 in Zhu *et al.* 2018. [a]*KRAS* G4 are unreported preliminary values provided by the Dr. Aaron Fleming and still undergoing further analysis.

The position of the Gh within the G4 had a more dramatic impact on Gh removal by NEIL1 than mNeil3 Δ324. The highest extent of Gh removal by NEIL1 was observed with Gh located at a core position within the G4 in 4-track G4s. The extent of NEIL1 mediated Gh removal was 40% greater when Gh was located at a core position compared to loop position within *RAD17* 4-track G4 (Table 3.3). The presence of Gh in a core position in the *RAD17* 4-track G4 decreases the T_m about 25 °C compared to non-lesion containing G4 (Table 3.7).[137] A similar drop in the thermal stability has been observed in *VEGF* and *KRAS* 4-track sequences when damage was inserted at the core position (Table 3.7).[85,137] Introduction of Gh into the G-tetrad results in loss of planarity and hydrogen bonds that help to stabilize the tetrad and overall G4. This decrease in stability of the G4 may make it more readily remodeled, facilitating the ability of NEIL1 to position the Gh lesion in a conformation needed for base excision catalysis.

In previous work, presence of an additional 5-track of guanines downstream of the four G-tracks required for G4 formation, has been proposed to serve as a "spare tire" for the G4, where the 5th track can replace the G-track containing the damage to stabilize the G4 structure.[135] With *VEGF*, the presence of the 5th track greatly increases Gh-excision located within the core by NEIL1, as reported previously. With the *KRAS* G4, the presence of the 5th track enhanced Gh removal from both core and loop positions, while in the RAD17 G4, there was a small decrease in Gh excision in the presence of the 5th track. All Gh-containing 5-track G4's evaluated in this study have similar T_m's to the 5-track G4 without damage indicating maintenance of G4 structure. These results suggest that the 5th track may restructure the G4 in such a fashion that positions the Gh in a manner that facilitates its excision, and the impact of the 5th track on the structure is dependent on the specific G4. However, further studies examining the G4 structure in the presence of enzyme

will help to identify the location of the 5th track and if the 5th track stabilizes G4 during base excision.

In contrast to NEIL1, mNeil3 Δ324 excision is not enhanced for Gh located within the G4 core nor with G4s sequences containing the additional G 5th track. These substrate specific differences are likely related to structural differences between the two glycosylases. NEIL3 lacks two of the void filling residues present in NEIL1, Arg118 and Phe120, which are known to play important roles in NEIL1 excision of damaged lesions in duplex DNA.[140] Specifically, Phe120 serves as wedge between the base opposite the lesion causing a bend in the DNA and may also contribute to the identification of non-planar bases like Gh in duplex DNA.[140] Arg118 forms a H-bond with the opposite base in duplex DNA and may influence opposite base preferences of NEIL1.[46] The lack of the equivalent Arg and Phe and additional negatively charged residues in NEIL3 provides a rationale for the preference for lesion removal from single stranded over duplex DNA contexts. Notably, NEIL3 has been observed to unhook abasic site crosslinks,[24] which would proceed in an alternative fashion to the base flipping mechanism of DNA glycosylases. The lack of void filling residues compared to that of NEIL1, paired with the insensitivity to core damage and the presence of the 5th track suggest that the increased flexibility and accessibility of the lesion does not influence excision by mNeil3, and rather, mNeil3 may recognize damage in various G4s similarly.

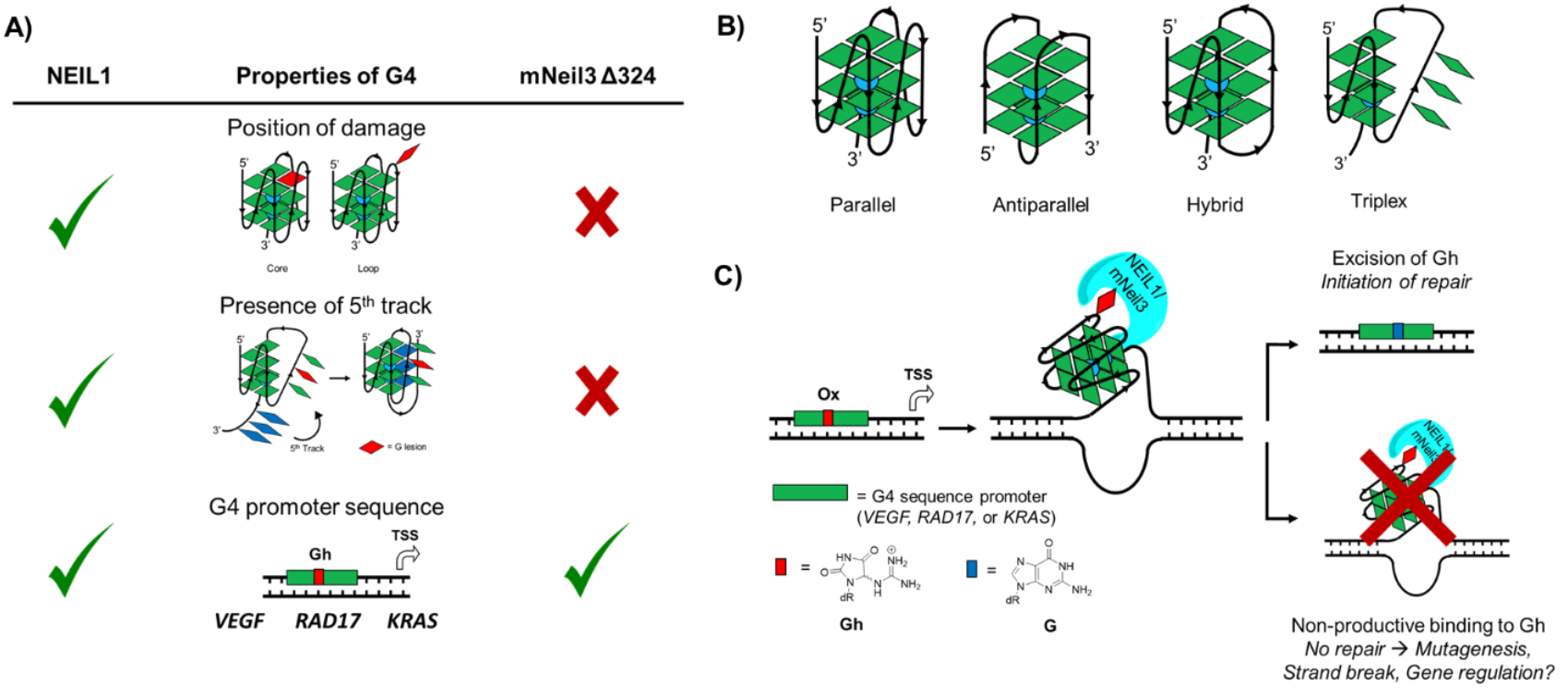

Figure 3.11: Factors and consequences of excision of Gh from G4.

(A) The promoter sequence has the greatest influence on excision of Gh from G4 structures for both Edited (Ed) NEIL1 and mNeil3 Δ324. Ed NEIL1 is more sensitive to the position of damage and the presence of the 5th track where as mNeil3 Δ324 is not. (B) Topologies of G4 structure. (C) The cellular implications of Gh removal and repair by NEIL glycosylase. Initiation of BER by NEIL1 or mNeil3 can either lead to restoration of the guanine base, or non-productive binding that could have a number of effects, including mutagenesis, strand breaks, or possible participation in G4 mediated gene regulation.

Reduced excision may relate to roles biological NEIL1 and mNeil3

A striking feature of Gh removal within G4s by NEIL1 and mNeil3 Δ324 is that a significant fraction of the Gh is not removed. The overall extent of Gh removed ranges from 10% to 70%, with differences due to the G4 sequence, Gh lesion position, and specific NEIL glycosylase. Increasing the concentration of G4 DNA or NEIL enzyme did not change the extent Gh removed. In contrast, Gh excision by NEIL1 in duplex DNA proceeds efficiently and to completion. We have observed that some lesion substrates, such as 5-OHU, Ug and DHT, are not completely removed by NEIL1, and the levels of lesion removed are strongly influenced by the opposite base and the NEIL1 isoform.[49,139] We have proposed that this feature of reduced excision may be due to non-productive binding of NEIL1 and may be a way to regulate excision in different contexts and other different conditions.[49,139] NEIL1 has been shown to slow replication fork progression functioning as a "cowcatcher" to identify DNA damage in oxidatively stressed cells. In its role as the "cowcatcher", NEIL1 binds the lesion but does not immediately excise it, signaling the need for repair.[45,82] It is possible NEIL1 binding to G4s could function in a similar fashion. NEIL3 has been found to localize to telomeres,[96] which consists of many G4 structures. This localization occurs during S phase, a stage in the cell cycle where DNA is highly susceptible to oxidation. Indeed, the binding of NEIL1 or NEIL3 to Gh within a G4 may be an important aspect of their cellular function and be related to whether the "damage" should be removed and replaced or serve as means to regulate transcription or replication (Figure 3.11C).

Potential NEIL involvement with G4 mediated gene regulation

The ability of the NEIL glycosylases to interact with G4 structures is intriguing as increasing amounts of literature suggest that G4s play a role in gene regulation. Gh, like OG, may be "epigenetic" and influence gene transcription. Previous work has shown that formation of OG

within a PQS, followed by excision by OGG1, leads to recruitment of APE1 as an activation factor for gene expression.[102] Cogoi *et al.* also noted a regulatory like property from guanine oxidation with the *KRAS* G4, where OG enhanced the recruitment of MAZ and hnRNP, two nuclear factors that are essential for transcription.[138] Because Gh is a further oxidation product of OG, this lesion could be playing similar roles in G4 structures. NEIL1 associated Werner syndrome protein (WRN),[90] which has the ability to unravel G4s, may allow NEIL1 to further access damage in G4's.[84] Additionally, Y-box protein 1 (YB-1) can regulate NEIL1 lyase activity and stimulate NEIL1,[143] and in turn NEIL1 can stimulate OGG1 in the removal OG.[83] While these interactions can modulate the response to oxidative stress, WRN and YB-1 have been observed in activating transcription, suggesting that NEIL1 may not simply be acting as a DNA repair enzyme.[9] The unproductive binding observed here with NEIL1 and mNeil3 may be a signal for repair or transcription, which is a pattern that has been noted with other BER pathway enzymes. To further elucidate this potential role additional cellular studies are needed to support our biochemical results.

Herein, we have elucidated the unique features of oxidative damage containing G4s that influence excision of Gh by NEIL1 and mNeil3 Δ324. The sequence had the greatest influence on the excision with greater base removal from *RAD17* and *KRAS* G4. Overall, less excision was observed from the *VEGF* G4. NEIL1 is more sensitive to the position of damage and presence of the 5th track, whereas the core position and the 5th track in the *RAD17* and *VEGF* sequences enhance the removal of Gh. In contrast, mNeil3 Δ324 remained largely insensitive to core vs loop position or the presence of a 5th track. Both NEIL1 and mNeil3 Δ324 do not have complete removal of Gh despite the lesion being an excellent substrate for both glycosylases in their preferred contexts. Oxidation of guanine in G4 has been considered epigenetic and the subsequent binding

of BER enzymes in promoter G4 is essential to this process. The incomplete excision and subsequent non-productive binding of NEIL1 or NEIL3 to Gh containing G4 suggest that the NEIL glycosylase may play a role in this epigenetic mechanism, but further investigation is warranted to elucidate NEIL's exact role.

Future work

The NEIL glycosylases are capable of excising a wide range of lesions from several DNA contexts. The work presented here has established a relationship between G4 sequence on the impact of excision. However, the only lesion probed in these studies was Gh. The NEIL glycosylases may also excise lesions such as Tg, FapyG, and 5-OHU differently in a G4 context compared to duplex. This work is currently in progress by other members of the David laboratory. Additionally, NEIL2 was not evaluated in these studies. NEIL2 is known to be associated with transcription coupled BER[48] and may play a role in G4 gene activation scheme that relies on activity by BER glycosylases. NEIL2 does have a higher activity on AP sites than the lesion themselves, so NEIL2 may play a similar role to APE1 in this gene activation pathway or process the AP site and help to erase the signal.

Materials and Methods

General methods and materials. DNA oligonucleotides containing OG were synthesized at the University of Utah Core Facility (University of Utah Medical School), and the OG phosphoramidite was purchased from Glen Research. The oligonucleotides were cleaved and deprotected following Glen Research's protocol for OG-containing DNA strands. All other lesion-free oligonucleotides were purchased from IDT. All oligonucleotides were purified via HPLC on a Shimadzu Prominence instrument with a Dionex PA100 anion-exchange column. [γ-^{32}P]ATP was purchased from Perkin Elmer, and T4 polynucleotide kinase from New England BioLabs.

Microspin G-50 columns were purchased from GE Life Sciences. Storage phosphor autoradiography was performed on either a Typhoon 9400 (GE) phosphorimager, or a Molecular Dynamics Storm 840 phosphorimager system. ImageQuaNT software version 8.2.0 (GE Life Sciences) was used for image quantification, and GraFit version 5.0.2 (Erithacus Software) was used to determine rate constants and percent completion values. All buffers and acrylamide solutions were made with distilled, deionized water purified from a Milli-Q PF system. All other reagents were purchased from VWR, Fisher Scientific, or Millipore-Sigma.

Substrate DNA preparation. All Gh-containing G4s reported in Table 3.8 were prepared from OG containing oligos synthesized at the University of Utah Core Facility. OG containing oligos underwent selective OG oxidation using K_2IrBr_6 and purified from the OG-containing oligonucleotides as previously described.[85] ESI-MS analysis confirmed the identity of the lesion containing oligonucleotides. The appropriate lesion-containing G4 was 5' end-labeled with [γ-^{32}P]ATP using T4 polynucleotide kinase at 37 °C, and then purified using a G-50 spin column per manufacturer's protocol. Additional nonradioactive G4 DNA was added to the labeled strand to allow for a final yield of 5% labeled DNA. The G4 mixture was allowed to fold by heating to 90 °C for 5 min and cooling to 4 °C overnight in folding buffer (20 mM Tris-HCl pH 7.6, 10 mM EDTA, and 100 mM KCl). Labeled G4 substrates were stored at -20 °C and used for both G4 glycosylase and electrophoretic mobility shift assays as described below. To generate single stranded G4 sequence, 5% labeled DNA was heated at 90 °C for 5 min allowed to cool in the following buffer: 20 mM Tris-HCl pH 7.6, 10 mM EDTA, and 100 mM LiCl. For G4 duplex, 5% labeled DNA was annealed to a 20% excess of the nonradioactive complementary strand in annealing buffer (20 mM Tris-HCl, pH7.6, 10 mM EDTA, 100 mM KCl) by heating to 90 °C for 5 min and cooling to 4 °C overnight.

Table 3.8: Sequences used in G4 glycosylase studies.

G4	Damage position	Sequence
VEGF 4	Loop	5'-CGGGGCGGGCC**X**GGGGCGGGGT-3'
VEGF 4	Core	5'-CGGGGCGGGCCG**X**GGGCGGGGT-3'
VEGF 5	Loop	5’-CGGGGCGGGCC**X**GGGGCGGGGTCCCGGCGGGGC-3’
VEGF 5	Core	5’-CGGGGCGGGCCGG**X**GGCGGGGTCCCGGCGGGGC-3’
RAD17 4	Core	5’-CCGGGAGGGACT**X**GGCTGGGGCA-3’
RAD17 4	Loop	5’-CCGGGAGGGACTGGGCT**X**GGGCA-3’
RAD17 5	Core	5’-CCGGGAGGGACT**X**GGCTGGGGCAGGCTGGGGCG-3’
RAD17 5	Loop	5’-CCGGGAGGGACTGGGCT**X**GGGCAGGCTGGGGCG-3’
KRAS 4	Core	5’-AGGGCGGTGT**X**GGAAGAGGGA-3’
KRAS 4	Loop	5’-AGGGCGGTGTGGGAA**X**AGGGA-3’
KRAS 5	Core	5’-AGGGCGGTGT**X**GGAAGAGGGAAGAGGGGGA-3’
KRAS 5	Loop	5’-AGGGCGGTGTGGGAA**X**AGGGAAGAGGGGGA-3’
Non- G4		**Sequence**
H30		5’-TGTTCATCATGGGTC**X**TCGGTATATCCCAT-3’

X indicates position of Gh. In G4, the lesion is placed in either the core of the G-tetrad or the loop region.

Enzyme purification. C-terminally His-tagged edited (R242) and unedited (K242) NEIL1 were purified as described previously by expressing NEIL1 in Rosetta 2 (DE3) pLysS cell strains from Novagen using a pET30a plasmid containing the NEIL1 gene. The active site concentrations of the enzymes were determined using previously reported methods.[136] Purified enzymes were stored at -80 °C. NTHL1 and truncated mouse and human NEIL3 were provided from Dr. Susan Wallace and her research group at the University of Vermont.

NEIL3 Δ324 was purified in similar to methods previously reported.[140] Briefly, NEIL3 Δ324 was over expressed in Rosetta 2 (DE3) pLysS cell strains from Novagen using a pET30a plasmid containing the NEIL3 Δ324 gene. Cells were lysed via sonication and followed by centrifugation. To the supernatant, imidazole and NaCl (20 m*M* and 1 *M* final concentration respectively) were added to the resuspended pellet and batch bound to Ni2+-NTA resin (Qiagen) for 1 h. The slurry was poured over a PD10 column and allowed to flow through via gravity. The

resin was washed with 10 ml wash buffer (20 m*M* sodium phosphate buffer pH 7.5, 10 % glycerol, 1 *M* NaCl and 20 m*M* imidazole) followed by elution buffer (20 m*M* sodium phosphate buffer pH 7.5, 10 % glycerol, 300 m*M* NaCl and 500 m*M* imidazole). The elutant was then concentrated with Amicon ultrafiltration cell with a 10,000 MWCO filter while stirring and diluted 10-fold with heparin buffer A (40 mM Hepes–NaOH pH 7.0, 10% glycerol, 5 mM β-mercaptoethanol), NEIL3 Δ324 were further purified by a 5 ml HiTrap Heparin column (Buffer A: 40 mM Hepes–NaOH pH 7.0, 150 mM NaCl, 10% glycerol, 5 mM β-mercaptoethanol; Buffer B: 40 mM Hepes–NaOH pH 7.0, 1 M NaCl, 10% glycerol, 5 mM β-mercaptoethanol). Protein concentration was determined via Bradford assay, and active site concentration was determine using previously reported methods with single stranded Gh-containing *RAD17* 4 track core oligo.[136]

Representative glycosylase assays. For the representative glycosylase assays, 20 nM of substrate DNA was incubated at 37°C with 200 nM of active enzyme, either Edited (R242) or Unedited (K242) NEIL1, NEIL3 Δ324, or NTHL1, in glycosylase assay buffer (20 mM Tris-HCl pH 7.6, 10 mM EDTA, 0.1 mg/mL BSA and 100 mM KCl). Aliquots were removed from the reaction mixture at 30 minutes and immediately quenched in 0.2 M NaOH. Then the mixture was heated to 90 °C for 5 minutes and cooled down on ice. Formamide denaturing dye (80 % formamide, 0.025 % bromophenol blue, 0.025 % xylene cyanol in TBE buffer) was added to each aliquot and heated to 90 °C for 5 minutes. All samples were electrophoresed on 15 % (19:1) denaturing polyacrylamide gel with 1X TBE buffer at 1500 V for 1.5 hours. The polyacrylamide gel was exposed to Molecular Dynamics phosphorimager screen for at least 18 h.

Kinetic parameters measured using Glycosylase assay. The glycosylase activity of Edited (Ed - R242) NEIL1 and mNeil3 Δ324towards G4 DNA substrates was measured under single-turnover conditions ([Enz]>[DNA]) as previously described.[49] Briefly, 20 nM of G4 DNA was

incubated at 37 °C with 200 nM of active enzyme in G4 glycosylase assay buffer (20 mM Tris-HCl pH 7.6, 10 mM EDTA, 0.1 mg/mL BSA and 100 mM KCl). Aliquots were removed from the reaction mixture at various time points ranging from 20 s to 60 min, and the reactions were quenched in 0.2M NaOH, heated to 90 °C for 5 min, and flash frozen on ice. Equivalent amounts of formamide denaturing dye (80% formamide, 0.025% bromophenol blue, 0.025% xylene cyanol in 1X TBE) was added to each aliquot and heated once again to 90 °C for 5 min before electrophoresis on a 15% (19:1) denaturing polyacrylamide gel in 1X TBE at 1500 V for 1.5 h and visualization by storage phosphor autoradiography. The analysis of the data and determination of the rate constants and percent completion values was analogous to that previously reported for NEIL and data were either fit to a one-exponential equation $[P]_t = A_0[1 - \exp(-k_g t)]$ or two-exponential equation $[P]_t = A_0[1 - \exp(-k_g' t)] + B_0[1 - \exp(-k_g'' t)]$ to determine the rates of product formation (k_g or k_g' and k_g") and their associated amplitudes, A_0 and B_0.[49,139] For experiments in which the reaction was too fast to measure manually, a Kintek RQF-3 Rapid-Quench instrument was utilized as previously reported.[52]

Chapter 4 Monitoring DNA repair capacity of NEIL substrates in cells

Contributions of others: Dr. Jongchan Yeo developed and validated the pTurbo reporter for monitoring the repair for Gh and Tg by NEIL1 in MEF cells. The FapyG-containing oligonucleotide was synthesized and characterized by Dr. Haozhe Yang from the laboratory of Dr. Marc Greenberg. The 2'ribo-fluoro-OG phosphoramidite was synthesized and incorporated into oligonucleotide by Dr. Sheng Cao of the David Laboratory.

Introduction

Modified bases can be indicators of oxidative stress and associated with many diseases including cancer neurodegenerative diseases and metabolic disorders.[2,144] A wide range of modifications are formed in a cellular context requiring repair to maintain genomic integrity.[2,144,145] DNA damage can disrupt cellular processes, such as replication and transcription, and introduce mutations leading to disease progression. The study of lesion formation and repair have been critical to understanding diseases, such as cancer, and how our cells thwart oncogenesis by genomic maintenance.[2,144,145] Our cells have several pathways for combating the diverse range of lesions. The base excision repair pathway, initiated by DNA glycosylases, is responsible for the recognition and repair of many of these modifications. The lesions guanidinohydantoin (Gh), thymine glycol (Tg), and 2,6-diamino-4-hydroxy-5-formamidopyrimidine (FapyG) are good substrates of NEIL1 and have been well characterized *in vitro.*[38,56,136] Gh and FapyG are non-planar and helix distorting lesions and stall activity of DNA and RNA polymerases,[10,146] and in cases where replications occurs, they are mutagenic leading to G-to-T transversion mutations.[11,146] Tg has also been shown to block activity of polymerases involved in both replication and transcription.[14] However, cellular conditions can impact lesion specific repair and efficiency, and the development of cellular reporter assays can provide a benchmark for repair levels of these NEIL substrates in a cellular context.

The David laboratory has established a mammalian cellular reporter assay to evaluate the OG:A specific repair by WT and cancer associated variants of MUTYH.[147] This assay features a reporter plasmid where the installation of a site-specific OG:A mismatch introduces a stop codon in the coding region of a green-fluorescent protein (GFP). MUTYH-mediated excision of the mispaired A, followed by downstream BER results in replacement of the A with C, and restoration

of an amino acid codon for expression of full-length GFP. Repair can be monitored by the proportion of transfected cells (RFP positive) that also express GFP.[147] Similar reporter systems have been developed by the Samson and Nagel laboratories to probe repair by other BER glycosylases and other repair pathways, such as NER or direct repair.[148] They leverage a diverse number of lesions to monitor different repair pathways and evaluate the repair of the lesion itself. These probes have been used to study DNA repair capacity along multiple disease cell lines as repair can vary due to different expression levels of enzymes associated in DNA repair pathways.[148,149] The type of damage have the potential to impact repair capacity warranting further study. The repair of lesions, Gh, Tg, and FapyG have never been evaluated in a cellular context. Monitoring the repair capacity of specific lesions in several cell lines can then be leveraged as a diagnostic tool to understand disease. While there are several assays monitoring the repair of many DNA repair pathways, there is no published assay to monitor cellular repair by specific lesions and potentially evaluate repair by NEIL1.

Dr. Jongchan Yeo of the David laboratory had developed and validated a reporter plasmid to monitor the repair of NEIL1 in mouse embryonic fibroblasts (MEF) cells.[150] The NEIL1 pTurbo reporter plasmid was adapted from a similar reporter developed by the Wang laboratory for the incorporation of transcriptionally blocking lesion to evaluate repair *in vitro* and in mammalian cells.[151] The NEIL1 substrates Tg, Gh, and FapyG have been shown to stall DNA and RNA polymerases[14,152,153] making them well suited for this plasmid design. Validation of NEIL1 specific repair was performed by comparing repair in WT MEF and *Neil1-/-* MEF via flow cytometry. For both the Gh and Tg lesion, repair in *Neil1-/-* MEFs was greatly diminished compared to that of WT MEFs suggesting that the absence of Neil1 was responsible for reduction in GFP expression.[150] From *in vitro* biochemical analysis, Tg, Gh, and FapyG are all known to be excellent

substrates for NEIL1 and are efficiently processed.[56,136] However, further evaluation is needed to examine if we can observe repair across multiple cell lines and if there will be differences in repair across the cell types and under different conditions.

In this chapter, I used a GFP expression reporter plasmid to monitor the repair of Tg, Gh and FapyG in HEK293FT, HeLa and U87 cells. The levels of NEIL1 vary in these cell lines, and we hypothesized that extents of repair of these lesions may similarly vary. Variations in repair as monitored by our reporter system can be indications of cellular DNA repair function, especially in cancer cells which may have deficits or alterations in DNA repair.[154,155] Additionally, I evaluated the repair of 2'-F-Gh as a molecular probe that is resistant to NEIL1 mediated repair. 2'-fluorinated deoxyribose modifications have been useful chemical biology tools for the study of many DNA glycosylases.[67,68,156,157] The addition of the fluorine at C2' can slow or inhibit the breaking of the N-glycosidic carried out by DNA glycosylases. 2'-F-Tg and 2'-F-Gh have been shown to dramatically inhibit the efficiency of base excision by NEIL1.[67,68] Here, I installed 2'-F-Gh into our reporter assay to evaluate it as mean of inhibiting or reducing repair.

Finally, we began examining RNA editing of NEIL1 transcript in a cellular context. As discussed in chapter 2, two isoforms of NEIL1 exist due to an RNA editing event catalyzed by ADAR1. The NEIL1 pre-mRNA has a codon encoding for a lysine at position 242 in the NEIL1 lesion recognition loop of NEIL1. A-to-I editing of ADAR1 at position 725 of the NEIL1 transcript producing in a codon change and resulting in an arginine at position 242. The David laboratory has well characterized the activity of unedited NEIL1 (UE-Lys242) and edited NEIL1 (Ed-Arg242). This single amino acid change can greatly alter the substrate specificity of the NEIL1 glycosylase. The UE NEIL1 excises Tg ~30 faster than Ed NEIL1.[136] Generally, the unedited isoform can more rapidly excise oxidized pyrimidines to that of Ed NEIL1, but characteristics of

lesion can influence excision. Here, we conducted some preliminary studies examining the influence of ADAR1 on NEIL1 activity in a cellular context. We began by establishing the editing levels of the NEIL1 transcript in HEK293FT, HeLa, and U87 cell lines and increased the editing of NEIL1 transcript with treatment of interferon alpha (IFN-α), which has been previously shown to increase ADAR1 expression.[158] We then explored repair of Gh and Tg lesions in HEK293FT, HeLa, and U87 cells treated with IFN-α to increase ADAR1 expression and editing of NEIL1 transcript. Regardless of lesion, repair by NEIL1 decreased across all cell lines upon IFN-α treatment.

Results

Generation of lesion pTurbo reporter plasmid and installation of lesions

The lesion reporter plasmid was previously designed by Dr. Jongchan Yeo from the David laboratory and discussed in detail in his doctoral dissertation.[150] Briefly, this lesion plasmid reporter (pTurbo - pT) was adapted from the pTurboGFP-Hha10 reporter plasmid developed to quantitatively assess the impact of DNA damage on transcription efficiency and fidelity *in vitro* and in mammalian cells by the Wang laboratory.[159] This method employs the site-specific incorporation of a DNA lesion downstream of the CMV promoter of GFP with the generation of gapped plasmid using nicking enzymes for the efficient installation.[151] The design of pTurboGFP-Hha10 was adapted for the study of NEIL1-initiated repair in mammalian cells to allow for the incorporation of transcriptionally blocking lesions in the H30 sequence that was previously used for the *in vitro* enzyme assays for NEIL1. Some of the best NEIL1 substrates, Tg, Gh, and FapyG, stall the activity of DNA and RNA polymerases.[14,146,152] and if installed upstream of reporter gene, could thwart transcription.

To generate lesion containing plasmid, Nt.BstNBI nicking endonuclease is used to generate a single strand nick in the template strand of the plasmid. The resulting 43 nucleotide (nt) oligo from plasmid nicking is removed by annealing to its complement. The gapped plasmid is purified away from excess complement and annealed duplex with Macherey-Nagel DNA purification kit. 5'-phosphorylated lesion containing oligonucleotide, H30, (30nt) and short downstream filling oligonucleotide (13nt) were annealed into gap of pTurbo and ligated with T4 ligase. To remove any unsuccessful ligation reactions, the ligation reaction was treated with T5 exonuclease to digest any remaining gapped plasmid and subsequently purified with DNA purification kit (Figure 4.1A). Plasmid generation was monitored via agarose gel electrophoresis (Figure 4.1B). Since the development of the pTurbo plasmid by Dr. Yeo, modifications to plasmid generation have allowed for higher yield of the final lesion containing product. First, purification of the pTurbo plasmid was conducted with a CsCl gradient procedure (see methods) compared to traditional use of mini-prep or midi-prep plasmid preparation kits. These kits have an alkaline lysis step for cell lysis and may damage the starting plasmid. With CsCl gradient purification, higher yields of final lesion containing plasmid were obtained (data not shown). Additionally, the use of Macherey-Nagel DNA purification kit led to higher yields at purification steps opposed to other methods, such as spin filter purification or ethanol purification.

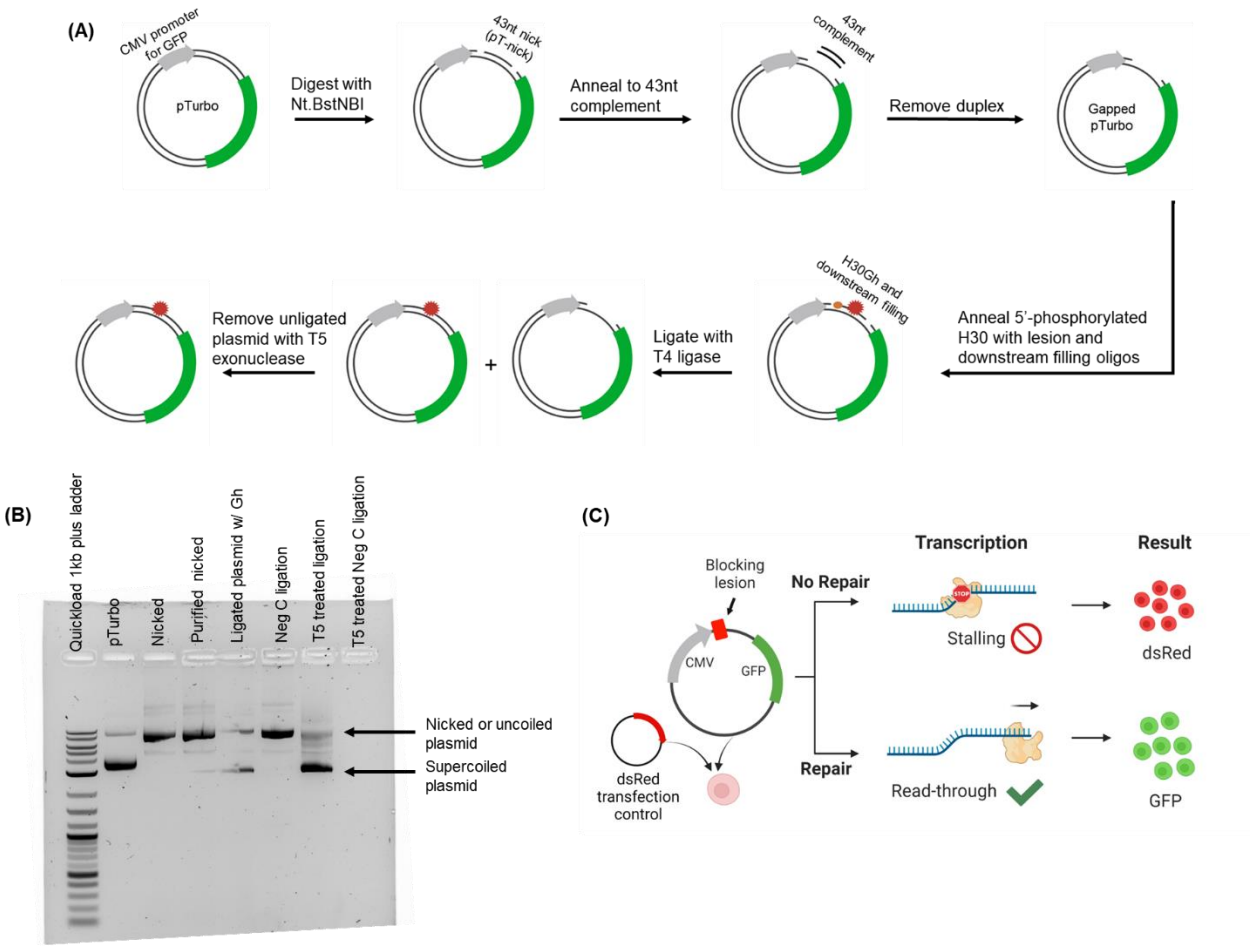

Figure 4.1: Construction of lesion reporter and monitoring lesion repair.

(A) Schematic of incorporation of lesion (Ex: Gh) into pTurbo reporter plasmid. A single strand 43nt nick (pT-nick) is introduced downstream of the CMV promoter to GFP. pT-nick is annealed to excess complement and the gapped plasmid is purified from excess duplex. 5'-phosphorylated H30 lesion containing oligo, and downstream oligonucleotides are annealed to into gap and ligated with T4 ligase. Unligated plasmid is digested with T5 exonuclease, and ligated plasmid is purified from T5 exonuclease and digested plasmid. Purified plasmid is used for flow cytometry. (B) Agarose gel verification on steps conducted in the scheme in part A. Plasmid with gap due to endonuclease reaction will shift higher in agarose gel. Ligated plasmid or unprocessed plasmid will show a higher mobility band indicating intact supercoiled plasmid. (C) Repair scheme for pTurbo reporter plasmid. Once transfected into mammalian cells, repair of installed lesion will allow for transcription of GFP and subsequent protein expression. Transfection will be measured using a co-transfected RFP (dsRed) control. The absence of repair will lead to persistence of lesion, stalling RNA polymerase, and no GFP expression. Figure generated on biorender.

Monitoring of repair Gh, Tg, and FapyG in human cell lines

Next, I evaluated the repair of Gh, Tg and FapyG in human cell lines to establish base line levels of repair for these lesions and to gain insights into repair capacity of these lesions. These lesions have never been evaluated in human cells lines and could demonstrate differences in repair across each cell line. Gh, Tg and FapyG were installed into the pTurbo reporter plasmid to evaluate repair across the cell lines. I was able also to evaluate the FapyG lesion in this system due to improvements in synthetic methods generated by the Greenberg laboratory.[160] FapyG is also an excellent substrate for NEIL1,[56] however, synthesis of this substrate and incorporation of FapyG into an oligonucleotide via solid phase DNA synthesis is challenging due to nucleobase sensitivity to base and heat.[160] The annealing step of pTurbo generation was performed at lower temperature to prevent depurination of the lesion and successfully incorporated in a similar fashion to Tg and Gh.

To begin bridging this gap, we monitored the repair of three NEIL1 substrates, Gh, Tg, and FapyG in the HEK293FT, HeLa, and U87 human cell lines. Additionally, HeLa and U87 are cancer cell lines arising from cervical cancer and glioblastoma respectively, and cancer cells are known to have altered function in their biochemical pathways to maintain self-sufficiency, evade apoptosis, sustain angiogenesis, replicate limitlessly, and invade tissue and metastasize.[161] The repair of FapyG, Gh, and Tg in HEK293FT, HeLa, and U87 cells were evaluated by transfecting lesion containing plasmid and monitored after 48 h via flow cytometry. pTurbo was co-transfected with plasmid expressing a red-fluorescent protein (RFP), dsRed, as a transfection control and a carrier plasmid, pUC19, which has been shown to assist in cellular uptake.[149] Percent repair was calculated as a percentage of GFP and RFP positive cells over all RFP expressing cells, and percent repair was normalized to a GFP and RFP positive control (Figure 4.1C).

In each cell line, we observed varying levels of repair of all three lesions. The greatest level of repair was observed in the HEK293FT cell line, with comparable extents of repair for all lesions with >90% repair (Figure 4.2, Figure 4.3, Table 4.1). Greater differences were observed in the HeLa and U87 cell lines, where the lowest level of repair was observed in HeLa cell lines. If we compare across the lesions evaluated, repair levels for each lesion were different and varied between the cell lines. Of the lesions studied, FapyG was repaired to the greatest extent in all cell lines, followed by Gh and Tg (Figure 4.3, Table 4.1) .

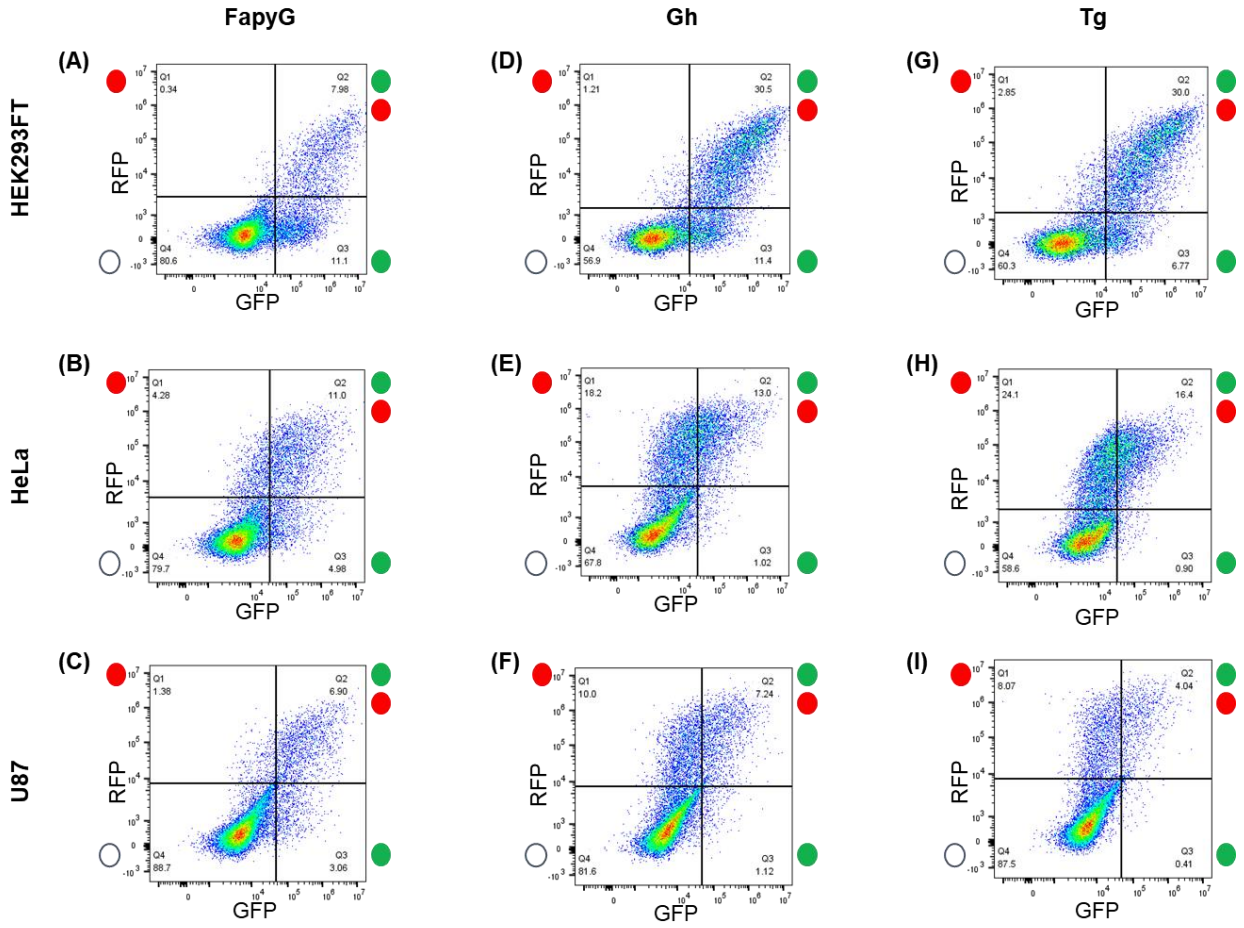

Figure 4.2: Representative plots of FapyG, Gh, and Tg repair in HEK293FT, HeLa, and U87 cells. Representative flow cytometry density plots of red (RFP) versus green (GFP) fluorescence in HEK293FT, HeLa, and U87 cells transfected with FapyG (A, B, C), Gh (D, E, F), or Tg (G, H, I) containing pTurbo reporter and dsRed plasmids.

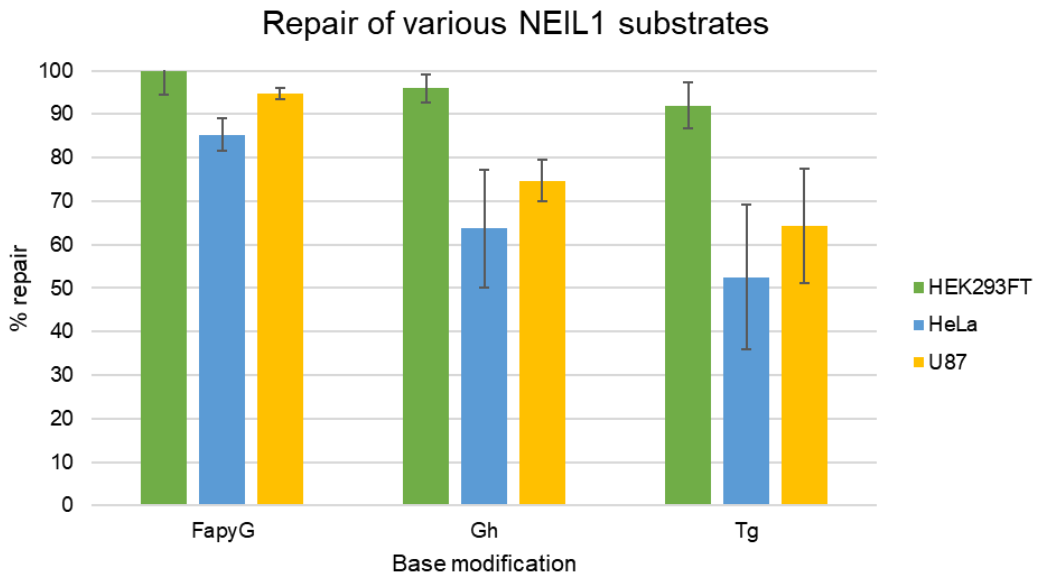

Figure 4.3: Repair of Gh, Tg, and FapyG in HEK293FT, HeLa, and U87 cell lines.

Mean percent repair after 48 h was calculated by the ratio of GFP and RFP positive cells to total RFP positive cells and normalized to the GFP/RFP positive control.

Table 4.1: Percent repair of Gh, Tg, and FapyG repair in HEK, HeLa, and U87 cell lines.

Cell line	FapyG (% repair[a])	Gh (% repair[a])	Tg (% repair[a])
HEK293FT	105 ± 5	96 ± 3	92 ± 5
HeLa	85 ± 4	64 ± 13	52 ± 16
U87	95 ± 2	75 ± 5	64 ± 13

[a]Repair of lesion contain lesion pTurbo reporter plasmid was monitored after 48 h. Percent repair was calculated by the comparison of cells expressing GFP and RFP to those only expressing RFP [%repair=100*(GFP+RFP+/RFP+)] and normalized to GFP/RFP positive control.

2'-F-Gh is repaired in HEK, HeLa, and U87 cell lines

2'-Fluorinated nucleotides have been used as chemical biology tools for probing features of DNA damage recognition and excision by DNA glycosylases. The addition of fluorine on the 2' position of the deoxyribose sugar of the nucleotide can inhibit or slow the bond breaking

between the N1/N9-C1' catalyzed by the DNA glycosylase. Specifically, the incorporation of fluorine at the 2'-position destabilizes the C1-O4' oxocarbenium ion transition state formed during glycosylase catalyzed glycosidic bond hydrolysis (Figure 4.4A).[162,163] 2'-F-Tg and 2'-F-Gh have been shown to dramatically resistant to NEIL1 mediated repair.[67,68] Additionally, 2'-F-Tg and 2'-F-Gh were used in electrophoretic mobility shift assays with the two isoforms of NEIL1, and both isoforms have similar affinities to 2'-F-Tg and 2'-F-Gh containing DNA, suggesting that differential processing is related to the lesion excision step rather than lesion binding.[67,68] 2'-F-Gh has provided critical insights into NEIL1 activity in our biochemical assays, but 2'-F-Gh has never been explored in a cellular context. Here, 2'-F-Gh was incorporated in the lesion pTurbo plasmid reporter to investigate 2'-F-Gh inhibition in a cellular context.

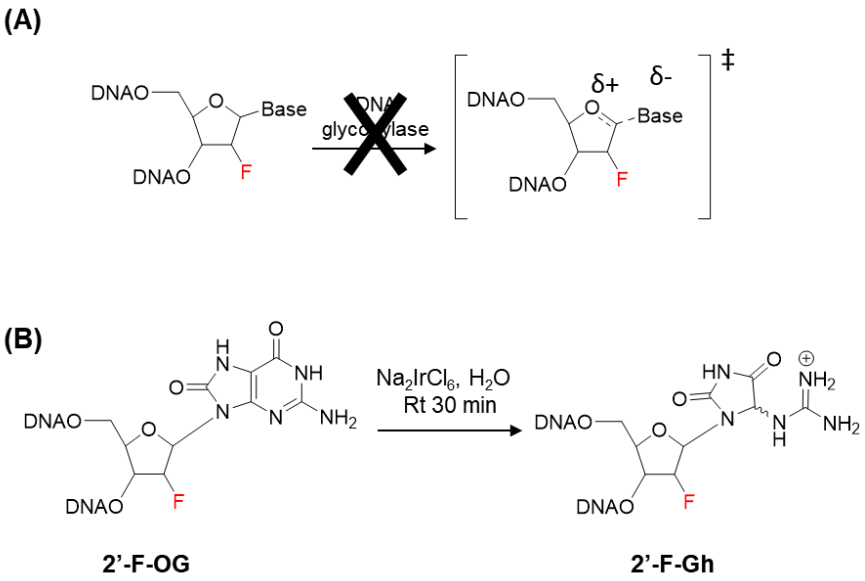

Figure 4.4: 2'-F-Gh as molecular probe for DNA repair.

(A) The addition of the fluorine atom to the 2' position of the deoxyribose sugar is expected to destabilize the transition state for glycosidic bond cleavage. (B) Selective oxidation 2'-F-OG allows for the formation of 2'-F-Gh. Figures adapted from Cao et al. 2020.

To generate 2'-F-Gh containing oligonucleotide, 2'-F-OG oligonucleotides were selectively oxidized with Na_2IrCl_6 for the generation of Gh and Sp lesions in oligonucleotide using methods developed by Burrows and coworkers (Figure 4.4B).[164,165] Oxidized oligonucleotides were purified via HPLC and separated from 2'-F-OG oligonucleotide and confirmed by ESI-MS. 2'-F-Gh was installed into the lesion pTurbo reporter plasmid as previously discussed. In these experiments, only the 2'-F-riboGh were performed due to availability, while ribo and arabino conformations of the deoxyribose sugar do have slightly different impacts on NEIL1 activity *in vitro*.[68]

2'-F-Gh-containing pTurbo plasmid were transfected into HEK293FT, HeLa, and U87 cells using the same method as Gh-containing pTurbo plasmid. Surprisingly, the overall percent repair 2'-F-Gh was similar to repair of Gh across all three cells lines (Figure 4.5, Figure 4.6, and Table 4.2). In HEK293FT cells, repair of 2'-F-riboGh was comparable to Gh containing plasmid (98% ± 1% and 96% ± 3%, respectively). On the other hand, repair of 2'-F-Gh was higher (76% ± 5%) than the repair of Gh (64% ± 13%) in HeLa cells Only the U87 cell line demonstrated decreased repair of 2'-F-Gh (69% ± 4%) compared to Gh (75% ± 5%). The addition of 2'-fluoro to the deoxyribose sugar does not impede repair in cells, and this lesion may be repaired by other mechanisms than by BER.

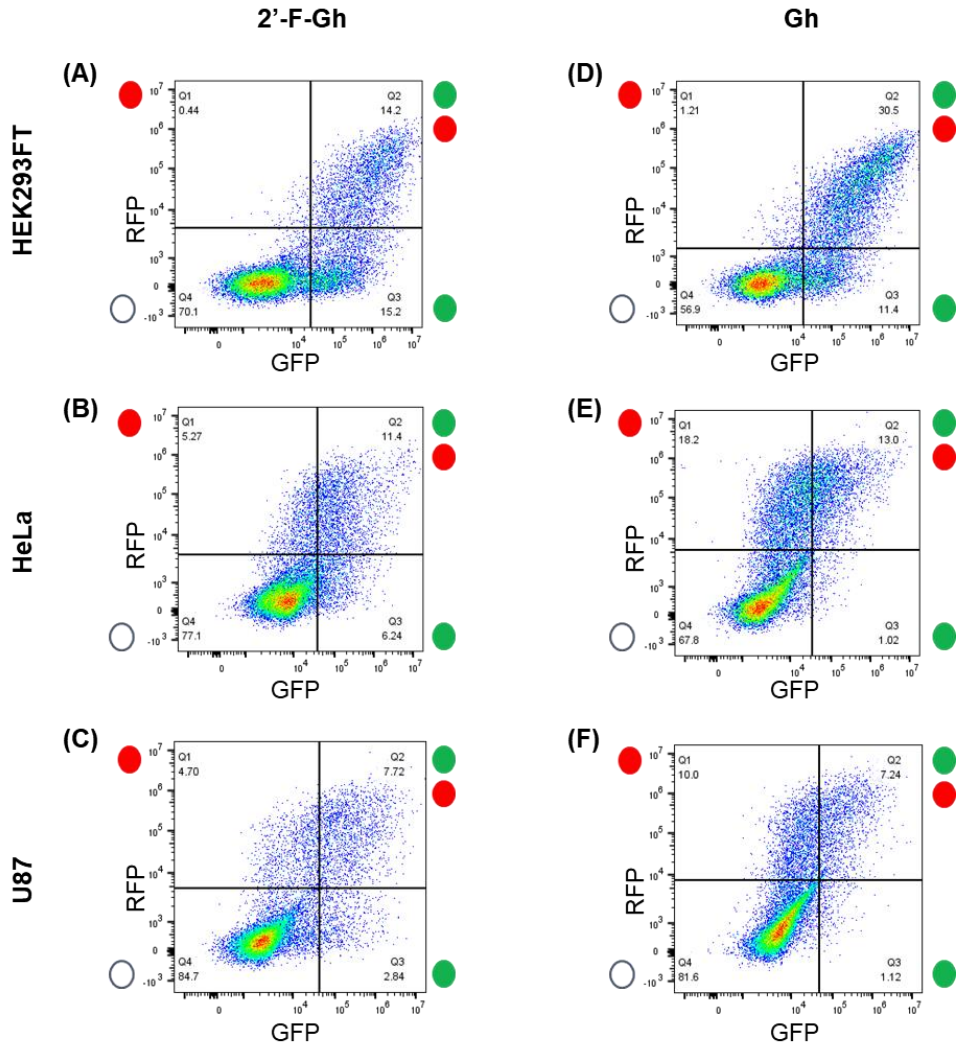

Figure 4.5:Representative plots of 2'-F-Gh and Gh repair in HEK293FT, HeLa, and U87 cells.

Representative flow cytometry density plots of red (RFP) versus green (GFP) fluorescence in HEK293FT, HeLa, and U87 cells transfected with 2'-F-Gh (A, B, C) or Gh (D, E, F) containing pTurbo reporter and dsRed plasmids.

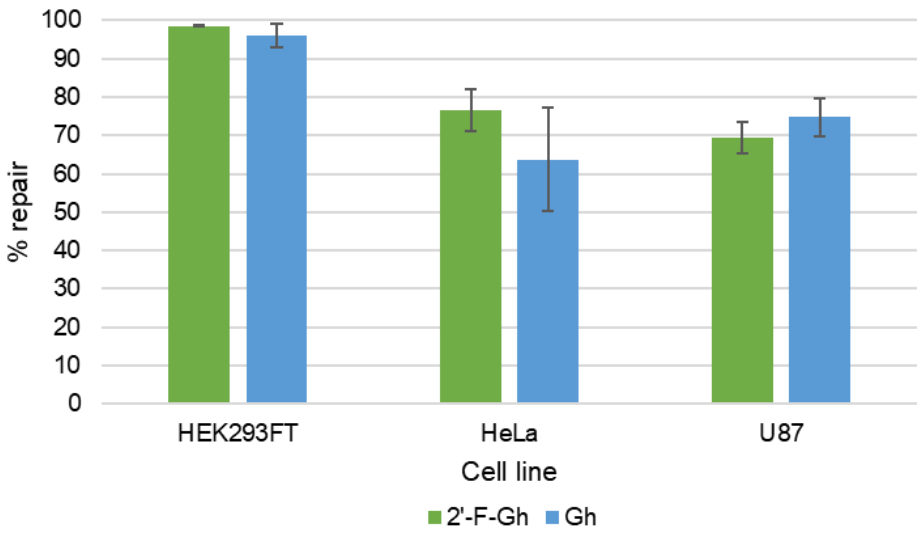

Figure 4.6: Repair of 2'-F-Gh repair in HEK293FT, HeLa, and U87 cell lines compared to Gh.

Percent repair after 48 h was calculated by the ratio of GFP and RFP positive cells to total RFP positive cells and normalized to the GFP/RFP positive control.

Table 4.2: Percent repair of 2'-F-Gh and Gh repair in HEK, HeLa, and U87 cell lines.

Cell line	2'-F-Gh (% repair[a])	Gh (% repair[a])
HEK293FT	98 ± 1	96 ± 3
HeLa	76 ± 5	64± 13
U87	69 ± 4	75 ± 5

[a]Repair of lesion containing pTurbo reporter plasmid was monitored after 48 h. Percent repair was calculated by the comparison of cells expressing both GFP and RFP to those only expressing RFP [%repair=100*(GFP+RFP+/RFP+)] and normalized to GFP/RFP positive control.

IFN-α treatment decreases repair of Gh and Tg in cell lines

Two isoforms of NEIL1 exist due to RNA editing of the NEIL1 pre-mRNA by ADAR1.[136] As discussed in chapter 2, this editing event can alter specificity of NEIL1 activity on different lesion substrates. A balance of the two isoforms is likely needed for the efficient removal of all NEIL1 substrates.[139] In a cellular context, repair by the two isoforms has yet to be explored. Here, we examine the repair of Gh and Tg lesions in the three cell lines, which all have varying levels of ADAR1 expression with HEK293FT having the highest level of ADAR1 expression followed by HeLa and U87.[166,167] However, ADAR1 expression does not always correlate with editing level, and each cell line will need to be evaluated for editing of the NEIL1 transcript.[166] In methods developed previously by the Beal laboratory, total RNA is isolated, and using RT-PCR, the editing region of the NEIL1 transcript was amplified and submitted for Sanger sequencing to characterize editing levels. The ratio of A to G was quantified to evaluate the percent editing of the NEIL1 transcript in each cell line.[136] We found that HEK293FT cell lines had the highest level of editing at 50% ± 2%, while HeLa and U87 had more comparable levels of editing of the NEIL1 transcript at 42% ± 2% and 46% ± 7% respectively. Additionally, we evaluated whether editing levels in each cell line changed in response to changes in ADAR1 expression level with treatment of interferon-α (IFN-α), which can stimulate the transcription of ADAR1 p150.[168] Each cell line was cultured with IFN-α 24 h prior to RNA isolation. Similar to previously reported work,[136] IFN-α treatment of all cell lines resulted in an increase in editing of the NEIL1 transcript as seen by increased G reads from Sanger sequencing (Figure 4.7, Table 4.3). All cell lines had comparable increase in editing of the NEIL1 transcript, showing around 70% editing across the three cell lines (Table 4.3).

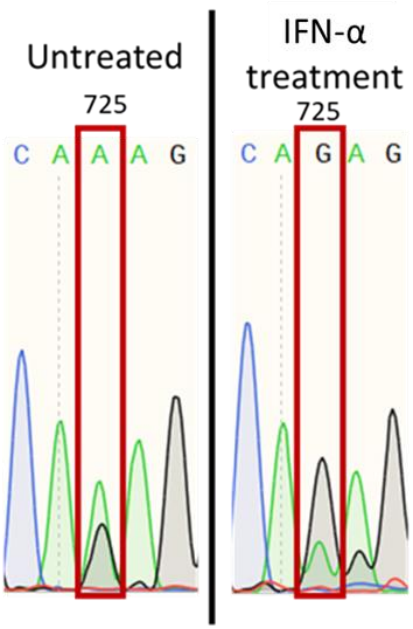

Figure 4.7: NEIL1 editing response to IFN-α.

Sequence traces at the recoding site (position 725) by ADAR1 in cDNA from HeLa cells cultured in the absence of IFN-α (left) and in the presence of IFN-α (right).

Table 4.3: Editing levels of NEIL1 transcript in HEK293FT, HeLa, and U87 cell lines.

Cell line	Untreated (% G:A[a])	IFN-α treated (% G:A[a])
HEK293FT	50 ± 2	73 ± 2
HeLa	42 ± 2	67 ± 3
U87	46 ± 7	75 ± 3

[a]NEIL1 editing in response to IFN-α. Percent editing of NEIL1 transcript in cell lines cultured in the absence and presence of IFN-α. Total RNA isolated and RT-PCR was performed to amplify editing region of NEIL1 transcript. PCR product was purified and submitted to Sanger sequencing. Sequence traces were analyzed by SnapGene for A to G changes.

After observing the increase in editing levels between all three cell lines, IFN-α treatment was added to the flow cytometry process to evaluate if altering the balance of edited and unedited NEIL1 impacts repair. Our previous results *in vitro* showed that the unedited isoform excised Tg ~30-fold faster than Ed NEIL1, while the rate was only 3-fold greater by edited isoform with the lesion Gh.[136] In these preliminary studies to evaluate increasing Ed NEIL1 levels, IFN-α was added

to cultured cells 24 h prior to transfection with plasmid reporter, and flow cytometry was performed 48 h after transfection. RNA editing levels for cells undergoing flow cytometry were approximated by culturing a corresponding plate of cells from the same initial cell stock and cultured identical conditions as the cells for flow cytometry experiments. Cells for RT-PCR were transfected with control plasmids (pTurbo, dsRed, pUC19) due to limited stock of lesion containing pTurbo plasmid, and HEK 293FT and HeLa cells transfected with control plasmids showed nearly identical editing levels to cells transfected with lesion containing plasmid (data not shown.) Overall, there was a modest increase in editing levels in cells treated with IFN-α indicating a likely higher level of edited NEIL1 in our flow cytometry experiments (Table 4.4).

The repair of Gh and Tg both display decreases in repair upon treatment with IFN-α (Figure 4.8, Figure 4.9, and Table 4.5). A small decrease in repair was observed between the IFN-α treated population and untreated population in the HEK293FT cells. Greater differences can be seen in the HeLa and U87 cell lines in each treatment group for both the Tg and Gh lesion (Figure 4.9 and Table 4.5). Based on our observation of Ed and UE NEIL1 *in vitro*, differences in lesion processing were expected when the population of NEIL1 editing was altered in a cellular context. Since UE NEIL1 more efficiently excised Tg, we anticipated that in IFN-α treated cells, where editing was higher and contained a greater population of Ed NEIL1, there would be a decrease in repair of Tg. This prediction was reflected in our flow cytometry experiments. The greatest decrease was observed in the HeLa cell line with 52% ± 16% repair in the untreated population and 35% ± 14% repair in the IFN-α treated cells. Smaller decreases around 7% in the repair of Tg was observed in HEK293FT and U87 cell lines (Table 4.5). The repair of Gh showed a similar decrease in the IFN-α treated cells, which was not expected due to the ability of both edited and UE NEIL1 to efficiently remove Gh.

Table 4.4: Approximate editing levels for flow cytometry assays treated with or without IFN-α.

Cell line	Untreated (% G:A[a])	IFN-α treated (% G:A[a])
HEK	50 ± 9	78 ± 3
HeLa	48 ± 3	63 ± 4
U87[b]	51 ± 6	61 ± 6

[a]Percent editing of NEIL1 transcript in cell lines cultured in the absence and presence of IFN-α matched to flow cytometry experiments. IFN- α was added to cell culture 24hr prior to transfection. Total RNA was isolated 48 hours after transfection, and RT-PCR was performed to amplify editing region of NEIL1 transcript. PCR product was purified and submitted to Sanger sequencing. Sequence traces were analyzed by SnapGene for A to G changes. [b]Results were not performed in triplicate.

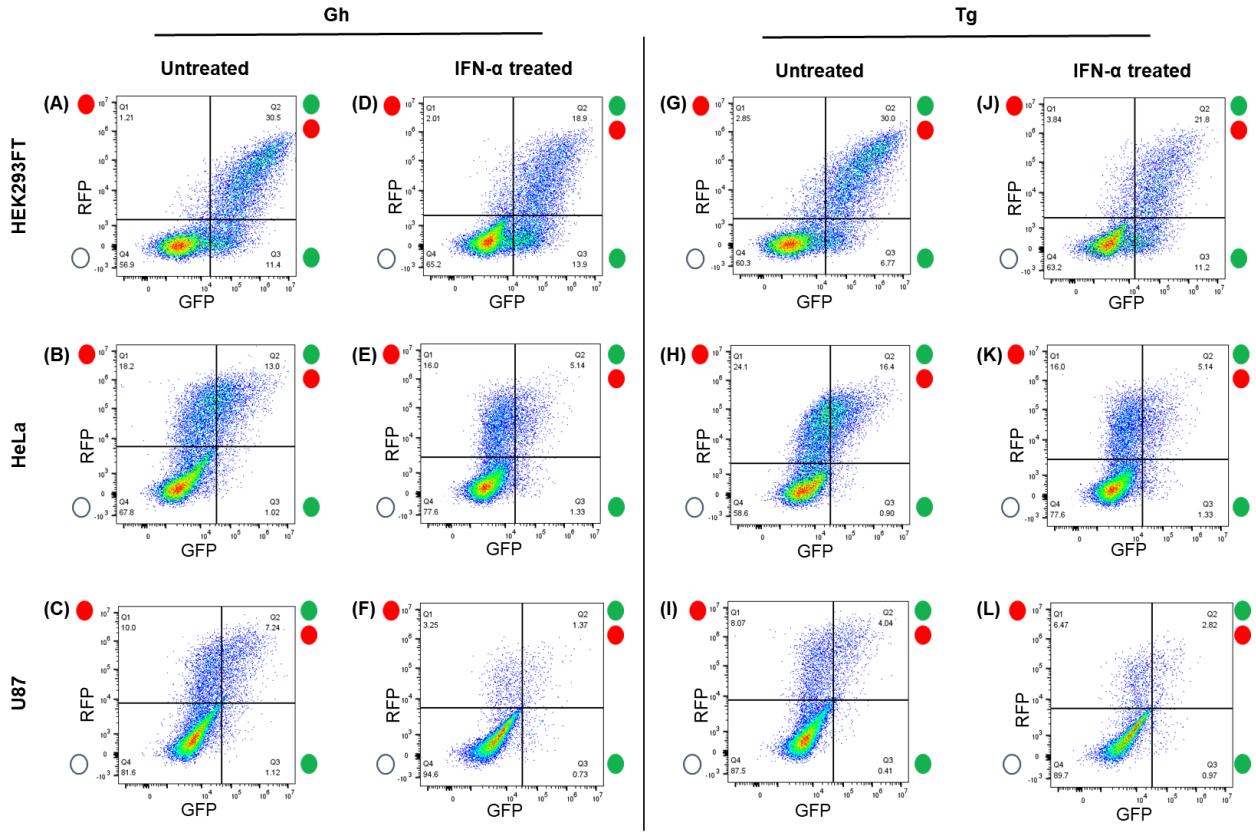

Figure 4.8: Representative plots of Gh, and Tg repair in HEK293FT, HeLa, and U87 cells treated with IFN-α.

Representative flow cytometry density plots of red (RFP) versus green (GFP) fluorescence in HEK293FT, HeLa, and U87 cells transfected with Gh (A, B, C, D, E, F,) or Tg (G, H, I, J, K, L) containing pTurbo reporter and dsRed plasmids. Cells were either untreated (A, B, C, G, H, I) or treated with IFN-α (D, E, F, J, K, I) 24 h prior to transfection.

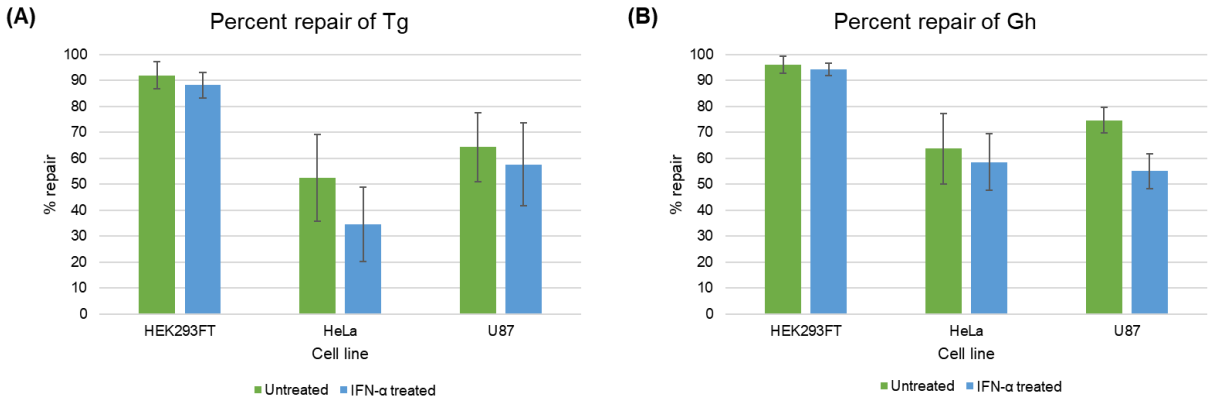

Figure 4.9: Repair of Gh and Tg in repair in HEK293FT, HeLa, and U87 cell lines treated with and without IFN-α.

Repair of (A) Gh or (B) Tg containing reporter plasmid with or without IFN-α treatment was monitored after 48 h. Percent repair was calculated by the comparison of cells expressing GFP and RFP to those only expressing RFP [%repair=100*(GFP+RFP+/RFP+)] and normalized to GFP/RFP positive control.

Table 4.5: Percent repair of Gh and Tg repair in HEK293FT, HeLa, and U87 cell lines treated with and without IFN-α.

Gh repair		
Cell line	Untreated (% repair)	IFN- α treated (% repair)
HEK293FT	96 ± 3	94 ± 2
HeLa	64± 13	58± 11
U87	75 ± 5	55 ± 7
Tg Repair		
Cell line	Untreated (% repair)	IFN- α treated (% repair)
HEK293FT	92 ± 5	88 ± 5
HeLa	52 ± 16	35 ± 14
U87	64 ± 13	58 ± 16

[a]Repair of lesion containing reporter plasmid was monitored after 48 h. Cells were treated with IFN- α 24 h prior to transfection with reporter plasmids. Percent repair was calculated by the comparison of cells expressing GFP and RFP to those only expressing RFP [%repair=100*(GFP+RFP+/RFP+)] and normalized to GFP/RFP positive control.

Discussion

This work establishes a baseline level of repair for FapyG, Gh, and Tg in a reporter system that replies on blocking of transcription. All three lesions are known to be excellent substrates for NEIL1 and in *in vitro* assays, they are rapidly excised from duplex DNA by NEIL1. In the context of our cellular reporter, we observe more variability in repair. FapyG is repaired to the greatest extent followed by Gh and Tg, and this trend is consistent across all three cell lines. When examining repair across the cell lines, the cancer cell lines, HeLa and U87, show reduced repair of all three lesions compared to HEK293FT. This trend does not align with the expression levels of NEIL1 in each type of cell. Like many other glycosylases, the expression level of NEIL1 is generally low (<15 transcripts per million (TPM)). HeLa cells have the greatest expression of NEIL1 with approximately 11.8 TPM, followed by HEK293 (9.1 TPM), and U87 having the lowest expression (1.1 TPM).[169] However, these results show the global repair capacity for each lesion in a cellular context and notably show decreased repair in the cancer cell lines, HeLa and U87.

Other pathways do exist for the repair of Gh, Tg, and FapyG as they are also substrates for NER and the BER glycosylases NEIL2 and NTHL1.[38] Additionally, FapyG is a good substrate for OGG1.[108] NER removes many helix distorting lesions, like Gh, Tg, and FapyG,[170–173] and the stalling of RNA pol II can recruit proteins necessary to for the NER complex and initiate repair in transcription coupled (TC) NER.[174,175] NEIL2 is also known to associate with RNA pol II and similarly function with TC-BER.[38] Finally, Tg is a substrate for the BER glycosylase NTHL1.[38] However, NEIL1 is still likely a major contributor of removal of these lesions. In Dr. Yeo's studies evaluating the repair of Gh and Tg *Neil1-/-* MEF and WT MEF, baseline levels of repair in the *Neil1-/-* MEFs was 20% suggests that NEIL1 is the primary means of initiating repair these

lesions.[150] A similar pattern may also exist the human cell lines evaluated here, but further analysis with the generation of knockout cell lines or siRNA knockdowns are needed to define the contribution of NEIL1. Similarly, siRNA knockdown would help to delineate the role of the several repair mechanisms on the processing of these substrates.

The 2'-F analog of Gh was also evaluated in the NEIL1 pTurbo plasmid to assess it as a chemical biology tool in this reporter system. NEIL1 does have high specificity for the lesion, and have been shown to slow or stall NEIL1 activity.[68] However, our results show similar levels of repair to the *native lesion*, Gh, across all three cell lines. Some repair is expected with 2'-F-Gh, as both isoforms NEIL1 can excise 2'-F-riboGh in *in vitro* biochemical assays; however, this excision was inefficient (~60% base removed after 60 min).[68] The presence of 2'-F did slow lesion excision despite NEIL1's high affinity for the substate.[68] However, 2-'F-Gh repair is suggestive of other repair pathways to repair Gh that do not involve glycosylases, such as NER. Another pathway could be translesion polymerases that are allowing bypass of the blocking lesion to observe GFP protein production and not necessarily classic excision repair.[176] Additionally, only the 2'-F-riboGh configuration was evaluated in this assay. There could be decreased repair observed with the arabino configuration of the 2'-F ribose sugar; the arabino configuration of 2'-F-Gh was found to stall the lyase activity of NEIL1 leading to the formation of a Schiff base intermediate.[177] If such a complex was to form in a cellular context, this may further thwart repair. In addition, future work may also want to consider the repair of the fluorinated lesion via other pathways such as NER, which can also excise Gh.[170]

Finally, I began some preliminary work assessing role of having two isoforms of NEIL1 in a cellular context. Previous biochemical analysis demonstrated substrate preferences between Ed and UE NEIL1. A modest 3-fold difference in the excision of Gh was observed between the two

isoforms of NEIL1, but a more striking ~40 fold difference was observed with UE NEIL1 compared to Ed NEIL1 for the Tg lesion.[136] First, I began by evaluating the editing levels of each cell line and found that HEKF239FT had the highest editing level followed by HeLa and U87 cell lines. When treated with IFN-α to increase the expression of ADAR1 and ultimately the editing of the NEIL1 transcript, the editing levels of all three cell lines was around 70% (Table 4.3). All three cell lines were treated with IFN-α and repair of Gh and Tg was monitored using the lesion pTurbo reporter plasmid via flow cytometry. We expected that in IFN-α treated cells, with a greater presence of Ed NEIL1, there may be comparable or higher repair of Gh in our cellular assay and reduced levels of repair of the Tg lesion. However, for both lesions and across all three cell lines, a reduction in repair was observed in cells treated with IFN-α. In the HEK293FT and HeLa cell lines, repair of Gh was similar with a slight decrease in the IFN-α treated cells (Figure 4.6B, Table 4.5). Repair of Gh in U87 decreased by 20% (Table 4.5). While a decrease in the repair of Gh was not expected, treatment with IFN-α may be impacting more than just the expression of ADAR1 and increasing the editing of the NEIL1 transcript.

IFN-α is an important signaling agent participating several pathways including the initiation of immune response and DNA repair.[178] IFN-α is also an indicator of chronic inflammation,[178] and chronic inflammation results in an increase in oxidative stress and the DNA repair response.[179,180] Additionally, ADAR1 expression is increased with IFN-α,[158] and ADAR1 plays a role in innate immunity during immune response and recoding events.[166] The NEIL1 pre-mRNA is one of many substrates for ADAR1 responsible for a single amino acid change in the glycosylase. As discussed previously, this editing event can greatly alter substrate specificity of the NEIL1 glycosylase *in vitro,* but there is still a lack of understanding in the biological consequences of this editing event.[139] In cases of multiple myeloma with ADAR1 hyperediting,

the NEIL1 transcript was found to be completely edited with hallmarks of increased levels of DNA damage.[71,72] The lack of balance between the two isoforms of NEIL1 may reduce repair of lesions in cancer. These preliminary studies demonstrate that there is a difference in repair when Ed NEIL1 levels are increased in a cellar context, but further study is needed to delineate the origin of these differences, and whether or not they related to the ratio of Ed versus UE NEIL1. With increased expression of ADAR1, additional editing events beyond NEIL1 maybe taking place having a global impact on DNA repair. Additionally, our method of increasing ADAR1 expression with the treatment of IFN-α could also be playing a role in the observed reduction in repair as IFN-α participates in a plethora of signally pathways.[178] Systems containing a singular isoform of NEIL1 could reveal isoform specific consequences in a cellular context without the need to alter ADAR1 expression levels and remove the variability of ADAR1 acting on its other editing targets.

These studies establish a baseline level of repair for FapyG, Tg, Gh and 2'-F-Gh across multiple mammalian cell lines. Understanding the mechanism of repair can be useful for monitoring the DNA repair capacity and role of DNA repair in disease. Lesion reporter plasmids can be a powerful chemical biology tool for assessing repair capacity especially in diseases with are associated with DNA repair pathways. For many types of cancer and other diseases, repair capacity can be altered by enzyme expression levels and influence disease progression.[155] Reduced function due to mutations in DNA repair enzymes have allowed for the accumulation of DNA damage and can initiate disease progression.[181] On the other hand, some SNPs of BER glycosylases have been identified to increase their activity that can lead to a potential buildup of toxic BER intermediates, such as strand breaks.[180] Characterization of these lesions from cellular reporter assays can be insightful in establishing how a mutation relates to disease.[155]

Additionally, lesion specific repair assays can be valuable in assessing enzyme specific activity in a cellular context and a tool for evaluating inhibitors for DNA repair enzymes. The DNA repair pathways are targets for many chemotherapeutics in the treatment of cancer.[181] Inhibition of repair activity can allow for the increased accumulation of damage leading to apoptosis. New methods targeting all pathways are under development including a recent inhibitor of the BER glycosylase OGG1.[182–184] Functional cell-based assays are useful tool to examine DNA damage and repair as they reflect the influence of factors such as protein expression and stability.[155] Their continued development have implications in public health, defining mechanisms of disease and personalized medicine.

Future work

Examining repair in a cellular context can give important insights into the molecular basis of NEIL1 recognition and excision of various substrates. However, there is room for further improvements in the plasmid. A new generation of this plasmid containing dsRed control would remove the need for co-transfection of the dsRed containing plasmid similar to the repair plasmid for MUTYH.[147] Co-transfection of multiple reporter plasmids with a transfection control plasmid have been demonstrated as effective means of monitoring multiple repair pathways.[149,185] However, incorporation of the transfection control on the reporter plasmid could ensure that the reporter and transfection control gene were transfected at the same efficiency. Additionally, the development of a reporter plasmid with substrates of NEIL1 in the GFP gene that rely on mutagenetic lesions are currently underway by Savannah Conlon. This would allow us to explore many additional substrates that are not blocking lesions, such as 5-OHU. Another avenue of exploration is examining the role that BER glycosylases like NEIL1, NEIL2, and NEIL3 or other repair pathways, such as NER, play in repair in a cellular context. Utilizing cell lines that express

varying amount of each pathway or using siRNA to knockdown different repair pathways may help to further delineate impact that each pathway has on repair of different lesions.

Finally, the cellular consequences of RNA editing on NEIL1 are still not well understood. We hypothesize that the balance of Ed and UE NEIL1 is important for the recognition and repair of a wide range of oxidative damage.[139] Complete editing of the NEIL1 transcript due to ADAR1 hyper editing has been observed in patients with multiple myeloma,[71] and the absence of UE NEIL1 may allow for the persistence of lesion. In these studies, we conducted preliminary analysis using IFN-α to increase ADAR1 expression and the editing levels of NEIL1, but other methods could be used to increase ADAR1 expression or increase Ed NEIL1 levels. First, monitoring the level of repair in the cells undergoing flow cytometry would give a more than approximation of editing levels of these cells, but methods to do so were not available at that time. Transfection of ADAR1 containing plasmid could be used to increase ADAR1 expression and has been employed by the Beal laboratory to increase ADAR1 levels and increase editing. Additionally, the formation of Ed only or UE only NEIL1 containing cell lines could be used. Savannah Conlon and I have developed a strategy to express only one NEIL1 isoform in *NEIL1* knockout cell lines. Monitoring repair of different lesions like Gh and Tg in Ed or UE only cell lines may allow us to define the cellular impact of each isoform on repair.

Materials and Methods

General material and methods. T4 polynucleotide kinase, Nt.BstNBI restriction endonuclease, T4 ligase, and T5 exonuclease enzymes were obtained from New England BioLabs. All solutions and buffers were prepared using deionized water from a Milli-Q PF System. MALDI-MS of oligonucleotides was obtained using a 3-hydroxypicolinic acid matrix on a Bruker UltraFlextreme MALDI TOF/TOF at the University of California, Davis or at Mass Spectrometry

Lab, School of Chemical Sciences, University of Illinois at Urbana-Champaign. High resolution ESI-MS for HRMS was obtained on an Applied Biosystem Qtrap Linear Ion Trap Spectrometer at the University of California, Davis. ImageQuant version 5.4 was used for the analysis of gel electrophoresis. All other chemicals and reagents were purchased from VWR, Fisher Scientific, Invitrogen or Sigma and used without further purification.

CsCl purification of pTurbo plasmid. Chemically competent DH5α cells were transformed with pTurbo reporter plasmid. A 1L culture was grown up from bacterial colony with kanamycin antibiotic appropriate for pTurbo. Cell culture was pellet and resuspended in ice cold 10 mM Tris-HCl, pH 8.0, 0.1 M NaCl, 1mM EDTA, pH 8.0 buffer and pellet again to rinse media from cell pellet. Cell pellet was resuspended with 400 mg lysozyme and EDTA (0.17 M final concentration) and gently mixed. SDS and NaCl was added to final concentrations of 5% SDS and 1M NaCl and incubated on ice for 1 h. Cell lysates were pelleted, and the supernatant was decanted and strained through cheese cloth. 2 volumes of 100% ethanol were added to the supernatant and incubated for 2 h to precipitate plasmid DNA. Pelleted DNA was resuspended in 1x TE and NaI solutions was added for final concentration of 7.6M NaI and incubated for 5 min at room temperature. 1 volume of isopropanol added to mixture and allowed to incubate for 15 min a room temperature for plasmid DNA precipitation followed by pelleting of DNA via centrifugation. Pellet was resuspended in 1x TE buffer, RNase A was added for a final concentration of 50µg/mL, incubated for 15 min at room temperature to digest RNA in plasmid DNA suspension. 0.1 volume of 3M sodium acetate and 1 volume of isopropanol was added prior to centrifugation to pellet plasmid DNA. Pellet was rinsed with cold 70% ethanol and allowed to air dry prior to resuspending in 1mL of 1x TE. A sample of suspension was run on an agarose gel to verify presence of plasmid DNA.

Plasmid DNA suspension was added to 20.8 g CsCl and 10 mg of Ethidium bromide in 15 mL of 1x TE. Solution was centrifuged in ultracentrifuge at 50,000 rpm at 20 ºC overnight for a minimum of 10 h to separate supercoiled plasmid DNA from nicked plasmid. Long wave UV light was used to visualize and extract band of supercoiled plasmid DNA. DNA was rinsed in 1 volume of cold n-butanol saturated with TE, centrifuged to pellet plasmid, and removed Ethidium bromide from plasmid. Repeated n-butanol rinse and centrifugation until the organic phase ran clear. Suspended plasmid DNA pellet in 70% ethanol and left at 4 ºC overnight to precipitate DNA. Plasmid DNA was pelleted and resuspended in 1x TE and concentration verified on nanodrop.

Preparation of lesion containing oligonucleotides. OG and Tg phosphoramidites were purchased from Glen Research and used without further purification. DNA oligonucleotides containing OG and Tg, were synthesized at the University of Utah Medical School's DNA/Peptide core facility. FapyG phosphoramidite was synthesized and incorporated into H30 sequence and purified as in the laboratory of Dr. Marc Greenberg as previously reported.[160] 2'-F-OG-containing oligonucleotide was synthesized and characterized by Dr. Sheng Cao of the David laboratory as previously reported.[68] Downstream filling oligo was order from IDT. All oligonucleotides were HPLC purified using a Beckman Gold Nouveau or Shimadzu Liquid Chromatography system with a Dionex DNApac100 ion-exchange column using a 30-100% gradient of 90:10 H_2O/acetonitrile with 2 M ammonium acetate. To generate Gh containing oligonucleotide, OG-containing and 2'-F-OG-containing oligonucleotide was selectively oxidized with Na_2IrCl_6, and 2'-F-OG and 2'-F-Gh containing oligonucleotides were separated via HPLC as reported previously.[68] Isolated fractions were lyophilized and desalted using with a Waters SEP-PAK C18 column. Masses of oligonucleotides were confirmed by MADLI and ESI-MS, and DNA concentrations were determined using the Abs 260 nm.

Table 4.6: Oligonucleotide sequences used instillation of pTurbo reporter plasmid.

H30 Downstream filling 43nt pT-nick complement	5'– TGTTCATCATGGGTC**X**TCGGTATATCCCAT – 3' 5'– GCAAGTCCGGA – 3' 5'–TCCGGACTCTTGCATATACCGAAGACCCATGATGAACA– 3'
	X = Gh, Tg, FapyG, or 2'-F-Gh

Incorporation lesion containing oligonucleotides into pTurbo plasmid. 4 µg CsCl purified pTurbo plasmid was incubated with 20 units of Nt.BstNBI restriction enzyme with 1x NEB buffer 3.1 for 2 h at 55 °C and then inactivated at 80 °C for 20 min. Nicking of plasmid was confirmed on agarose gel. Next, 50 pmol (20x excess) of complement oligo to the nicked region was added to nicked plasmid reaction and brought to a final concentration of 50 mM NaCl. Sample was run on thermocycler to remove nicked single stranded oligo via annealing to excess complement by first denaturing at 95 °C for 30 s followed by 10 cycles of 80 °C for 30 s and 8 °C for 30 sec with a 50% ramp speed. Nicked plasmid was purified away from nicked and complement oligo using Macherey-Nagel DNA purification kit per manufacturer's instructions. Purified nicked pTurbo plasmid was combined with 20x molar excess of 5'-phosphorylated H30 lesion-containing oligonucleotide and 5'-phosphorylated 13nt H30 downstream filing oligonucleotide and 1x ligase buffer (NEB) heated to 90 °C for 5 min and allowed to slowly cool to room temperature for annealing of lesion-containing and downstream filling oligo into the gap of nicked pTurbo plasmid. For FapyG lesion, the initial heating at the heating step was conducted at 55 °C to preserve modification and prevent depurination. 400 units of T4 ligase was added to annealed plasmid and ligated at 16 °C overnight per manufacturer's instructions. Ligation was verified via agarose gel. Ligated plasmid mixture was treated with 10 units of T5 exonuclease for 30 min to digest unligated plasmid. Digested plasmid was purified with Macherey-Nagel DNA purification kit per manufacturer's instructions. Plasmid concentration was determined via agarose gel.

Cell culture, transfection, and flow cytometry of HEK293FT, HeLa, and U87 cell lines. HEK293FT, HeLa, and human glioblastoma U87 cells were grown and maintained in Dulbecco's Modified Eagle Medium (DMEM) (Gibco) with 10% FBS containing 2 mM GlutaMax (Gibco) and 1x non-essential amino acids. Approximately, 2 x 10^4 cells (~20% confluency) were plated in 24 well plates 2 h prior to transfection. For transfection, 0.4 µg total of plasmid DNA was combined with Opti-MEM reduced serum media (Gibco) and Attractene Transfection Reagent (Qiagen) per manufacturer's protocol. Mixture was well mixed and incubated for 15 min at room temperature to allow for complex formation prior to adding transfection complexes to cell, which were at ~40% confluency. Transfected cells were incubated at 37 °C, 5% CO_2 for 48 h before harvesting for flow cytometry at ~70-100% confluency. Cells were harvested by trypsinization and pelleted to remove growth media. Pelleted cells were resuspended in 5% (vol/vol) FBS in PBS buffer and filtered. Flow cytometry was performed on Beckman Coulter Cytoflex 4 laser Flow Cytometer. Percent repair was measured by [% repair =100*(GFP+RFP+/RFP+)] and normalized to GFP+RFP+ control.

Isolation of RNA and evaluation of NEIL1 editing levels. To evaluate NEIL1 editing levels in HEK293FT, HeLa, and U87 cells, cells were grown to ~100% confluency (10^7 cells) and total RNA was isolated using RNAqueous Total RNA Isolation Kit (Thermo Fisher). RT and nested PCR was performed to monitor editing level of NEIL1 transcript as previously reported.[136] Briefly, nested RT-PCR was performed in triplicate using Access RT-PCR kit (Qiagen) for 30 cycles and then followed by Phusion Hot Start II DNA Polymerase (Thermo Fisher) for the second PCR of 30 cycles with target specific primers. Oligonucleotides for RT PCR (TFOF and TCOR) and nested PCR (TCIR and TCIR) were as follows: N1-TCOF 5′-TCCAGACCTGCTGGAGCTAT-3′, N1-TCOR 5′-TGGCCTTGGATTTCTTTTTG-3′, N1-TCIF 5′-CCCAAGGAAGTGGTCCAGTTGG-

3′, and N1-TCIR 5′-CTGGAACCAGATGGTACGGCC-3′. PCR product was purified by agarose gel and QIAquick Gel Extraction kit (Qiagen). PCR product was submitted for Sanger Sequencing, and sequence traces were analyzed by SNAP gene for A to G changes.

To increase ADAR1 expression and editing levels of NEIL1 transcript, cells were treated with Human interferon-α (2A) (Millipore Sigma) as reported previously. IFN-α (10^5 U⁄mL) stocks were made in PBS containing 1% FBS. Cells were grown to ~70% confluence (10^7 cells), washed, and treated with media containing 10^3 U⁄mL IFN-α. Cells were cultured an additional 24 h in media containing IFN-α before cell lysis and RNA isolation. For cells undergoing flow cytometry, cells were plated at ~15% confluency 24hrs prior to IFN-α treatment and cultured for an additional 24 h prior to transfection. To approximate the editing levels of NEIL1 for cells undergoing flow cytometry, additional plate of cells was cultured in tandem with cells for flow cytometry coming from the same initial cell stock. Cells for RT-PCR were treated in an identical fashion to cells for flow cytometry and treated with IFN-α 24 h prior to transfections. Cells for RT-PCR were transfected with control plasmid to lesions containing plasmid, as control plasmid showed identical editing levels to lesion containing plasmid. RNA was isolated 48 hours after transfection, and RT-PCR was performed to evaluate editing levels as described above.

References

(1) Lindahl, T. *Instability and Decay of the Primary Structure of DNA*; 1993.

(2) Hoeijmakers, J. H. J. Genome Maintenance Mechanisms for Preventing Cancer. *Nature* **2001**, *411* (6835), 366–374.

(3) Stokstad, E. Cellular Secrets of DNA Repair Win Nobel Prize for Chemistry. *Science (80).* **2015**.

(4) Lindahl, T. Instability and Decay of the Primary Structure of DNA. *Nature* **1993**, *362* (6422), 709–715.

(5) Talpaert-Borlè, M. Formation, Detection and Repair of AP Sites. *Mutat. Res. Mol. Mech. Mutagen.* **1987**, *181* (1), 45–56.

(6) Giorgio, M.; Trinei, M.; Migliaccio, E.; Pelicci, P. G. Hydrogen Peroxide: A Metabolic by-Product or a Common Mediator of Ageing Signals? *Nat. Rev. Mol. Cell Biol. 2007 89* **2007**, *8* (9), 722–728.

(7) Dedon, P. C.; Tannenbaum, S. R. Reactive Nitrogen Species in the Chemical Biology of Inflammation. *Arch. Biochem. Biophys.* **2004**, *423* (1), 12–22.

(8) Fleming, A. M.; Burrows, C. J. On the Irrelevancy of Hydroxyl Radical to DNA Damage from Oxidative Stress and Implications for Epigenetics. *Chem. Soc. Rev.* **2020**, *49* (18), 6524–6528.

(9) Fleming, A. M.; Burrows, C. J. Formation and Processing of DNA Damage Substrates for the HNEIL Enzymes. *Free Radic. Biol. Med.* **2017**, *107*, 35–52.

(10) Henderson, P. T.; Delaney, J. C.; Muller, J. G.; Neeley, W. L.; Tannenbaum, S. R.; Burrows, C. J.; Essigmann, J. M. The Hydantoin Lesions Formed from Oxidation of 7,8-Dihydro-8-Oxoguanine Are Potent Sources of Replication Errors in Vivo. *Biochemistry* **2003**, *42* (31), 9257–9262.

(11) Kornyushyna, O.; Burrows, C. J. Effect of the Oxidized Guanosine Lesions Spiroiminodihydantoin and Guanidinohydantoin on Proofreading by Escherichia Coli DNA Polymerase I (Klenow Fragment) in Different Sequence Contexts. *Biochemistry* **2003**, *42* (44), 13008–13018.

(12) Cooke, M. S.; Evans, M. D.; Dizdaroglu, M.; Lunec, J. Oxidative DNA Damage: Mechanisms, Mutation, and Disease. *FASEB J.* **2003**, *17* (10), 1195–1214.

(13) Kreutzer, D. A.; Essigmann, J. M. Oxidized, Deaminated Cytosines Are a Source of C → T Transitions in Vivo. *Proc. Natl. Acad. Sci. U. S. A.* **1998**, *95* (7), 3578–3582.

(14) Johnson, R. E.; Yu, S. L.; Prakash, S.; Prakash, L. Yeast DNA Polymerase Zeta (ζ) Is Essential for Error-Free Replication Past Thymine Glycol. *Genes Dev.* **2003**, *17* (1), 77–87.

(15) Tubbs, J. L.; Tainer, J. A. DNA Damage: Alkylation. In *Encyclopedia of Biological Chemistry*; Elsevier, 2013; pp 9–15.

(16) Richardson, F. C.; Richardson, K. K. Sequence-Dependent Formation of Alkyl DNA Adducts: A Review of Methods, Results, and Biological Correlates. *Mutat. Res. Mol. Mech. Mutagen.* **1990**, *233* (1–2), 127–138.

(17) Barnes, J. L.; Zubair, M.; John, K.; Poirier, M. C.; Martin, F. L. Carcinogens and DNA Damage. *Biochem. Soc. Trans.* **2018**, *46* (5), 1213–1224.

(18) McCullough, A. K.; Lloyd, R. S. Mechanisms Underlying Aflatoxin-Associated Mutagenesis – Implications in Carcinogenesis. *DNA Repair (Amst).* **2019**, *77* (March), 76–86.

(19) Lyko, F. The DNA Methyltransferase Family: A Versatile Toolkit for Epigenetic Regulation. *Nat. Rev. Genet. 2017 192* **2017**, *19* (2), 81–92.

(20) Lindahl, T. An N Glycosidase from Escherichia Coli That Releases Free Uracil from DNA Containing Deaminated Cytosine Residues. *Proc. Natl. Acad. Sci. U. S. A.* **1974**, *71* (9), 3649–3653.

(21) Mouret, S.; Baudouin, C.; Charveron, M.; Favier, A.; Cadet, J.; Douki, T. Cyclobutane Pyrimidine Dimers Are Predominant DNA Lesions in Whole Human Skin Exposed to UVA Radiation. *Proc. Natl. Acad. Sci. U. S. A.* **2006**, *103* (37), 13765–13770.

(22) Avendaño, C.; Menéndez, J. C. DNA Alkylating Agents. *Med. Chem. Anticancer Drugs* **2008**, 139–176.

(23) MacMillan, K. S.; Boger, D. L. Fundamental Relationships between Structure, Reactivity, and Biological Activity for the Duocarmycins and CC-1065. *J. Med. Chem.* **2009**, *52* (19), 5771–5780.

(24) Imani Nejad, M.; Housh, K.; Rodriguez, A. A.; Haldar, T.; Kathe, S.; Wallace, S. S.; Eichman, B. F.; Gates, K. S. Unhooking of an Interstrand Cross-Link at DNA Fork Structures by the DNA Glycosylase NEIL3. *DNA Repair (Amst).* **2020**, *86*, 102752.

(25) Yang, Z.; Nejad, M. I.; Varela, J. G.; Price, N. E.; Wang, Y.; Gates, K. S. A Role for the Base Excision Repair Enzyme NEIL3 in Replication-Dependent Repair of Interstrand DNA Cross-Links Derived from Psoralen and Abasic Sites. *DNA Repair (Amst).* **2017**, *52* (573), 1–11.

(26) Sancar, A. Structure and Function of DNA Photolyase and Cryptochrome Blue-Light Photoreceptors. *Chem. Rev.* **2003**, *103* (6), 2203–2238.

(27) Margison, G. P.; Santibáñez-Koref, M. F. O6-Alkylguanine-DNA Alkyltransferase: Role in Carcinogenesis and Chemotherapy. *Bioessays* **2002**, *24* (3), 255–266.

(28) Yi, C.; He, C. DNA Repair by Reversal of DNA Damage. *Cold Spring Harb. Perspect. Biol.* **2013**, *5* (1), a012575–a012575.

(29) Li, X.; Heyer, W. D. Homologous Recombination in DNA Repair and DNA Damage Tolerance. *Cell Res. 2008 181* **2008**, *18* (1), 99–113.

(30) Chang, H. H. Y.; Pannunzio, N. R.; Adachi, N.; Lieber, M. R. Non-Homologous DNA End Joining and Alternative Pathways to Double-Strand Break Repair. *Nat. Rev. Mol. Cell*

Biol. **2017**, *18* (8), 495–506.

(31) Kisker, C.; Kuper, J.; Van Houten, B. Prokaryotic Nucleotide Excision Repair. *Cold Spring Harb. Perspect. Biol.* **2013**, *5* (3), a012591–a012591.

(32) Li, G.-M. Mechanisms and Functions of DNA Mismatch Repair. *Cell Res.* **2008**, *18* (1), 85–98.

(33) Trasviña-Arenas, C. H.; Demir, M.; Lin, W. J.; David, S. S. Structure, Function and Evolution of the Helix-Hairpin-Helix DNA Glycosylase Superfamily: Piecing Together the Evolutionary Puzzle of DNA Base Damage Repair Mechanisms. *DNA Repair (Amst).* **2021**, *108* (September).

(34) Mullins, E. A.; Rodriguez, A. A.; Bradley, N. P.; Eichman, B. F. Emerging Roles of DNA Glycosylases and the Base Excision Repair Pathway. *Trends Biochem. Sci.* **2019**, *44* (9), 765–781.

(35) David, S. S.; Williams, S. D. Chemistry of Glycosylases and Endonucleases Involved in Base-Excision Repair. *Chem. Rev.* **1998**, *98* (3), 1221–1262.

(36) Robertson, A. B.; Klungland, A.; Rognes, T.; Leiros, I. DNA Repair in Mammalian Cells: Base Excision Repair: The Long and Short of It. *Cell. Mol. Life Sci.* **2009**, *66* (6), 981–993.

(37) Prakash, A.; Doublié, S.; Wallace, S. S. The Fpg/Nei Family of DNA Glycosylases: Substrates, Structures, and Search for Damage. In *Progress in Molecular Biology and Translational Science*; Elsevier B.V., 2012; Vol. 110, pp 71–91.

(38) Lee, A. J.; Wallace, S. S. The DNA Glycosylases That Recognize and Remove Free Radical-Damaged Pyrimidines. In *The Base Excision Repair Pathway*; WORLD SCIENTIFIC, 2017; pp 117–188.

(39) Liu, M.; Bandaru, V.; Bond, J. P.; Jaruga, P.; Zhao, X.; Christov, P. P.; Burrows, C. J.; Rizzo, C. J.; Dizdaroglu, M.; Wallace, S. S. The Mouse Ortholog of NEIL3 Is a Functional DNA Glycosylase in Vitro and in Vivo. *Proc. Natl. Acad. Sci. U. S. A.* **2010**, *107* (11), 4925–4930.

(40) Dizdaroglu, M.; Burgess, S. M.; Jaruga, P.; Hazra, T. K.; Rodriguez, H.; Lloyd, R. S. Substrate Specificity and Excision Kinetics of Escherichia Coli Endonuclease VIII (Nei) for Modified Bases in DNA Damaged by Free Radicals. *Biochemistry* **2001**, *40* (40), 12150–12156.

(41) Lavrukhin, O. V.; Lloyd, R. S. Involvement of Phylogenetically Conserved Acidic Amino Acid Residues in Catalysis by an Oxidative DNA Damage Enzyme Formamidopyrimidine Glycosylase. *Biochemistry* **2000**, *39* (49), 15266–15271.

(42) Vik, E. S.; Alseth, I.; Forsbring, M.; Helle, I. H.; Morland, I.; Luna, L.; Bjørås, M.; Dalhus, B. Biochemical Mapping of Human NEIL1 DNA Glycosylase and AP Lyase Activities. *DNA Repair (Amst).* **2012**, *11* (9), 766–773.

(43) Liu, M.; Doublié, S.; Wallace, S. S. Neil3, the Final Frontier for the DNA Glycosylases That Recognize Oxidative Damage. *Mutation Research - Fundamental and Molecular*

Mechanisms of Mutagenesis. NIH Public Access March 2013, pp 4–11. https://doi.org/10.1016/j.mrfmmm.2012.12.003.

(44) Liu, M.; Imamura, K.; Averill, A. M.; Wallace, S. S.; Doublié, S. Structural Characterization of a Mouse Ortholog of Human NEIL3 with a Marked Preference for Single-Stranded DNA. *Structure* **2013**, *21* (2), 247–256.

(45) Hegde, M. L.; Hegde, P. M.; Bellot, L. J.; Mandal, S. M.; Hazra, T. K.; Li, G. M.; Boldogh, I.; Tomkinson, A. E.; Mitra, S. Prereplicative Repair of Oxidized Bases in the Human Genome Is Mediated by NEIL1 DNA Glycosylase Together with Replication Proteins. *Proc. Natl. Acad. Sci. U. S. A.* **2013**, *110* (33).

(46) Doublié, S.; Bandaru, V.; Bond, J. P.; Wallace, S. S. The Crystal Structure of Human Endonuclease VIII-like 1 (NEIL1) Reveals a Zincless Finger Motif Required for Glycosylase Activity. *Proc. Natl. Acad. Sci. U. S. A.* **2004**, *101* (28), 10284–10289.

(47) Rodriguez, A. A.; Wojtaszek, J. L.; Greer, B. H.; Haldar, T.; Gates, K. S.; Williams, R. S.; Eichman, B. F. An Autoinhibitory Role for the GRF Zinc Finger Domain of DNA Glycosylase NEIL3. *J. Biol. Chem.* **2020**, jbc.RA120.015541.

(48) Eckenroth, B. E.; Cao, V. B.; Averill, A. M.; Dragon, J. A.; Doublié, S. Unique Structural Features of Mammalian NEIL2 DNA Glycosylase Prime Its Activity for Diverse DNA Substrates and Environments. *Structure* **2020**, *28*, 1–14.

(49) Yeo, J.; Lotsof, E. R.; Anderson-Steele, B. M.; David, S. S. RNA Editing of the Human DNA Glycosylase NEIL1 Alters Its Removal of 5-Hydroxyuracil Lesions in DNA. *Biochemistry* **2021**, *60* (19), 1485–1497.

(50) Bandaru, V. A Novel Human DNA Glycosylase That Removes Oxidative DNA Damage and Is Homologous to Escherichia Coli Endonuclease VIII. *DNA Repair (Amst).* **2002**, *1* (7), 517–529.

(51) David, S. S.; O'Shea, V. L.; Kundu, S. Base-Excision Repair of Oxidative DNA Damage. *Nature* **2007**, *447* (7147), 941–950.

(52) Krishnamurthy, N.; Zhao, X.; Burrows, C. J.; David, S. S. Superior Removal of Hydantoin Lesions Relative to Other Oxidized Bases by the Human DNA Glycosylase HNEIL1. *Biochemistry* **2008**, *47* (27), 7137–7146.

(53) Grin, I. R.; Zharkov, D. O. Eukaryotic Endonuclease VIII-like Proteins: New Components of the Base Excision DNA Repair System. *Biochemistry. (Mosc).* **2011**, *76* (1), 80–93.

(54) Jaruga, P.; Birincioglu, M.; Rosenquist, T. A.; Dizdaroglu, M. Mouse NEIL1 Protein Is Specific for Excision of 2,6-Diamino-4-Hydroxy-5- Formamidopyrimidine and 4,6-Diamino-5-Formamidopyrimidine from Oxidatively Damaged DNA. *Biochemistry* **2004**, *43* (50), 15909–15914.

(55) Zhang, Q. M.; Yonekura, S. I.; Takao, M.; Yasui, A.; Sugiyama, H.; Yonei, S. DNA Glycosylase Activities for Thymine Residues Oxidized in the Methyl Group Are Functions of the HNEIL1 and HNTH1 Enzymes in Human Cells. *DNA Repair (Amst).* **2005**, *4* (1), 71–79.

(56) Minko, I. G.; Vartanian, V. L.; Tozaki, N. N.; Coskun, E.; Coskun, S. H.; Jaruga, P.; Yeo, J.; David, S. S.; Stone, M. P.; Egli, M.; Dizdaroglu, M.; McCullough, A. K.; Lloyd, R. S. Recognition of DNA Adducts by Edited and Unedited Forms of DNA Glycosylase NEIL1. *DNA Repair (Amst).* **2020**, *85* (August), 102741.

(57) Spruijt, C. G.; Gnerlich, F.; Smits, A. H.; Pfaffeneder, T.; Jansen, P. W. T. C.; Bauer, C.; Münzel, M.; Wagner, M.; Müller, M.; Khan, F.; Eberl, H. C.; Mensinga, A.; Brinkman, A. B.; Lephikov, K.; Müller, U.; Walter, J.; Boelens, R.; Van Ingen, H.; Leonhardt, H.; Carell, T.; Vermeulen, M. Dynamic Readers for 5-(Hydroxy)Methylcytosine and Its Oxidized Derivatives. *Cell* **2013**, *152* (5), 1146–1159.

(58) Slyvka, A.; Mierzejewska, K.; Bochtler, M. Nei-like 1 (NEIL1) Excises 5-Carboxylcytosine Directly and Stimulates TDG-Mediated 5-Formyl and 5-Carboxylcytosine Excision. *Sci. Rep.* **2017**, *7* (1), 9001.

(59) Schomacher, L.; Han, D.; Musheev, M. U.; Arab, K.; Kienhöfer, S.; Von Seggern, A.; Niehrs, C. Neil DNA Glycosylases Promote Substrate Turnover by Tdg during DNA Demethylation. *Nat. Struct. Mol. Biol.* **2016**, *23* (2), 116–124.

(60) Jia, L.; Shafirovich, V.; Geacintov, N. E.; Broyde, S. Lesion Specificity in the Base Excision Repair Enzyme HNeil1: Modeling and Dynamics Studies. *Biochemistry* **2007**, *46* (18), 5305–5314.

(61) Perlow-Poehnelt, R. A.; Zharkov, D. O.; Grollman, A. P.; Broyde, S. Substrate Discrimination by Formamidopyrimidine-DNA Glycosylase: Distinguishing Interactions within the Active Site. *Biochemistry* **2004**, *43* (51), 16092–16105.

(62) Athanasiadis, A.; Rich, A.; Maas, S. Widespread A-to-I RNA Editing of Alu-Containing MRNAs in the Human Transcriptome. *PLoS Biol.* **2004**, *2* (12), e391.

(63) Li, J. B.; Levanon, E. Y.; Yoon, J.-K.; Aach, J.; Xie, B.; Leproust, E.; Zhang, K.; Gao, Y.; Church, G. M. Genome-Wide Identification of Human RNA Editing Sites by Parallel DNA Capturing and Sequencing. *Science* **2009**, *324* (5931), 1210–1213.

(64) Yeo, J.; Goodman, R. A.; Schirle, N. T.; David, S. S.; Beal, P. A. RNA Editing Changes the Lesion Specificity for the DNA Repair Enzyme NEIL1. *Proc. Natl. Acad. Sci. U. S. A.* **2010**, *107* (48), 20715–20719.

(65) Maydanovych, O.; Beal, P. A. Breaking the Central Dogma by RNA Editing. *Chemical Reviews*. American Chemical Society August 2006, pp 3397–3411. https://doi.org/10.1021/cr050314a.

(66) Wiederhold, L.; Leppard, J. B.; Kedar, P.; Karimi-Busheri, F.; Rasouli-Nia, A.; Weinfeld, M.; Tomkinson, A. E.; Izumi, T.; Prasad, R.; Wilson, S. H.; Mitra, S.; Hazra, T. K. AP Endonuclease-Independent DNA Base Excision Repair in Human Cells. *Mol. Cell* **2004**, *15* (2), 209–220.

(67) Onizuka, K.; Yeo, J.; David, S. S.; Beal, P. A. NEIL1 Binding to DNA Containing 2′-Fluorothymidine Glycol Stereoisomers and the Effect of Editing. *ChemBioChem* **2012**, *13* (9), 1338–1348.

(68) Cao, S.; Rogers, J.; Yeo, J.; Anderson-Steele, B.; Ashby, J.; David, S. S. 2′-Fluorinated

Hydantoins as Chemical Biology Tools for Base Excision Repair Glycosylases. *ACS Chem. Biol.* **2020**, *15* (4), 915–924.

(69) Zhu, C.; Lu, L.; Zhang, J.; Yue, Z.; Song, J.; Zong, S.; Liu, M.; Stovicek, O.; Gao, Y. Q.; Yi, C. Tautomerization-Dependent Recognition and Excision of Oxidation Damage in Base-Excision DNA Repair. *Proc. Natl. Acad. Sci. U. S. A.* **2016**, *113* (28), 7792–7797.

(70) Liu, M.; Zhang, J.; Zhu, C.; Zhang, X.; Xiao, W.; Yan, Y.; Liu, L.; Zeng, H.; Gao, Y. Q.; Yi, C. DNA Repair Glycosylase HNEIL1 Triages Damaged Bases via Competing Interaction Modes. *Nat. Commun. 2021 121* **2021**, *12* (1), 1–12.

(71) Teoh, P. J.; An, O.; Chung, T. H.; Chooi, J. Y.; Toh, S. H. M.; Fan, S.; Wang, W.; Koh, B. T. H.; Fullwood, M. J.; Ooi, M. G.; de Mel, S.; Soekojo, C. Y.; Chen, L.; Ng, S. B.; Yang, H.; Chng, W. J. Aberrant Hyperediting of the Myeloma Transcriptome by ADAR1 Confers Oncogenicity and Is a Marker of Poor Prognosis. *Blood* **2018**, *132* (12), 1304–1317.

(72) Xu, L. Di; Öhman, M. ADAR1 Editing and Its Role in Cancer. *Genes*. MDPI AG January 1, 2019. https://doi.org/10.3390/genes10010012.

(73) Anadón, C.; Guil, S.; Simó-Riudalbas, L.; Moutinho, C.; Setien, F.; Martínez-Cardús, A.; Moran, S.; Villanueva, A.; Calaf, M.; Vidal, A.; Lazo, P. A.; Zondervan, I.; Savola, S.; Kohno, T.; Yokota, J.; De Pouplana, L. R.; Esteller, M. Gene Amplification-Associated Overexpression of the RNA Editing Enzyme ADAR1 Enhances Human Lung Tumorigenesis. *Oncogene* **2016**, *35* (33), 4407–4413.

(74) Canugovi, C.; Shamanna, R. A.; Croteau, D. L.; Bohr, V. A. Base Excision DNA Repair Levels in Mitochondrial Lysates of Alzheimer's Disease. *Neurobiol. Aging* **2014**, *35* (6), 1293–1300.

(75) Das, A.; Boldogh, I.; Jae, W. L.; Harrigan, J. A.; Hegde, M. L.; Piotrowski, J.; Pinto, N. D. S.; Ramos, W.; Greenberg, M. M.; Hazra, T. K.; Mitra, S.; Bohr, V. A. The Human Werner Syndrome Protein Stimulates Repair of Oxidative DNA Base Damage by the DNA Glycosylase NEIL1. *J. Biol. Chem.* **2007**, *282* (36), 26591–26602.

(76) Canugovi, C.; Yoon, J. S.; Feldman, N. H.; Croteau, D. L.; Mattson, M. P.; Bohr, V. A. Endonuclease VIII-like 1 (NEIL1) Promotes Short-Term Spatial Memory Retention and Protects from Ischemic Stroke-Induced Brain Dysfunction and Death in Mice. *Proc. Natl. Acad. Sci. U. S. A.* **2012**, *109* (37), 14948–14953.

(77) Sampath, H.; Batra, A. K.; Vartanian, V.; Carmical, J. R.; Prusak, D.; King, I. B.; Lowell, B.; Earley, L. F.; Wood, T. G.; Marks, D. L.; McCullough, A. K.; R Stephen, L. Variable Penetrance of Metabolic Phenotypes and Development of High-Fat Diet-Induced Adiposity in NEIL1-Deficient Mice. *Am. J. Physiol. Endocrinol. Metab.* **2011**, *300* (4), E724.

(78) Vartanian, V.; Lowell, B.; Minko, I. G.; Wood, T. G.; Ceci, J. D.; George, S.; Ballinger, S. W.; Corless, C. L.; McCullough, A. K.; Lloyd, R. S. The Metabolic Syndrome Resulting from a Knockout of the NEIL1 DNA Glycosylase. *Proc. Natl. Acad. Sci. U. S. A.* **2006**, *103* (6), 1864–1869.

(79) Yang, B.; Figueroa, D. M.; Hou, Y.; Babbar, M.; Baringer, S. L.; Croteau, D. L.; Bohr, V. A. NEIL1 Stimulates Neurogenesis and Suppresses Neuroinflammation after Stress. *Free Radic. Biol. Med.* **2019**, *141* (June), 47–58.

(80) Hazra, T. K.; Kow, Y. W.; Hatahet, Z.; Imhoff, B.; Boldogh, I.; Mokkapati, S. K.; Mitra, S.; Izumi, T. Identification and Characterization of a Novel Human DNA Glycosylase for Repair of Cytosine-Derived Lesions. *J. Biol. Chem.* **2002**, *277* (34), 30417–30420.

(81) Hildrestrand, G. A.; Rolseth, V.; Bjørås, M.; Luna, L. Human NEIL1 Localizes with the Centrosomes and Condensed Chromosomes during Mitosis. *DNA Repair (Amst).* **2007**, *6* (10), 1425–1433.

(82) Rangaswamy, S.; Pandey, A.; Mitra, S.; Hegde, M. Pre-Replicative Repair of Oxidized Bases Maintains Fidelity in Mammalian Genomes: The Cowcatcher Role of NEIL1 DNA Glycosylase. *Genes (Basel).* **2017**, *8* (7), 175.

(83) Mokkapati, S. K.; Wiederhold, L.; Hazra, T. K.; Mitra, S. Stimulation of DNA Glycosylase Activity of OGG1 by NEIL1: Functional Collaboration between Two Human DNA Glycosylases. *Biochemistry* **2004**, *43* (36), 11596–11604.

(84) Tang, W.; Robles, A. I.; Beyer, R. P.; Gray, L. T.; Nguyen, G. H.; Oshima, J.; Maizels, N.; Harris, C. C.; Monnat, R. J. The Werner Syndrome RECQ Helicase Targets G4 DNA in Human Cells to Modulate Transcription. *Hum. Mol. Genet.* **2016**, *25* (10), 2060–2069.

(85) Zhou, J.; Fleming, A. M.; Averill, A. M.; Burrows, C. J.; Wallace, S. S. The NEIL Glycosylases Remove Oxidized Guanine Lesions from Telomeric and Promoter Quadruplex DNA Structures. *Nucleic Acids Res.* **2015**, *43* (8), 4039–4054.

(86) Hailer, M. K.; Slade, P. G.; Martin, B. D.; Rosenquist, T. A.; Sugden, K. D. Recognition of the Oxidized Lesions Spiroiminodihydantoin and Guanidinohydantoin in DNA by the Mammalian Base Excision Repair Glycosylases NEIL1 and NEIL2. *DNA Repair (Amst).* **2005**, *4* (1), 41–50.

(87) Makasheva, K. A.; Endutkin, A. V.; Zharkov, D. O. Requirements for Dna Bubble Structure for Efficient Cleavage by Helix-Two-Turn-Helix Dna Glycosylases. *Mutagenesis* **2020**, *35* (1), 119–128.

(88) Das, A.; Wiederhold, L.; Leppard, J. B.; Kedar, P.; Prasad, R.; Wang, H.; Boldogh, I.; Karimi-Busheri, F.; Weinfeld, M.; Tomkinson, A. E.; Wilson, S. H.; Mitra, S.; Hazra, T. K. NEIL2-Initiated, APE-Independent Repair of Oxidized Bases in DNA: Evidence for a Repair Complex in Human Cells. *DNA Repair (Amst).* **2006**, *5* (12), 1439–1448.

(89) Mandal, S. M.; Hegde, M. L.; Chatterjee, A.; Hegde, P. M.; Szczesny, B.; Banerjee, D.; Boldogh, I.; Gao, R.; Falkenberg, M.; Gustafsson, C. M.; Sarkar, P. S.; Hazra, T. K. Role of Human DNA Glycosylase Nei-like 2 (NEIL2) and Single Strand Break Repair Protein Polynucleotide Kinase 3′-Phosphatase in Maintenance of Mitochondrial Genome. *J. Biol. Chem.* **2012**, *287* (4), 2819–2829.

(90) Das, S.; Chattopadhyay, R.; Bhakat, K. K.; Boldogh, I.; Kohno, K.; Prasad, R.; Wilson, S. H.; Hazra, T. K. Stimulation of NEIL2-Mediated Oxidized Base Excision Repair via YB-1 Interaction during Oxidative Stress. *J. Biol. Chem.* **2007**, *282* (39), 28474–28484.

(91) Kang, L.; Zou, X.; Zhang, G.; Xiang, J.; Wang, Y.; Yang, M.; Chen, X.; Wu, J.; Guan, A. H. A Variant in a MicroRNA Binding Site in NEIL2 3′UTR Confers Susceptibility to Age-related Cataracts. *FASEB J.* **2019**, *33* (9), 10469–10476.

(92) Pau, C. T.; Mosbruger, T.; Saxena, R.; Welt, C. K. Phenotype and Tissue Expression as a Function of Genetic Risk in Polycystic Ovary Syndrome. *PLoS One* **2017**, *12* (1), e0168870.

(93) Lillenes, M. S.; Espeseth, T.; Støen, M.; Lundervold, A. J.; Frye, S. A.; Rootwelt, H.; Reinvang, I.; Tønjum, T. DNA Base Excision Repair Gene Polymorphisms Modulate Human Cognitive Performance and Decline during Normal Life Span. *Mech. Ageing Dev.* **2011**, *132* (8–9), 449–458.

(94) Osorio, A.; Milne, R. L.; Kuchenbaecker, K.; Vaclová, T.; Pita, G.; Alonso, R.; Peterlongo, P.; Blanco, I.; de la Hoya, M.; Duran, M.; Díez, O.; Ramón y Cajal, T.; Konstantopoulou, I.; Martínez-Bouzas, C.; Andrés Conejero, R.; Soucy, P.; McGuffog, L.; Barrowdale, D.; Lee, A.; Arver, B.; Rantala, J.; Loman, N.; Ehrencrona, H.; Olopade, O. I.; Beattie, M. S.; Domchek, S. M.; Nathanson, K.; Rebbeck, T. R.; Arun, B. K.; Karlan, B. Y.; Walsh, C.; Lester, J.; John, E. M.; Whittemore, A. S.; Daly, M. B.; Southey, M.; Hopper, J.; Terry, M. B.; Buys, S. S.; Janavicius, R.; Dorfling, C. M.; van Rensburg, E. J.; Steele, L.; Neuhausen, S. L.; Ding, Y. C.; Hansen, T. v. O.; Jønson, L.; Ejlertsen, B.; Gerdes, A. M.; Infante, M.; Herráez, B.; Moreno, L. T.; Weitzel, J. N.; Herzog, J.; Weeman, K.; Manoukian, S.; Peissel, B.; Zaffaroni, D.; Scuvera, G.; Bonanni, B.; Mariette, F.; Volorio, S.; Viel, A.; Varesco, L.; Papi, L.; Ottini, L.; Tibiletti, M. G.; Radice, P.; Yannoukakos, D.; Garber, J.; Ellis, S.; Frost, D.; Platte, R.; Fineberg, E.; Evans, G.; Lalloo, F.; Izatt, L.; Eeles, R.; Adlard, J.; Davidson, R.; Cole, T.; Eccles, D.; Cook, J.; Hodgson, S.; Brewer, C.; Tischkowitz, M.; Douglas, F.; Porteous, M.; Side, L.; Walker, L.; Morrison, P.; Donaldson, A.; Kennedy, J.; Foo, C.; Godwin, A. K.; Schmutzler, R. K.; Wappenschmidt, B.; Rhiem, K.; Engel, C.; Meindl, A.; Ditsch, N.; Arnold, N.; Plendl, H. J.; Niederacher, D.; Sutter, C.; Wang-Gohrke, S.; Steinemann, D.; Preisler-Adams, S.; Kast, K.; Varon-Mateeva, R.; Gehrig, A.; Stoppa-Lyonnet, D.; Sinilnikova, O. M.; Mazoyer, S.; Damiola, F.; Poppe, B.; Claes, K.; Piedmonte, M.; Tucker, K.; Backes, F.; Rodríguez, G.; Brewster, W.; Wakeley, K.; Rutherford, T.; Caldés, T.; Nevanlinna, H.; Aittomäki, K.; Rookus, M. A.; van Os, T. A. M.; van der Kolk, L.; de Lange, J. L.; Meijers-Heijboer, H. E. J.; van der Hout, A. H.; van Asperen, C. J.; Gómez Garcia, E. B.; Hoogerbrugge, N.; Collée, J. M.; van Deurzen, C. H. M.; van der Luijt, R. B.; Devilee, P.; Olah, E.; Lázaro, C.; Teulé, A.; Menéndez, M.; Jakubowska, A.; Cybulski, C.; Gronwald, J.; Lubinski, J.; Durda, K.; Jaworska-Bieniek, K.; Johannsson, O. T.; Maugard, C.; Montagna, M.; Tognazzo, S.; Teixeira, M. R.; Healey, S.; Olswold, C.; Guidugli, L.; Lindor, N.; Slager, S.; Szabo, C. I.; Vijai, J.; Robson, M.; Kauff, N.; Zhang, L.; Rau-Murthy, R.; Fink-Retter, A.; Singer, C. F.; Rappaport, C.; Geschwantler Kaulich, D.; Pfeiler, G.; Tea, M. K.; Berger, A.; Phelan, C. M.; Greene, M. H.; Mai, P. L.; Lejbkowicz, F.; Andrulis, I.; Mulligan, A. M.; Glendon, G.; Toland, A. E.; Bojesen, A.; Pedersen, I. S.; Sunde, L.; Thomassen, M.; Kruse, T. A.; Jensen, U. B.; Friedman, E.; Laitman, Y.; Shimon, S. P.; Simard, J.; Easton, D. F.; Offit, K.; Couch, F. J.; Chenevix-Trench, G.; Antoniou, A. C.; Benitez, J. DNA Glycosylases Involved in Base Excision Repair May Be Associated with Cancer Risk in BRCA1 and BRCA2 Mutation Carriers. *PLOS Genet.* **2014**, *10* (4), e1004256.

(95) Benítez-Buelga, C.; Baquero, J. M.; Vaclova, T.; Fernández, V.; Martín, P.; Inglada-Perez, L.; Urioste, M.; Osorio, A.; Benítez, J. Genetic Variation in the NEIL2 DNA Glycosylase Gene Is Associated with Oxidative DNA Damage in BRCA2 Mutation Carriers. *Oncotarget* **2017**, *8* (70), 114626.

(96) Zhou, J.; Chan, J.; Lambelé, M.; Yusufzai, T.; Stumpff, J.; Opresko, P. L.; Thali, M.; Wallace, S. S. NEIL3 Repairs Telomere Damage during S Phase to Secure Chromosome Segregation at Mitosis. *Cell Rep.* **2017**, *20* (9), 2044–2056.

(97) Skarpengland, T.; Holm, S.; Scheffler, K.; Gregersen, I.; Dahl, T. B.; Suganthan, R.; Segers, F. M.; Østlie, I.; Otten, J. J. T.; Luna, L.; Ketelhuth, D. F. J.; Lundberg, A. M.; Neurauter, C. G.; Hildrestrand, G.; Skjelland, M.; Bjørndal, B.; Svardal, A. M.; Iversen, P. O.; Hedin, U.; Nygard, S.; Olstad, O. K.; Krohg-Sørensen, K.; Slupphaug, G.; Eide, L.; Kuśnierczyk, A.; Folkersen, L.; Ueland, T.; Berge, R. K.; Hansson, G. K.; Biessen, E. A. L.; Halvorsen, B.; Bjøras, M.; Aukrust, P. Neil3-Dependent Base Excision Repair Regulates Lipid Metabolism and Prevents Atherosclerosis in Apoe-Deficient Mice. *Sci. Rep.* **2016**, *6* (1), 1–13.

(98) Regnell, C. E. E.; Hildrestrand, G. A. A.; Sejersted, Y.; Medin, T.; Moldestad, O.; Rolseth, V.; Krokeide, S. Z. Z.; Suganthan, R.; Luna, L.; Bjørås, M.; Bergersen, L. H. H. Hippocampal Adult Neurogenesis Is Maintained by Neil3-Dependent Repair of Oxidative DNA Lesions in Neural Progenitor Cells. *Cell Rep.* **2012**, *2* (3), 503–510.

(99) Massaad, M. J.; Zhou, J.; Tsuchimoto, D.; Chou, J.; Jabara, H.; Janssen, E.; Glauzy, S.; Olson, B. G.; Morbach, H.; Ohsumi, T. K.; Schmitz, K.; Kyriacos, M.; Kane, J.; Torisu, K.; Nakabeppu, Y.; Notarangelo, L. D.; Chouery, E.; Megarbane, A.; Kang, P. B.; Al-Idrissi, E.; Aldhekri, H.; Meffre, E.; Mizui, M.; Tsokos, G. C.; Manis, J. P.; Al-Herz, W.; Wallace, S. S.; Geha, R. S. Deficiency of Base Excision Repair Enzyme NEIL3 Drives Increased Predisposition to Autoimmunity. *J. Clin. Invest.* **2016**, *126* (11), 4219–4236.

(100) He, Y. F.; Li, B. Z.; Li, Z.; Liu, P.; Wang, Y.; Tang, Q.; Ding, J.; Jia, Y.; Chen, Z.; Li, N.; Sun, Y.; Li, X.; Dai, Q.; Song, C. X.; Zhang, K.; He, C.; Xu, G. L. Tet-Mediated Formation of 5-Carboxylcytosine and Its Excision by TDG in Mammalian DNA. *Science (80-.).* **2011**, *333* (6047), 1303–1307.

(101) Maiti, A.; Drohat, A. C. Thymine DNA Glycosylase Can Rapidly Excise 5-Formylcytosine and 5-Carboxylcytosine: Potential Implications for Active Demethylation of CpG Sites. *J. Biol. Chem.* **2011**, *286* (41), 35334–35338.

(102) Fleming, A. M.; Ding, Y.; Burrows, C. J. Oxidative DNA Damage Is Epigenetic by Regulating Gene Transcription via Base Excision Repair. *Proc. Natl. Acad. Sci. U. S. A.* **2017**, *114* (10), 2604–2609.

(103) Huppert, J. L.; Balasubramanian, S. Prevalence of Quadruplexes in the Human Genome. *Nucleic Acids Res.* **2005**, *33* (9), 2908–2916.

(104) Fleming, A. M.; Zhu, J.; Howpay Manage, S. A.; Burrows, C. J. Human NEIL3 Gene Expression Regulated by Epigenetic-Like Oxidative DNA Modification. *J. Am. Chem. Soc.* **2019**, *141* (28), 11036–11049.

(105) Duclos, S.; Aller, P.; Jaruga, P.; Dizdaroglu, M.; Wallace, S. S.; Doublié, S. Structural and

Biochemical Studies of a Plant Formamidopyrimidine-DNA Glycosylase Reveal Why Eukaryotic Fpg Glycosylases Do Not Excise 8-Oxoguanine. *DNA Repair (Amst).* **2012**, *11* (9), 714–725.

(106) David, S. S.; O'Shea, V. L.; Kundu, S. Base-Excision Repair of Oxidative DNA Damage. *Nature* **2007**, *447* (7147), 941–950.

(107) Zhao, X.; Krishnamurthy, N.; Burrows, C. J.; David, S. S. Mutation versus Repair: NEILl Removal of Hydantoin Lesions in Single-Stranded, Bulge, Bubble, and Duplex DNA Contexts. *Biochemistry* **2010**, *49* (8), 1658–1666.

(108) Krishnamurthy, N.; Haraguchi, K.; Greenberg, M. M.; David, S. S. Efficient Removal of Formamidopyrimidines by 8-Oxoguanine Glycosylases. *Biochemistry* **2008**, *47* (3), 1043–1050.

(109) Purmal, A. A.; Kow, Y. W.; Wallace, S. S. Major Oxidative Products of Cytosine, 5-Hydroxycytosine and 5-Hydroxyuracil, Exhibit Sequence Context-Dependent Mispairing in Vitro. *Nucleic Acids Res.* **1994**, *22* (1), 72–78.

(110) Purmal, A. A.; Lampman, G. W.; Bond, J. P.; Hatahet, Z.; Wallace, S. S. Enzymatic Processing of Uracil Glycol, a Major Oxidative Product of DNA Cytosine. *J. Biol. Chem.* **1998**, *273* (16), 10026–10035.

(111) Manlove, A. H.; McKibbin, P. L.; Doyle, E. L.; Majumdar, C.; Hamm, M. L.; David, S. S. Structure–Activity Relationships Reveal Key Features of 8-Oxoguanine: A Mismatch Detection by the MutY Glycosylase. *ACS Chem. Biol.* **2017**, *12* (9), 2335–2344.

(112) Rogers, J. Creating a Chemical Toolbox: The Chemical Synthesis of Modified Nucleotides as Probes of DNA Repair Glycosylases, Univeristy of California, Davis, 2007.

(113) Imamura, K.; Averill, A.; Wallace, S. S.; Doublié, S. Structural Characterization of Viral Ortholog of Human DNA Glycosylase NEIL1 Bound to Thymine Glycol or 5-Hydroxyuracil-Containing DNA. *J. Biol. Chem.* **2012**, *287* (6), 4288–4298.

(114) Michelson, A. Z.; Rozenberg, A.; Tian, Y.; Sun, X.; Davis, J.; Francis, A. W.; O'Shea, V. L.; Halasyam, M.; Manlove, A. H.; David, S. S.; Lee, J. K. Gas-Phase Studies of Substrates for the DNA Mismatch Repair Enzyme MutY. *J. Am. Chem. Soc.* **2012**, *134* (48), 19839–19850.

(115) Maiti, A.; Morgan, M. T.; Drohat, A. C. Role of Two Strictly Conserved Residues in Nucleotide Flipping and N-Glycosylic Bond Cleavage by Human Thymine DNA Glycosylase. *J. Biol. Chem.* **2009**, *284* (52), 36680–36688.

(116) Morgan, M. T.; Bennett, M. T.; Drohat, A. C. Excision of 5-Halogenated Uracils by Human Thymine DNA Glycosylase: Robust Activity for DNA Contexts Other than CpG. *J. Biol. Chem.* **2007**, *282* (38), 27578–27586.

(117) Sun, X.; Lee, J. K. Acidity and Proton Affinity of Hypoxanthine in the Gas Phase versus in Solution: Intrinsic Reactivity and Biological Implications. *J. Org. Chem.* **2007**, *72* (17), 6548–6555.

(118) Bennett, M. T.; Rodgers, M. T.; Hebert, A. S.; Ruslander, L. E.; Eisele, L.; Drohat, A. C. Specificity of Human Thymine DNA Glycosylase Depends on N-Glycosidic Bond Stability. *J. Am. Chem. Soc.* **2006**, *128* (38), 12510–12519.

(119) Michelson, A. Z.; Chen, M.; Wang, K.; Lee, J. K. Gas-Phase Studies of Purine 3-Methyladenine DNA Glycosylase II (AlkA) Substrates. *J. Am. Chem. Soc.* **2012**, *134* (23), 9622–9633.

(120) Bhate, A.; Sun, T.; Li, J. B. ADAR1: A New Target for Immuno-Oncology Therapy. *Molecular Cell*. Cell Press March 7, 2019, pp 866–868. https://doi.org/10.1016/j.molcel.2019.02.021.

(121) Oka, N.; Greenberg, M. M. The Effect of the 2-Amino Group of 7,8-Dihydro-8-Oxo-2′-Deoxyguanosine on Translesion Synthesis and Duplex Stability. *Nucleic Acids Res.* **2005**, *33* (5), 1637–1643.

(122) Bodepudi, V.; Shibutani, S.; Johnson, F. Synthesis of 2′-Deoxy-7,8-Dihydro-8-Oxoguanosine and 2′-Deoxy-7,8-Dihydro-8-Oxoadenosine and Their Incorporation into Oligomeric DNA. *Chem. Res. Toxicol.* **1992**, *5* (5), 608–617.

(123) Porello, S. L.; Leyes, A. E.; David, S. S. Single-Turnover and Pre-Steady-State Kinetics of the Reaction of the Adenine Glycosylase MutY with Mismatch-Containing DNA Substrates. *Biochemistry* **1998**, *37* (42), 14756–14764.

(124) Krishnamurthy, N.; Zhao, X.; Burrows, C. J.; David, S. S. Superior Removal of Hydantoin Lesions Relative to Other Oxidized Bases by the Human DNA Glycosylase HNEIL1. *Biochemistry* **2008**, *47* (27), 7137–7146.

(125) Huppert, J. L.; Balasubramanian, S. G-Quadruplexes in Promoters throughout the Human Genome. *Nucleic Acids Res.* **2007**, *35* (2), 406–413.

(126) Biffi, G.; Tannahill, D.; McCafferty, J.; Balasubramanian, S. Quantitative Visualization of DNA G-Quadruplex Structures in Human Cells. *Nat. Chem.* **2013**, *5* (3), 182–186.

(127) Manna, S.; Sarkar, D.; Srivatsan, S. G. A Dual-App Nucleoside Probe Provides Structural Insights into the Human Telomeric Overhang in Live Cells. *J. Am. Chem. Soc.* **2018**, *140* (39), 12622–12633.

(128) Sun, D.; Liu, W. J.; Guo, K.; Rusche, J. J.; Ebbinghaus, S.; Gokhale, V.; Hurley, L. H. The Proximal Promoter Region of the Human Vascular Endothelial Growth Factor Gene Has a G-Quadruplex Structure That Can Be Targeted by G-Quadruplex-Interactive Agents. *Mol. Cancer Ther.* **2008**, *7* (4), 880–889.

(129) Siddiqui-Jain, A.; Grand, C. L.; Bearss, D. J.; Hurley, L. H. Direct Evidence for a G-Quadruplex in a Promoter Region and Its Targeting with a Small Molecule to Repress c-MYC Transcription. *Proc. Natl. Acad. Sci. U. S. A.* **2002**, *99* (18), 11593–11598.

(130) Cogoi, S.; Xodo, L. E. G-Quadruplex Formation within the Promoter of the KRAS Proto-Oncogene and Its Effect on Transcription. *Nucleic Acids Res.* **2006**, *34* (9), 2536–2549.

(131) Miller, K. M.; Forment, J. V; Bradshaw, C. R.; Nikan, M.; Britton, bastien; Oelschlaegel, T.; Xhemalce, B.; Balasubramanian, S.; Jackson, S. P. Small-Molecule–Induced

DNA Damage Identifies Alternative DNA Structures in Human Genes. **2012**.

(132) Neeley, W. L.; Essigmann, J. M. Mechanisms of Formation, Genotoxicity, and Mutation of Guanine Oxidation Products. *Chemical Research in Toxicology*. American Chemical Society April 2006, pp 491–505. https://doi.org/10.1021/tx0600043.

(133) Zhou, J.; Liu, M.; Fleming, A. M.; Burrows, C. J.; Wallace, S. S. Neil3 and NEIL1 DNA Glycosylases Remove Oxidative Damages from Quadruplex DNA and Exhibit Preferences for Lesions in the Telomeric Sequence Context. *J. Biol. Chem.* **2013**, *288* (38), 27263–27272.

(134) Fleming, A. M.; Zhou, J.; Wallace, S. S.; Burrows, C. J. A Role for the Fifth G-Track in G-Quadruplex Forming Oncogene Promoter Sequences during Oxidative Stress: Do These "Spare Tires" Have an Evolved Function? *ACS Cent. Sci.* **2015**, *1* (5), 226–233.

(135) Fleming, A. M.; Zhou, J.; Wallace, S. S.; Burrows, C. J. A Role for the Fifth G-Track in G-Quadruplex Forming Oncogene Promoter Sequences during Oxidative Stress: Do These "Spare Tires" Have an Evolved Function? *ACS Cent. Sci.* **2015**, *1* (5), 226–233.

(136) Yeo, J.; Goodman, R. A.; Schirle, N. T.; David, S. S.; Beal, P. A. RNA Editing Changes the Lesion Specificity for the DNA Repair Enzyme NEIL1. *Proc Natl Acad Sci U S A* **2010**, *107* (48), 20715–20719.

(137) Zhu, J.; Fleming, A. M.; Burrows, C. J. The RAD17 Promoter Sequence Contains a Potential Tail-Dependent G-Quadruplex That Downregulates Gene Expression upon Oxidative Modification. *ACS Chem. Biol.* **2018**, *13* (9), 2577–2584.

(138) Cogoi, S.; Ferino, A.; Miglietta, G.; Pedersen, E. B.; Xodo, L. E. The Regulatory G4 Motif of the Kirsten Ras (KRAS) Gene Is Sensitive to Guanine Oxidation: Implications on Transcription. *Nucleic Acids Res.* **2018**, *46* (2), 661–676.

(139) Lotsof, E. R.; Krajewski, A. E.; Anderson-Steele, B.; Rogers, J.; Zhang, L.; Yeo, J.; Conlon, S. G.; Manlove, A. H.; Lee, J. K.; David, S. S. NEIL1 Recoding Due to RNA Editing Impacts Lesion-Specific Recognition and Excision. *J. Am. Chem. Soc.* **2022**, *144* (32), 14578–14589.

(140) Liu, M.; Bandaru, V.; Holmes, A.; Averill, A. M.; Cannan, W.; Wallace, S. S. Expression and Purification of Active Mouse and Human NEIL3 Proteins. *Protein Expr. Purif.* **2012**, *84* (1), 130–139.

(141) Qin, Y.; Hurley, L. H. Structures, Folding Patterns, and Functions of Intramolecular DNA G-Quadruplexes Found in Eukaryotic Promoter Regions. *Biochimie* **2008**, *90* (8), 1149–1171.

(142) Zhou, J.; Liu, M.; Fleming, A. M.; Burrows, C. J.; Wallace, S. S. Neil3 and NEIL1 DNA Glycosylases Remove Oxidative Damages from Quadruplex DNA and Exhibit Preferences for Lesions in the Telomeric Sequence Context. *J. Biol. Chem.* **2013**, *288* (38), 27263–27272.

(143) Alemasova, E. E.; Moor, N. A.; Naumenko, K. N.; Kutuzov, M. M.; Sukhanova, M. V.; Pestryakov, P. E.; Lavrik, O. I. Y-Box-Binding Protein 1 as a Non-Canonical Factor of Base Excision Repair. *Biochim. Biophys. Acta - Proteins Proteomics* **2016**, *1864* (12),

1631–1640.

(144) Czarny, P.; Bialek, K.; Ziolkowska, S.; Strycharz, J.; Sliwinski, T. DNA Damage and Repair in Neuropsychiatric Disorders. What Do We Know and What Are the Future Perspectives? *Mutagenesis* **2020**, *35* (1), 79–106.

(145) Nelson, B. C.; Dizdaroglu, M. Implications of Dna Damage and Dna Repair on Human Diseases. *Mutagenesis*. Oxford University Press February 13, 2020, pp 1–3. https://doi.org/10.1093/mutage/gez048.

(146) Wiederholt, C. J.; Greenberg, M. M. Fapy·dG Instructs Klenow Exo- to Misincorporate Deoxyadenosine. *J. Am. Chem. Soc.* **2002**, *124* (25), 7278–7279.

(147) Raetz, A. G.; Xie, Y.; Kundu, S.; Brinkmeyer, M. K.; Chang, C.; David, S. S. Cancer-Associated Variants and a Common Polymorphism of MUTYH Exhibit Reduced Repair of Oxidative DNA Damage Using a GFP-Based Assay in Mammalian Cells. *Carcinogenesis* **2012**, *33* (11), 2301–2309.

(148) Nagel, Z. D.; Margulies, C. M.; Chaim, I. A.; McRee, S. K.; Mazzucato, P.; Ahmad, A.; Abo, R. P.; Butty, V. L.; Forget, A. L.; Samson, L. D. Multiplexed DNA Repair Assays for Multiple Lesions and Multiple Doses via Transcription Inhibition and Transcriptional Mutagenesis. *Proc. Natl. Acad. Sci. U. S. A.* **2014**, *111* (18).

(149) Piett, C. G.; Pecen, T. J.; Laverty, D. J.; Nagel, Z. D. Large-Scale Preparation of Fluorescence Multiplex Host Cell Reactivation (FM-HCR) Reporters. *Nat. Protoc.* **2021**, *16* (9), 4265–4298.

(150) Yeo, J. RNA Editing Changes the Lesion Specificity for the DNA Repair Enzyme HNEIL1, University of California, Davis, 2014.

(151) You, C.; Wang, Y. Quantitative Measurement of Transcriptional Inhibition and Mutagenesis Induced by Site-Specifically Incorporated DNA Lesions in Vitro and in Vivo. *Nat. Protoc.* **2015**, *10* (9), 1389–1406.

(152) Henderson, P. T.; Delaney, J. C.; Muller, J. G.; Neeley, W. L.; Tannenbaum, S. R.; Burrows, C. J.; Essigmann, J. M. The Hydantoin Lesions Formed from Oxidation of 7,8-Dihydro-8-Oxoguanine Are Potent Sources of Replication Errors in Vivo. *Biochemistry* **2003**, *42* (31), 9257–9262.

(153) Delaney, M. O.; Wiederholt, C. J.; Greenberg, M. M. Fapy·dA Induces Nucleotide Misincorporation Translesionally by a DNA Polymerase We Are Grateful for Support of This Research by the National Institutes of Health (CA-74954). *Angew. Chemie Int. Ed.* **2002**, *41* (5), 771.

(154) Hurley, L. H. DNA and Its Associated Processes as Targets for Cancer Therapy. *Nat. Rev. Cancer 2002 23* **2002**, *2* (3), 188–200.

(155) Owiti, N. A.; Nagel, Z. D.; Engelward, B. P. Fluorescence Sheds Light on DNA Damage, DNA Repair, and Mutations. *Trends in Cancer* **2021**, *7* (3), 240–248.

(156) Russelburg, L. P.; O'Shea Murray, V. L.; Demir, M.; Knutsen, K. R.; Sehgal, S. L.; Cao, S.; David, S. S.; Horvath, M. P. Structural Basis for Finding Og Lesions and Avoiding

Undamaged g by the Dna Glycosylase Muty. *ACS Chem. Biol.* **2020**, *15* (1), 93–102.

(157) Dow, B. J.; Malik, S. S.; Drohat, A. C. Defining the Role of Nucleotide Flipping in Enzyme Specificity Using 19F NMR. *J. Am. Chem. Soc.* **2019**, *141* (12), 4952–4962.

(158) Meltzer, M.; Long, K.; Nie, Y.; Gupta, M.; Yang, J.; Montano, M. The RNA Editor Gene ADAR1 Is Induced in Myoblasts by Inflammatory Ligands and Buffers Stress Response. *Clin. Transl. Sci.* **2010**, *3* (3), 73–80.

(159) Yuan, B.; OConnor, T. R.; Wang, Y. 6-Thioguanine and S6-Methylthioguanine Are Mutagenic in Human Cells. *ACS Chem. Biol.* **2010**, *5* (11), 1021–1027.

(160) Yang, H.; Tang, J. A.; Greenberg, M. M. Synthesis of Oligonucleotides Containing the N6-(2-Deoxy-α,β-d-Erythropentofuranosyl)-2,6-Diamino-4-Hydroxy-5-Formamidopyrimidine (Fapy·dG) Oxidative Damage Product Derived from 2′-Deoxyguanosine. *Chem. – A Eur. J.* **2020**, *26* (24), 5441–5448.

(161) Brooks, T. A.; Hurley, L. H. The Role of Supercoiling in Transcriptional Control of MYC and Its Importance in Molecular Therapeutics. *Nat. Rev. Cancer 2009 912* **2009**, *9* (12), 849–861.

(162) Berti, P. J.; McCann, J. A. B. Toward a Detailed Understanding of Base Excision Repair Enzymes: Transition State and Mechanistic Analyses of N-Glycoside Hydrolysis and N-Glycoside Transfer. *Chem. Rev.* **2006**, *106* (2), 506–555.

(163) Marquez, V. E.; Tseng, C. K. H.; Kelley, J. A.; Ford, H.; Roth, J. S.; Driscoll, J. S.; Mitsuya, H.; Aoki, S.; Broder, S.; Johns, D. G. Acid-Stable 2'-Fluoro Purine Dideoxynucleosides as Active Agents against HIV. *J. Med. Chem.* **1990**, *33* (3), 978–985.

(164) Luo, W.; Muller, J. G.; Rachlin, E. M.; Burrows, C. J. Characterization of Hydantoin Products from One-Electron Oxidation of 8-Oxo-7,8-Dihydroguanosine in a Nucleoside Model. *Chem. Res. Toxicol.* **2001**, *14* (7), 927–938.

(165) Kornyushyna, O.; Berges, A. M.; Muller, J. G.; Burrows, C. J. In Vitro Nucleotide Misinsertion Opposite the Oxidized Guanosine Lesions Spiroiminodihydantoin and Guanidinohydantoin and DNA Synthesis Past the Lesions Using Escherichia Coli DNA Polymerase I (Klenow Fragment). *Biochemistry* **2002**, *41* (51), 15304–15314.

(166) Eisenberg, E.; Levanon, E. Y. A-to-I RNA Editing — Immune Protector and Transcriptome Diversifier. *Nat. Rev. Genet. 2018 198* **2018**, *19* (8), 473–490.

(167) *Cell line - ADAR - The Human Protein Atlas*. https://www.proteinatlas.org/ENSG00000160710-ADAR/cell+line (accessed 2022-07-25).

(168) Patterson, J. B.; Samuel, C. E. Expression and Regulation by Interferon of a Double-Stranded-RNA-Specific Adenosine Deaminase from Human Cells: Evidence for Two Forms of the Deaminase. *Mol. Cell. Biol.* **1995**, *15* (10), 5376–5388.

(169) *Cell line - NEIL1 - The Human Protein Atlas*. https://www.proteinatlas.org/ENSG00000140398-NEIL1/cell+line (accessed 2022-04-25).

(170) McKibbin, P. L.; Fleming, A. M.; Towheed, M. A.; Van Houten, B.; Burrows, C. J.; David, S. S. Repair of Hydantoin Lesions and Their Amine Adducts in DNA by Base and Nucleotide Excision Repair. *J. Am. Chem. Soc.* **2013**, *135* (37), 13851–13861.

(171) Shafirovich, V.; Geacintov, N. E. Removal of Oxidatively Generated DNA Damage by Overlapping Repair Pathways. *Free Radic. Biol. Med.* **2017**, *107*, 53–61.

(172) Dianov, G. L.; Thybo, T.; Dianova, I. I.; Lipinski, L. J.; Bohr, V. A. Single Nucleotide Patch Base Excision Repair Is the Major Pathway for Removal of Thymine Glycol from DNA in Human Cell Extracts. *J. Biol. Chem.* **2000**, *275* (16), 11809–11813.

(173) Pascucci, B.; D'Errico, M.; Parlanti, E.; Giovannini, S.; Dogliotti, E. Role of Nucleotide Excision Repair Proteins in Oxidative DNA Damage Repair: An Updating. *Biochem. 2011 761* **2011**, *76* (1), 4–15.

(174) Fousteri, M.; Mullenders, L. H. F. Transcription-Coupled Nucleotide Excision Repair in Mammalian Cells: Molecular Mechanisms and Biological Effects. *Cell Res. 2008 181* **2008**, *18* (1), 73–84.

(175) Gregersen, L. H.; Svejstrup, J. Q. The Cellular Response to Transcription-Blocking DNA Damage. *Trends Biochem. Sci.* **2018**, *43* (5), 327–341.

(176) Waters, L. S.; Minesinger, B. K.; Wiltrout, M. E.; D'Souza, S.; Woodruff, R. V.; Walker, G. C. Eukaryotic Translesion Polymerases and Their Roles and Regulation in DNA Damage Tolerance. *Microbiol. Mol. Biol. Rev.* **2009**, *73* (1), 134–154.

(177) Cao, S. Synthesis of Fluorinated Analogs of Oxidative DNA Lesions and Their Use to Probe Features of Recognition and Repair by Base Excision Repair Glycosylases. *ProQuest Diss. Theses* **2010**, No. August, n/a.

(178) McNab, F.; Mayer-Barber, K.; Sher, A.; Wack, A.; O'Garra, A. Type I Interferons in Infectious Disease. *Nat. Rev. Immunol. 2015 152* **2015**, *15* (2), 87–103.

(179) Khansari, N.; Shakiba, Y.; Mahmoudi, M. Chronic Inflammation and Oxidative Stress as a Major Cause of Age-Related Diseases and Cancer. *Recent Pat. Inflamm. Allergy Drug Discov.* **2009**, *3* (1), 73–80.

(180) Roos, W. P.; Thomas, A. D.; Kaina, B. DNA Damage and the Balance between Survival and Death in Cancer Biology. *Nat. Rev. Cancer 2015 161* **2015**, *16* (1), 20–33.

(181) Helleday, T.; Petermann, E.; Lundin, C.; Hodgson, B.; Sharma, R. A. DNA Repair Pathways as Targets for Cancer Therapy. *Nat. Rev. Cancer 2008 83* **2008**, *8* (3), 193–204.

(182) Baquero, J. M.; Benítez-Buelga, C.; Rajagopal, V.; Zhenjun, Z.; Torres-Ruiz, R.; Müller, S.; Hanna, B. M. F.; Loseva, O.; Wallner, O.; Michel, M.; Rodríguez-Perales, S.; Gad, H.; Visnes, T.; Helleday, T.; Benítez, J.; Osorio, A. Small Molecule Inhibitor of OGG1 Blocks Oxidative DNA Damage Repair at Telomeres and Potentiates Methotrexate Anticancer Effects. *Sci. Reports 2021 111* **2021**, *11* (1), 1–14.

(183) Tahara, Y. K.; Auld, D.; Ji, D.; Beharry, A. A.; Kietrys, A. M.; Wilson, D. L.; Jimenez, M.; King, D.; Nguyen, Z.; Kool, E. T. Potent and Selective Inhibitors of 8-Oxoguanine DNA Glycosylase. *J. Am. Chem. Soc.* **2018**, *140* (6), 2105–2114.

(184) Donley, N.; Jaruga, P.; Coskun, E.; Dizdaroglu, M.; McCullough, A. K.; Lloyd, R. S. Small Molecule Inhibitors of 8-Oxoguanine DNA Glycosylase-1 (OGG1). *ACS Chem. Biol.* **2015**, *10* (10), 2334–2343.

(185) Nagel, Z. D.; Margulies, C. M.; Chaim, I. A.; McRee, S. K.; Mazzucato, P.; Ahmad, A.; Abo, R. P.; Butty, V. L.; Forget, A. L.; Samson, L. D. Multiplexed DNA Repair Assays for Multiple Lesions and Multiple Doses via Transcription Inhibition and Transcriptional Mutagenesis. *Proc. Natl. Acad. Sci. U. S. A.* **2014**, *111* (18), E1823.